DEPARTMENT OF CHEMICAL ENGINEERING
UNIVERSITY OF CAPE TOWN

The Effect of Carbon Dioxide on the Growth and Activity of *Leptospirillum ferriphilum*

Dissertation in partial fulfilment for the Degree of Magister Scientae

By
Linus Naik BSc[Engineering](Hons)

CeBER
CENTRE FOR BIOPROCESS ENGINEERING RESEARCH

November 2010

Ad Majorum Dei Gloriam

For my Father, Yogeshkumar and Mother, Shanarz,

who willingly gave up many luxuries for my education,
and without whom nothing would matter.
With humble love and appreciation.

For Celéste,

for your continued encouragements, love and support
from even before the beginning of this undertaking,
and without whom this would not be possible.
With love and affection, always.

Declarations

I, Linus Naik, declare that I know the meaning of plagiarism and declare that all the work in this document, save for that which is properly acknowledged, is my own. This dissertation is for the Degree of Magister Scientae (MSc) at the University of Cape Town and has not been submitted for any other degree at any other University.

Signed by candidate

28th day of November 2010

Linus Naik

Synopsis

Microbial oxidation rates catalysed by the acidophilic micro-organisms mediating mesophilic and thermophilic bioleaching of mineral sulphides have been well characterised under conditions typical of active tank leaching processes in the mineral industry. However, with the increasing need to beneficiate low grade ores, heap bioleaching processes are increasingly of interest. The physicochemical conditions within the heap bioleach differ considerably from the tank leaching system in terms of typical iron concentration, presence of dissolved salts and dissolved gases. This study focuses particularly on the kinetic description of the microbial ferrous oxidation rate and the microbial growth rate of the *Leptospirillum* species under conditions where the supply of carbon dioxide is limited.

The study presented uses the previously reported chemostat approach to generate rigorous biokinetics, using a ferrous sulphate-based medium in an ore-free environment to provide focus on the microbial reaction only. The effect of CO_2 concentration in the sparge gas on the ferrous iron oxidation rate and microbial growth rate supported in continuous culture of planktonic *Leptospirillum ferriphilum* is studied. Results have shown negligible variation in the ferrous iron oxidation rate and microbial growth supported across the range of carbon dioxide concentrations of 430 to 100 ppm in the sparge gas under the experimental conditions used. However, limitation of growth and ferrous iron oxidation was demonstrated at lower rates of CO_2 concentrations (up to 30 ppm). The suitability of the stoichiometric relationships typically used to qualify the ferrous oxidation rate with respect to microbial growth rate was also investigated and compared across the carbon dioxide concentrations used. It has been shown that the relationship breaks down under non-ideal conditions as the carbon dioxide availability is reduced.

Further, the study compares the ferrous iron oxidation rate of planktonic and sessile cells on a ceramic support, under these conditions of limited CO_2 availability in an attempt to understand the behaviour and carbon balance of these cells under different growth and stress conditions. In this study, a packed column was coupled to the chemostat STR with rapid recycle of the liquid phase between these. It was found that the number of cells in the sessile and planktonic populations in the presence of a solid phase was typically twice the number of cells in the planktonic phase. Following this, a sessile population at steady state was decoupled from the planktonic population and attached to another abiotic reactor to observe the ferrous oxidation potential of the sessile population on its own. It was found that the ferrous oxidation rate per unit carbon assimilated for the sessile population on its own reached levels as high as the purely planktonic culture.

The effect of CO_2 availability on the biomass population supported, the yield of biomass on ferrous iron oxidised and the maintenance requirements of the culture are discussed. It was found that the correlation between the biomass formed accounted for almost all the carbon dioxide assimilated in the planktonic system but the relationship broke down when the sessile population was introduced. The total organic carbon produced was significantly higher in the sessile system compared to the planktonic system. In the former, the total organic carbon comprised only a small fraction of monomeric organic acids determined by HPLC. Since the sample was not hydrolysed before the assay was done, this further supports the postulate that the extra organic carbon produced was used for the production of EPS in the presence of the solid support.

Acknowledgements

I would like to acknowledge those persons with whom I have been fortunate enough to work, those who have contributed to how much I enjoyed being at work and those who made the made the work bearable by making the time away from work enjoyable.

My supervisor, Professor Sue Harrison for her guidance and invaluable and indispensable involvement in my thesis project and for giving me the opportunity to learn so much.

My co-supervisor, Doctor Jochen Petersen for encouraging my ideas and always inspiring the engineer in me.

Professor Harro von Blottnitz for his interest in me as a student and for his trust and encouragement over my postgraduate career so far.

Fran Pocock, for her immeasurable help during the experimental phase of this project.

Sue Jobson and Bev Bailey for all the administrative work behind the scenes and creating a friendly work space for everyone

Cindy-Jade Africa, Alistair Hughes, Wynand van Zyl, Jia Fan, Elaine Govender and James Mwase amongst many others for company in the laboratory, in the work place, at conferences and in social life.

The Centre for Bioprocess Engineering Research (CeBER) which was formerly known as the Bioprocess Engineering Research Unit (BERU) for taking me on and for funding

BHP Billition for this opportunity and for funding

My closest and most long-term friends, Christopher Shilubane, Lloyd Joubert & Harshad Bhikha for the all good times since undergraduate and through to present day and for being my constants in this equation of life.

A very special thank you to Celeste Houston for all the love and support and mainly for being there through it all.

And to my family, my father, mother and sister, for everything.

Table of Contents

List of Figures

List of Tables

Glossary

Autotrophic	An organism that supplies all its' carbon requirement from carbon dioxide
Chemolithotroph	An organism which uses inorganic compounds as a source of chemical energy
Dilution rate	The rate of flow of medium divided by the volume of culture in a bioreactor. At steady state the dilution rate is equal to the microbial growth rate.
Haemocytometer	Microscope slide designed with gridlines and a fixed volume used to count the number of cells in a known volume
Hydrometallurgical	Pertaining to the extraction of metals using water based methods
Inoculate	To introduce (micro-organisms) into surroundings suited to their growth such, as a culture medium
Jarosite	A hydroxy-sulphate of potassium and iron ($KFe_3(OH)_6(SO_4)_2$) formed in ore deposits by the oxidation of iron sulphides
Planktonic	Micro-organisms suspended in aqueous solution
Pyrometallurgical	Pertaining to the extraction of metals using heat based methods
Pyruvate	A three carbon saccharide ($CH_3COCOOH$) found in living organisms. It plays a key role in he central carbon metabolism
Residence time	The average time spent by a given particle in a system (usually a chemical reactor system)
Sessile	Micro-organisms attached to a surface
Spectrophotometry	An analytical method used in chemical analyses to determine the concentration of compounds in a liquid medium. It is often used for metals which are coupled with ligands to form coloured complexes which have absorbance maxima at different wavelengths. It is a quantitative technique
Redox potential	The tendency of a chemical species to acquire electrons and therefore be reduced
Washout	The dilution rate at which the flow rate of cells out of the system exceeds the generation of cells within the system, meaning that cells will be purged

Chemical and Technical Abbreviations

AAS	Atomic Absorption Spectrum spectroscopy
Acetyl Co-A	Acetyl Coenzyme-A
ATP	Adenosine Tri-Phosphate
Bis-acrylamide	N, N'-Methylene-bis-acrylamide
CO_2	carbon dioxide
Coomassie Blue	Coomassie Brilliant Blue G-250
CSTR	Continuous Stirred Tank Reactor
Cu_2S	chalcocite
$CuFeS_2$	chalcopyrite
CuS	covellite
EPS	Extracellular/Exocellular Polymeric Substances
EOM	Extracellular Organic Monomers
Fe^{2+}	ferrous iron
Fe^{3+}	ferric iron
Fe_2S	pyrite
H_2SO_4	sulphuric acid
HPLC	High Pressure/Performance Liquid Chromatography
K_La	overall mass transfer coefficient
MeS	metal sulphide
$NAD(P)^+$	Nicotinamide Adenine Dinucleotide (Phosphate) [Oxidised]
NAD(P)H	Nicotinamide Adenine Dinucleotide (Phosphate) [Reduced]
NO_x	Nitrous oxides, including NO and NO_2 amongst others
pH	potential for Hydrogen ion concentration (a measure of acidity/alkalinity)
pK_a	logarithmic measure of the acid dissociation constant
ppm	parts per million (equivalent to mg/L in aqueous systems)
PLS	Pregnant Leach Solution
O_2	oxygen
RuBisCO	Ribulose Bisphosphate Carboxylase Oxygenase
S	sulphur
SO_2	sulphur dioxide
SO_x	sulphurous oxides (primarily SO_2)
SO_4^{2-}	sulphate ion
STR	Stirred Tank Reactor
Tris	Tris(hydroxymethyl)aminomethane
TOC	Total Organic Carbon

List of Symbols

symbol	*name/description*	*value/units*
a_i	chemical activity of relevant species ***i***	mol/dm^3
$[Cell]$	cell concentration	10^6 cells/ml
C_i	concentration of species ***i***	mol/dm^3
C_x	amount of carbon (as biomass) in the system	mmol/l
D	bioreactor dilution rate	1/hr
E	solution potential	mV
E_0	solution potential at standard state	mV
F	Faraday constant	9.649 C/mol
$[Fe^{2+}]_{inlet}$	concentration of ferrous iron in inlet	mmol/l
$[Fe^{2+}]_{outlet}$	concentration of ferrous iron in outlet	mmol/l
$\frac{[Fe^{3+}]}{[Fe^{2+}]}$	ratio of ferric iron to ferrous iron concentration	
ΔG^0	change in Gibbs free energy, std conditions	J/mol
g	acceleration due to gravity	9.81 m/s^2
I_m	Ionic strength	mol/dm^3
$K_{Fe^{2+}}$	apparent affinity constant	
$m_{Fe^{2+}}$	maintenance term	mmolFe^{2+}/(mmolC.hr)
μ	microbial growth rate	1/hr
n	number of electrons transferred	
$q_{Fe^{2+}}$	specific ferrous oxidation rate	mmolFe^{2+}/(mmolC.hr)
$q_{Fe^{2+}}^{max}$	maximum specific ferrous oxidation rate	mmolFe^{2+}/(mmolC.hr)
R	universal gas constant	8.3145 J/(mol.K)
r_{CO_2}	rate of carbon dioxide utilisation	mmol/(l.hr)
$r_{Fe^{2+}}$	rate of ferrous iron oxidation	mmol/(l.hr)
r_{O_2}	rate of oxygen utilisation	mmol/(l.hr)
T	temperature	K
$Y_{Fe^{2+}}^{max}$	maximum growth yield on the ferrous iron	mmolC/mmol Fe^{2+}
Z_i	ionic charge of species ***i***	mol/dm^3

1. Introduction

1.1 Background

Mineral bioleaching, a hydrometallurgical process which uses micro-organisms to facilitate the dissolution of metals from low grade sulphidic ores, occurs primarily in one of two forms: heap leaching or tank leaching. The form chosen depends on the scale of the operation and the grade of ore being processed, as well as its suitability for prior milling and concentration. For low grade ores heap leaching is the most apt process for mineral extraction. Other forms of extraction all include grinding and concentration which are energy intensive. Heap bioleaching does not require these and although the process is relatively slower, it has lower NO_x and SO_2 emissions compared to traditional pyrometallurgical processes. Heap leaching is a dynamic process comprised of many sub-systems. On the macro scale, a bed of ore is irrigated from the top and air introduced from the bottom. Soluble ferrous iron is present in the feed solution. On the micro scale, ferrous iron oxidation is coupled with oxygen reduction by the microbes in the heap to produce energy which in turn generates ferric iron, a leach agent. The protons liberated into solution are another leach agent. The metal ions and oxidised sulphur compounds are liberated into solution on sulphur oxidation and leave in the pregnant leach solution.

The process of microbial leaching involves many microbial species, classified into two major groupings: the iron oxidizers and the sulphur oxidizers. Some microbes are capable of oxidising both iron and sulphur while others perform only one or the other. *L. ferriphilum* is an iron oxidizer, converting ferrous iron to ferric iron. It is used in the microbial leaching of pyrite (FeS_2), chalcopyrite ($CuFeS_2$) and chalcocite (Cu_2S). *L. ferriphilum* has been found to be the dominant iron-oxidizing bacterium in industrial continuous-flow bio-oxidation tanks (Rawlings *et al.*, 1999; Coram & Rawlings, 2002). The high ferric: ferrous ion ratio present in tank leaching is less inhibitory to *L. ferriphilum* than to other mesophilic bacteria, such as *Acidithiobacillus ferrooxidans*, associated with both ferrous iron and sulphide oxidation. For this reason, *L. ferriphilum* is also found as a key micro-organism in well established heap and column bioleach systems at high redox potential under mesophilic conditions (De Wulf-Durand *et al.*, 1997). qRT-PCR analysis has shown that *At. thiooxidans*, *At. ferrooxidans* and *L. ferriphilum* were the three dominant micro-organisms in analysis of cultures from low temperature heap leaching simulation columns in Johannesburg, South Africa (Coram-Uliana *et al.*, 2006). Demergasso *et al.* (2005) found that *L. ferriphilum* was among the dominant populations along with *At. ferrooxidans* and *Ferroplasma acidiphilum* in low-grade copper sulphide run-of-mine test heaps using PCR and Denaturing Gel Gradient Electrophoresis (DGGE).

Many of the microbial strains implicated in facilitating mineral bioleaching, including *Leptospirillum ferriphilum,* are obligate chemolithoautotrophs, relying on the fixation of atmospheric carbon dioxide as their carbon source (autotrophic) and deriving their energy from the oxidation of inorganic compounds (lithotrophic). This implies that establishment of the biocatalytic phase is dependent on CO_2 availability. Stoichiometric relationships and rate equations have been measured empirically under optimum leach conditions appropriate for tank leaching (Breed & Hansford, 1999) to correlate CO_2 assimilation, microbial growth rate and the ferrous iron oxidation rate under optimal conditions in a steady state bioreactor.

The microbial growth rate is dependent on the availability of carbon dioxide which can be converted to organic carbon by the microbe, and the apportionment of the carbon fixed for growth. During industrial bioleaching operations, there is often a span of time between heap inoculation and effective leaching of ore, known as the "lag phase." This has been attributed to the time taken for the microbes involved in bioleaching to adapt and start growing successfully. Understanding of factors which govern the length of the lag phase is critical to ensure that heaps can start being effective soon after inoculation. Since carbon is needed for microbial growth, understanding the effect of carbon availability on microbial growth kinetics is important.

Once carbon dioxide is fixed by microbes, its usage is split into three main categories. Some of the carbon is used for cell maintenance, the basic metabolic processes that the cells need to perform to remain alive. Another portion is used in the formation of new biomass, which leads to further cellular reproduction. Lastly, a small portion is used in the synthesis of organic compounds to be used in certain cell activities. These include Extracellular Organic Monomers (EOM), and Extracellular Polymeric Substances (EPS). EPS is secreted to form bio-films on mineral surfaces and to enhance attachment to the mineral surface. *Leptospirillum ferriphilum* is known to be an EPS producing microbe (Ginsburg *et al.*, 2008). Since *Leptospirilla* only use ferrous iron as an energy source, they can be grown in continuous stirred tank reactors using an aqueous feed (i.e. without mineral ore or concentrate present). Initially, Boon *et al.* (1995) did the seminal work under ideal conditions to develop the constant relationships and comparative parameters for the system under ideal conditions for what was then thought to be predominantly *L. ferrooxidans* but was later typed as predominantly *L. ferriphilum*. Later, these parameters were used in rate analyses of non-ideal systems (Boon *et al.*, 1995; Breed and Hansford, 1999; Ojumu *et al.* 2008). So far, rate studies have been performed to compare the microbial growth rate and the ferrous iron oxidation rate of various micro-organisms under different physicochemical conditions. Parameters tested include the effects of pH, temperature, ionic strength and ferrous iron concentration on the microbial growth rate, to determine the effect of these stress conditions on the ferrous oxidation rate, and hence leach performance. All experiments were run in well aerated systems at moderate to favourable ferrous iron concentrations with efficient aeration to supply carbon dioxide. In studies to date, a fixed stoichiometry between ferrous iron oxidation and carbon dioxide fixation has been assumed.

In a recent study, Petersen and Ojumu (2006) suggested that up to 99% of the carbon dioxide fixed under these ideal conditions is used in the formation of new biomass. This was calculated by measuring the CO_2 uptake rate over the continuous stirred tank at steady state using off-gas analysis and the number of cells in the system by microscopic cell counts. A carbon equivalent (based on an elemental empirical formula for bioleach microbes) was used to calculate the fraction of CO_2 taken up to form new biomass. Studies have been performed to investigate the effect of carbon dioxide and oxygen limitation on the leaching rate of sulphidic minerals (Haddadin et al., 1992; Witne & Philips, 2000; Bouffard and Dixon, 2002). However, studies have not yet been performed to compare the effect of carbon dioxide availability on microbial kinetics and stoichiometry, or to attempt to verify the respirometric assumptions underpinning the respirometric approach under non-ideal conditions (especially gas-liquid mass transfer limitations).

Furthermore, while attachment of bioleaching micro-organisms to surfaces has been investigated (Harneit *et al.*, 2006; Africa *et al.*, 2010), the activity of sessile and planktonic cells has not been compared as a function of carbon dioxide availability, nor has the relative flux of carbon through the microbial metabolism been considered under different culture conditions or in the presence or absence of a solid surface. The presence of a solid surface may be expected to lead to an increase in EPS production with a concomitant shift in the carbon partitioning. It is also postulated that under stress, microbes may have lower growth rates and expend less energy on the production of biomass for growth and more on maintenance functions, including the production of stress proteins to counteract the stress factor (e.g. ionic stress).

1.2 Problem statement

It has been identified that during the process of heap bioleaching, carbon availability may be reduced. This reduced availability of carbon dioxide has been identified as reducing the performance of heap bioleaching (Petersen and Dixon, 2007; Petersen *et al.*, 2010) and has prompted this study investigating the effect of carbon dioxide availability on the growth and activity of *L. ferriphilum*.

1.3 Research objectives

It is apparent that the carbon utilization in bioleaching microbes has not been rigorously studied as a function of the process environment. Respirometric rate studies have been used to establish a stoichiometric relationship between the ferrous iron oxidation rate and the microbial growth rate (Boon *et al.*, 1995; Boon *et al.*, 1999). However, this relationship between the microbial growth rate and carbon utilization has not been fully described and has been assumed to be unaffected by growth conditions. Since some of the energy derived from ferrous iron oxidation is used in carbon dioxide uptake, there exists a relationship between the two rates. Progress in the understanding of these processes, their inter-relationship and how they change as a function of carbon dioxide availability is expected to be beneficial to microbial heap leaching practices.

In this study, the effect of carbon dioxide concentration in the sparge gas, and thereby the CO_2 transfer rate, on the ferrous oxidation rate, the CO_2 uptake rate and the microbial growth rate of *Leptospirillum ferriphilum* in submerged continuous tank culture was investigated. Changes in carbon utilization of the microbial strain with the addition of a non-mineral solid phase for attachment have been studied. The parameters varied were the carbon dioxide concentration in the air supply to *L. ferriphilum* cultured in a continuous stirred tank reactor across a range of dilution rates. Data were collected with respect to ferrous iron oxidation rate, microbial growth rate, yield and stoichiometry. In the second stage, a non-mineral solid support was added to the system and the experiments repeated to provide data to compare the rate between planktonic and sessile cells. The measurements taken included: redox potential, pH, $[Fe^{2+}]$, CO_2 uptake, O_2 uptake and total iron concentration. Microbial cell counts and the concentration of total organic carbon in the media and the effluent were determined for occasional sampling or intermittently to establish the proportion of CO_2 used for viable biomass formation and extracellular

organic products as well as the effect of the varying culture conditions on the microbial population respectively.

The aims of the study were thus fourfold:

- to determine the microbial growth kinetics as a function of carbon dioxide availability
- to verify the stoichiometric relationship between the carbon dioxide uptake rate and the ferrous oxidation rate in planktonic cells across a range of growth conditions through the comparison of analytical methods
- to investigate the associated partitioning of carbon fixed between viable biomass and extracellular organic materials, and
- to compare the activity of the sessile and planktonic populations.

The data generated can also be used to model the ferrous iron oxidation and growth of bacteria under known carbon dioxide stress. This, in turn, can be used to inform the predictive model of overall heap leaching kinetics.

1.4 Thesis outline

In this dissertation, the relevant literature is reviewed in Chapter 2, starting with an overview of bioleaching, the different types of bioleaching, in terms of the reactions which occur, those relevant to this study and the role of the micro-organisms in bioleaching from Sections 2.1 to 2.4. The kinetics of bioleaching are reviewed in Section 2.5 along with equations and assumptions underlying the respirometric approach. The principles behind the reduction-oxidation potential, a critical measurement in this study, are outlined in Section 2.6. Microbial energetics, the carbon uptake and utilisation and the effect of carbon dioxide limitation are discussed in Sections 2.7, 2.8 and 2.9 respectively. Some key concepts of bioleaching, namely mass transfer in bioleaching, carbon partitioning and the differences between planktonic and sessile cells are then highlighted in Sections 2.10, 2.11 and 2.12 respectively. Finally, hypotheses are drawn from the literature and an experimental approach is formulated in Section 2.13.

The experimental approach adopted in this project is outlined in Section 3. The materials used, the bacterial culture and the growth medium are presented in Sections 3.1, 3.2, and 3.3 respectively. The reactor set-up and operation is outlined from Section 3.5 to 3.6.3 and the analytical methods used are summarised in Section 3.7 with details in Appendix D.

The results and discussion are presented in two chapters. The effect of carbon dioxide concentration on the ferrous oxidation and growth rate of the purely planktonic system is presented in Chapter 4. A brief outline of the aim and the approach taken in this part of the study are provided in Section 4.1. An analysis of the base case study uses the planktonic system as a well mixed chemostat with normal compressed air supplied at approximately 360 ppm carbon dioxide is provided in Section 4.2. In Section 4.3, the full set of

results is presented using carbon dioxide concentrations of 30, 50, 100, 270, 340 and 450 ppm with subsequent discussions. The conclusions of the planktonic study are provided in Section 4.4.

In Chapter 5 the performance of sessile and planktonic cells is compared. Chapter 5 is divided into two separate sections. The kinetic study of carbon dioxide uptake and ferrous iron oxidation, carried out in Chapter 4 using planktonic *Leptospirillum ferriphilum*, is repeated in the presence of a sessile population at carbon dioxide concentrations of 340 ppm, 100 ppm, 50 ppm and 30 ppm. The sessile population is retained on a solid support in a column attached to the system. The results for this study are discussed in Section 5.1. Thereafter the sessile based population and planktonic stirred tank reactor populations from steady state operation are decoupled. The sessile population is attached to a new abiotic reactor running at steady state and the planktonic population is left to run without the sessile phase. The ferrous oxidation rate of the sessile population on the solid phase and the remaining planktonic population are monitored separately. This is referred to as the Decoupling study and is outlined and discussed in Section 5.2. Section 5.3 presents conclusions of these studies.

Carbon utilisation for biomass is discussed at the end of Chapters 4 and 5 in Sections 4.4 and 5.3 respectively. Carbon flux and utilisation for other organic compounds measured by total organic carbon and high performance liquid chromatography are also presented here.

The general conclusions and recommendations for future work are given in Chapter 6. This is followed by the list of references used and the appendices, which contain the media preparation, detailed analytical methods, raw data and sample calculations.

2. Literature Review and Project Definition

2.1 The role of bioleaching in metal recovery from minerals

The increasing necessity to process low grade ores has made heap bioleaching a favourable option as the ore does not require pre-concentration. The economic advantages of bioleaching, as well as the environmental concerns over traditional pyrometallurgical processes have prompted numerous studies into the bioleaching process in the minerals industry (Rawlings, 1997). The process has been used since the early 1960's, for example, in the leaching of uranium ore *in situ* in Spain (Munoz *et al.*, 2006); however, bioleaching (without the knowledge of the microbial phase) dates back to ancient times. The Rio Tinto (Red River) obtained its name from the red colour due to the high concentration of ferric iron and was known to be inhospitable to aquatic life (mainly due to acidity). In the 16th century, a priest, Delgardo, while investigating the phenomenon that iron dissolved in the river, also observed that copper precipitated out as the iron dissolved. This process is known as cementation and is still used today as one of the processes to extract copper from leach solution (Rawlings, 2002). The role of micro-organisms in mineral bioleaching was characterised in the late 1950's.

Liberation of metals from ore can be done via pyrometallurgy or hydrometallurgy. Pyrometallurgy is economically inefficient with lower grades of ore as it is very energy intensive through concentration, roasting and smelting. Pyrometallurgy is also associated with the environmental concerns of SO_x and NO_x emissions, its energy footprint and emission of toxic metals, e.g. arsenic, from concentrations bearing these compounds. Hydrometallurgy processes usually involve an acid leach or a pressure acid leach which liberate the metal from the ore into solution known as the pregnant leach solution (PLS). Bioleaching is characterised by the addition of micro-organisms in the leaching step to assist in provision of leaching agents. The PLS is then taken to metal extraction processes such as electro-winning, ion exchange or cementation depending on the properties of the leach solution and the mineral being recovered (Rawlings, 2002). SO_x and NO_x emissions are reduced or eliminated. Toxic metals such as arsenic can be managed into a stable precipitate. The process is outlined in Figure 2-1.

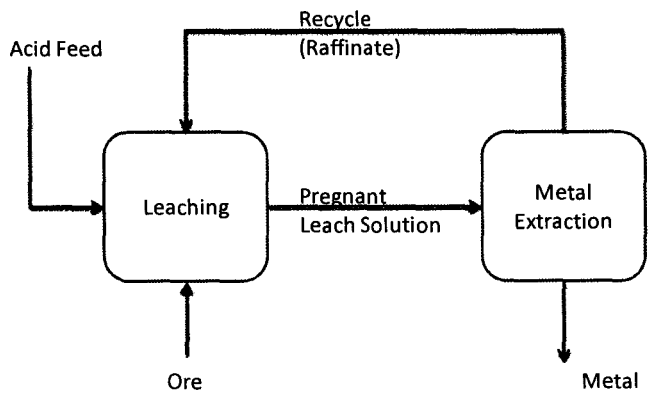

Figure 2-1. Block flow diagram of a typical leaching process

Mine tailings and wastes produced from physicochemical processes when exposed to air and rain may be biologically leached producing unwanted acid and metal pollution. Tailings from bioleaching operations are less chemically active, and the biological activity is reduced by at least the extent to which they have already been bioleached (Rawlings, 2002). Bioleaching also has clear advantages in the extraction of residual metals from waste streams (Brierley, 1978). For example, copper can be recovered from low grade ores and dumps left behind from previous mining operations by using the biological activity that takes place during controlled irrigation of the dump (Brierley, 1982).

2.2 Key elements and chemical reactions in bioleaching

There are two main categories of bioleaching carried out in industry today, namely irrigation or heap leaching and tank leaching. In tank leaching, the mineral slurry is processed through a series of continuously stirred tanks. Following contacting of the mineral concentrate, inorganic nutrients and water, the material passes through a series of aerated and agitated leaching tanks in which biological and mineral leaching reactions proceed. Typically temperature and pH adjustment are required (Van Aswegen *et al.*, 1991). When the biooxidation of the mineral concentrate is sufficiently complete (Schnell, 1997), a settling tank is used to prepare the pregnant leach solution (PLS). The majority of refractory gold-bearing ore is leached via tank leaching, and the tank system raises the potential for the leaching of high grade concentrates of base metals (Coram and Rawlings, 1999).

The second type of bioleaching is irrigation or heap leaching. Irrigation leaching is essentially a simple process with respect to equipment and operational set up and is less energy intensive as it does not use agitation, nor require the preparation of a concentrate. It has its drawbacks in that it is difficult to control. Irrigation type processes include dump leaching, heap leaching and *in situ* leaching. The metal recovered in by far the greatest quantities by heap bioleaching is copper, in excess of 30 million tonnes/annum (Brierley & Brierley, 1999). Dump leaching was initiated in the 1960's. One of the best known processes is the Kennecott Copper Mine in Utah (Brierley, 1997). The dumps consist of run-of-mine ore, piled into heaps, (up to 350m high) which goes through cycles of preconditioning, irrigation and rest, each of which may extend up to a year. The irrigation is carried out with an iron- and sulphate- rich acidic solution to aid the solubilisation of copper. The micro-organisms in the dump contribute by the regeneration of leaching agents. The result is a PLS containing copper. The metal extraction takes place in the form of solvent extraction and electro-winning (Schnell, 1997). *In situ* leaching is a very similar process, but different with respect to the form of mineral being leached. It involves the breaking up of ore bodies in place without mining, adding irrigant and collecting the PLS. It can be used for base metals, but the majority of uranium obtained from bioleaching is recovered by *in situ* leaching (Hallberg, 1995). Its chief challenges are liberation of the metal sulphide and control of the collection of PLS. Heap leaching is simply a more efficient way of dump leaching and is the most common bioleaching process, used mainly for the bioleaching of copper (Rawlings, 2002). The actual process is expanded in Section 2.3.

Understanding the chemistry behind the bioleaching process emphasises the significance of the microbial population. The following is an outline of the key chemical reactions involved in the bioleaching of sulphidic ores. The bioleaching of pyrite and chalcopyrite using mesophilic and thermophilic micro-

organisms has been extensively studied (Ackil & Cifti, 2003; Bevilaqua *et al.*, 2002; Gericke *et al.*, 2001; Norris, 1983; Petersen & Dixon, 2002). The mechanism for leaching is not the same for all minerals. This is not just with respect to different metals, i.e. zinc, nickel and copper, but even different copper sulphide minerals, e.g. chalcocite (Cu_2S), covellite (CuS) and chalcopyrite ($CuFeS_2$) undergo different leaching and oxidation reactions. Recent studies have suggested that the oxidation of sulphidic minerals proceeds via either the polysulphide intermediates or the thiosulphate pathway depending on the mineral (Rohwerder *et al.*, 2003; Sand *et al.*, 2001).

It is proposed that chalcopyrite is leached via the formation of polysulphide intermediates following chemical attack by the ferric iron and acid shown in Equation 1.

$$CuFeS_2 + 2Fe_2(SO_4)_3 \rightarrow CuSO_4 + 5FeSO_4 + 2S^0 \qquad \textbf{Equation 1}$$

The bioleaching micro-organisms continuously regenerate the polysulphide intermediates as shown in Equation 2 and Equation 3. These micro-organisms are present in the bioleach environment and the rate of the bioleaching process is expected to depend on the activity of the micro-organisms and the rate at which they regenerate the ferric iron as a key leaching agent, where mineral availability is sufficient.

$$2FeSO_4 + \tfrac{1}{2}O_2 + H_2SO_4 \rightarrow Fe_2(SO_4)_3 + H_2O \qquad \textbf{Equation 2}$$

$$2S^0 + 3O_2 + 2H_2O \rightarrow 2H_2SO_4 \qquad \textbf{Equation 3}$$

The biooxidation of pyrite occurs via the thiosulphate pathway solely by ferric attack leading to the acidification of the bioleach medium. This process is highlighted in Equation 4.

$$FeS_2 + 7Fe_2(SO_4)_3 + 8H_2O \rightarrow 15FeSO_4 + 8H_2SO_4 \qquad \textbf{Equation 4}$$

Chalcocite is a typical copper sulphide mineral processed at bioleaching operations. Some of the chalcocite heap operations began as oxide (chemical) leach operations and were converted to bioleach (oxidative) operations by heap aeration and inoculation when the oxide ore was depleted. Even if microbial inoculation is not forced, microbial-assisted air oxidation of ferrous iron and sulphur contributes to copper extraction if sulphide mineral is present in the heap (Watling, 2006). Millions of tonnes of low-grade copper rich tailings await the development of an efficient and economic bioleach process for chalcopyrite, which is both the most abundant and the most refractory copper sulphide. The bioleaching of chalcopyrite *in situ*, in dumps and in heaps is a practical option only because the low and slow recoveries are countered by the low processing costs (Schnell, 1997).

The leaching rate itself is governed by a number of factors including pH, temperature, redox potential, pulp density, particle size, availability of nutrients, O_2 and CO_2, presence of toxic elements etc.. These affect the activity of the micro-organisms as well as the chemistry of the dissolution process (Bailey &

Hansford, 1993; Boon & Heijnen, 1997; Deveci, 2002). Microbial growth kinetics and ferrous oxidation are reviewed in Section 2.5

2.3 Heap leaching and the sub-processes in heap leaching

Heap leaching, a more efficient way of dump leaching, is the most common bioleaching process used with most applications being for copper recovery (Rawlings, 2002). Typically, ore is crushed, acidified and agglomerated before it is stacked into heaps of 2 to 10 metres high on irrigation pads lined with, for example, polyethylene to avoid loss of solution. Irrigation pipes are laid on top of the heap. Aeration pipes are constructed into the heap at the bottom to permit forced aeration to provide oxygen and carbon dioxide. Although bioleaching micro-organisms are present on the ore, an inoculum is typically added during agglomeration or in the irrigation stream. The microbial cultures for inoculation are usually enriched in pond systems on the mine site or may be specifically cultured in tank reactors. Since some micro-organisms, e.g. *Acidithiobacillus caldus* cannot fix nitrogen from the air (Valdês *et al.*, 2008a), they benefit from the addition of inorganic nutrients containing combined nitrogen and phosphorus (Madigan *et al.*, 2003) especially during heap start-up. To date this is not common practice on an industrial scale. The process of heap leaching is outlined in Figure 2-2.

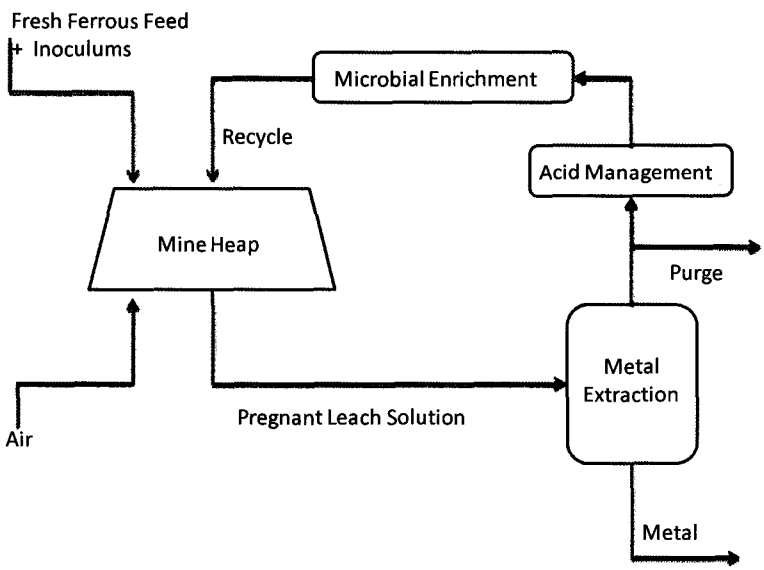

Figure 2-2. Block flow diagram of the heap bioleaching process

Although the configuration of the process may seem straight forward, the sub-processes and their interactions occurring in the heap leaching process are not yet fully understood (Petersen and Dixon, 2007). The gas transport into the liquid phase, and the microbial oxidation and growth rates play a key role in understanding the dynamics of bioleaching. In this section, the macro scale aspects of heap bioleaching are discussed. In Section 2.4, the role of micro-organisms is considered.

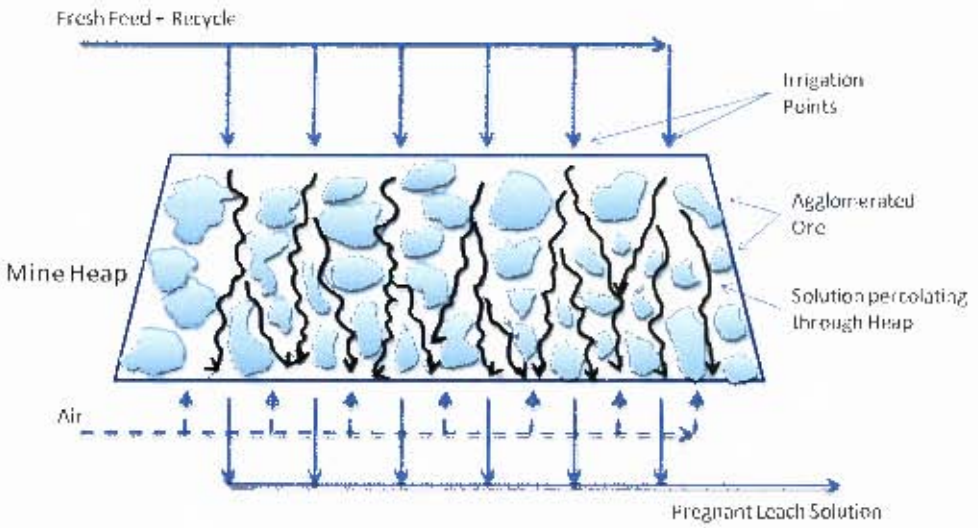

Figure 2-3. Diagrammatic representation of a typical heap in a heap leaching process (adapted from Dixon and Petersen, 2003)

Figure 2-3 conceptualises the large scale processes taking place in a heap leaching environment. As bioleaching is an exothermic process, the heat flow in the profile in the heap is also significant. The energy produced in the heap during leaching can raise temperature up to 70°C (Gautier *et al.*, 2008). The mass and energy transfer through the bed of ore encompass the solution flow, heat flow and gas flow as the main variables. It is noted that specific micro-organisms are only active under certain temperature ranges.

The diagram highlights heap leaching as dynamic process. While tank leaching is typically a well-mixed process, the heap environment is highly heterogeneous and unsaturated (Petersen and Dixon, 2007). The solution present can be divided into flowing and stagnant zones. The oxygen and carbon dioxide reactants are required to diffuse from the air pockets through solution films to the reaction surface. Mass transfer limitations result and concentration profiles of dissolved gasses, ions in feed solution and liberated metal vary greatly through the heap on both the macro- and micro-scale.

2.4 Micro-organisms in bioleaching

To date, the role of the micro-organisms has been identified as follows. The abiotic oxidation of ferrous ions to ferric ions is a slow process at temperatures below 60°C (Rubio & Garcia Frutos, 2002). Microbial oxidation of ferrous iron (Fe^{2+}) may occur 10^5 - 10^6 times faster than normal chemical oxidation at pH 2-3 (Bosecker, 1997). The key physiological requirements of micro-organisms involved in the heap bioleaching of sulphide minerals are, firstly, that they are chemolithotrophic, using ferrous iron and/or reduced inorganic sulphur sources as electron donors (Rawlings, 2002). Figure 2-4 illustrates the role of ferrous oxidising micro-organisms in the liberation of a metal from a sulphide ore. Sulphur oxidizing micro-organisms oxidize the sulphur to sulphate.

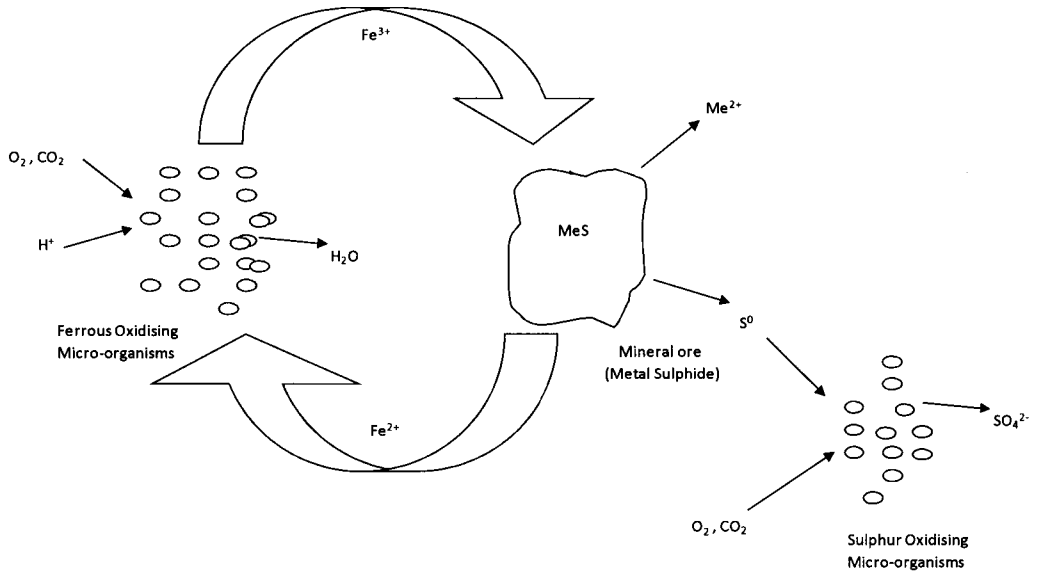

Figure 2-4. Simplification of the interaction between ferrous and sulphur oxidising micro-organisms and mineral ore (adapted from Breed, 2000)

Table 2-1 highlights some of the key iron and sulphur oxidisers involved in bioleaching and their properties. As the by-product of sulphur oxidation is sulphuric acid, bioleaching micro-organisms are acidophilic and are typically active between pH 1 and pH 2. Bacteria are considered acidophilic if they grow below pH 4.0 (Hallberg, 1995). This acidophily also applies to the micro-organisms which only oxidise ferrous iron. The micro-organisms are also classed according to their optimal growth temperature: psychrophiles (<20°C), mesophiles (30°C to 45°C), moderate thermophiles (45°C to 60°C) and thermophiles (60°C to 80°C).

Most of the primary bioleaching micro-organisms are able to fix CO_2, with varying levels of efficiency. Some carbon dioxide fixing species scavenge carbon dioxide at very low carbon dioxide concentrations while others require either elevated levels of CO_2 or a small amount of yeast extract (an alternative carbon source) to grow rapidly (Rawlings, 2002). A number of heterotrophic micro-organisms have been identified as key players in bioleaching. The carbon utilisation by the micro-organisms is reviewed further in Section 2.8.

Table 2-1. Key iron and sulphur oxidising acidophiles involved in bioleaching (adapted from Watling, 2006)

Micro-Organism	Trophic Characteristics	Energy Source	Temperature Category	Active pH Range
Acidianus ambivalens	chemolithoautotroph	S oxidation and reduction, poor (if any) Fe oxidation	hyperthermophile	1.5 - 2.5
Acidithiobacillus ferrooxidans	chemolithoautotroph	S oxidation, sulphides Fe oxidation (and Fe reduction as a facultative anaerobe)	mesophile	2.0 - 4.0
Acidithiobacillus thiooxidans	chemolithoautotroph	S oxidation, sulphides	mesophile	2.0 - 4.0
Acidithiobacillus caldus	mixotroph	S oxidation, sulphides	moderate thermophile	2.0 - 2.5
Ferroplasma acidophilum	heterotroph	Fe oxidation, pyrite	moderate thermophile	<1.0 - 2.0
Leptospirillum ferriphilum	chemolithoautotroph	Fe oxidation	mesophile, some thermotolerant strains	1.6 - 1.9
Leptospirillum ferrooxidans	chemolithoautotroph	Fe oxidation, pyrite	mesophile	1.5 - 1.7
Metallosphera hakonnensis	obligate chemolithoautotroph	S oxidation, sulphides	thermophile	1.0 - 4.0
Sulfolobus metallicus	mixotroph	S oxidation, sulphides	hyperthermophile	1.0 - 4.5
Sulfobacillus acidophilus	chemolithoautotroph	Fe oxidation & reduction, sulphides	moderate thermophile	1.0 - 2.5
Sulfobacillus thermosulfidooxidans	obligate chemolithoautotroph	S oxidation	moderate thermophile	1.0 - 2.5
Thiobacillus prosperus	obligate autotroph	S and Fe oxidation, sulphides	mesophile	2.0 opt.

The micro-organisms implicated in bioleaching are resistant to a range of metal ions in high concentrations. The leach solution often has a high concentration of dissolved ions, e.g. aluminium and magnesium which are commonly toxic to most other micro-organisms (Blight & Ralph, 2008; Ojumu *et al.*, 2008). This stress is intensified by nature of heap leaching, in which the leach solution is recycled, hence metal ions which are not removed in ion or solvent exchange accumulate in the raffinate.

The aforementioned properties explain why "biomining micro-organisms are ideally suited to growing in the inorganic environment created by the active aeration of a suspension of a suitable iron- and sulphur-containing mineral in water or during the passive aeration that takes place when a heap of the mineral is irrigated with water. Air provides the carbon source (CO_2) and the preferred electron acceptor (O_2), and the mineral ore supplies the electron donor (ferrous iron and/or reduced inorganic sulphur) and the water is the medium for the growth" (Rawlings, 2002).

Some of the bioleaching micro-organisms are capable of fixing atmospheric nitrogen. Nitrogen fixation requires an energy input and therefore lowers the growth yield. Supplementation of laboratory scale leach columns with soluble nitrogen, particularly as organic nitrogen significantly reduced the lag time and promoted bacterial growth (van Hille *et al.*, 2009). The addition of small quantities of fertilizer grade salts, e.g. ammonium sulphate and potassium phosphate to ensure that there is no nutrient limitation has been investigated in lab-scale columns but is not applied uniformly across all industrial scale processes.

In the heap leach environment, air supply is not uniform. Some regions are limited with respect to oxygen and carbon dioxide availability. In some heaps, this is overcome partially by enriching the aeration gas with carbon dioxide, as discussed in Section 2.8.

The above mentioned physiological characteristics have provided the basis for investigations into the activity of bioleaching micro-organisms, i.e. varying temperature, pH, carbon dioxide and oxygen concentrations, and the addition of nutrients. The understanding of the role of the microbial strains and the potential interactions within the bacterial population under the defined bioleaching conditions is essential for improving the efficiency of the bioleaching process (Akcil *et al.*, 2006). Researchers have shown that mixed microbial cultures of micro-organisms oxidise sulphide minerals more efficiently than pure cultures (Akcil & Cifti, 2003; Norris, 1983). The diversity was shown to depend on the conditions of the bioleach environment and relate largely to aforementioned factors (pH, temperature, pulp density etc.) (Johnson, 1998). The commensal interactions influence population dynamics. In the heap leach environment, there is a gradual succession of strains of micro-organisms as the temperature, concentration and pH profiles change. Furthermore, heterotrophs in the heap scavenge organic by-products from the autotrophs and become more dominant as the heap moves from a start-up phase to a pseudo-continuous phase.

The limited number of micro-organisms that have been discovered is partly a consequence of the selective methods of enrichment on isolation. The perceived importance of *Acidithiobacillus ferrooxidans* (formerly *Thiobacillus ferrooxidans*) is case in point. *At. ferrooxidans* was thought to play a major role in the biooxidation and bioleaching processes at temperatures ≤ 40°C because, when cultures were grown on soluble iron media in batch tests, *At. ferrooxidans* outcompeted *Leptospirillum ferriphilum* (previously thought to be *Leptospirillum ferrooxidans*). The seminal work of Rawlings *et al.* (1999) showed that the reverse is true in continuous tank bioreactors. Since then, the *Leptospirillum* component has been shown to consist of two major species and *Leptospirillum ferriphilum* has been identified as the predominant mesophile in many tank leaching industrial operations (Coram & Rawlings, 2002). This has been attributed to the strain's ability to scavenge ferrous iron, which is important in well mixed operating systems where the actual mineral leaching is limiting and not the ferrous oxidation rate. However, to date the molecular research relevant to bioleaching is still dominated by *At. ferrooxidans* studies and this remains the most well-understood micro-organism in bioleaching. While early studies suggest that *Lepstospirillum* species are unable to flourish on chalcopyrite ores (Stott *et al.*, 2003) and attribute this to the lack of tolerance to metal concentrations (Norris *et al.*, 1988) and passivation of the mineral surface by jarosite (Stott *et al.*, 2000), recent studies contradict this. Dermagasso *et al.* (2005) have identified *Leptospirillum* as a key microbe in the in chalcocite and chalcopyrite containing heaps. Further, Africa *et al.* (2010) demonstrated significant attachment of both *L. ferriphilum* and *At. ferrooxidans* to both pyrite and chalcopyrite.

2.5 Ferrous iron oxidation and microbial growth kinetics

In order to inform process optimisation, a significant body of literature has been established on ferrous iron oxidation rates and microbial growth rates. Following on from the seminal studies of Boon and Hansford (1996), much of the kinetic data has been collected through the combination of respirometry and microbial stoichiometry. The theoretical formulation of this approach, presented below, has been described in many sources (Boon *et al.*, 1994; Boon, 1996; Breed & Hansford, 1999; Ojumu, 2008). Several assumptions, made for the purpose of this approach, are outlined below:

1. Microbial biomass can be approximately represented by $CH_{1.8}O_{0.5}N_{0.2}$ (Jones & Kelly, 1983)
2. The carbon source is limited to CO_2
3. Energy for microbial growth, metabolic processes and cell maintenance is obtained solely from ferrous iron oxidation.
4. For planktonic micro-organisms, the production of extracellular polymeric substances (principally used for microbial attachment to mineral ore) is not significant (Ojumu *et al.*, 2008). Hence, it has been typically assumed that all CO_2 assimilation contributes to metabolically active cells.
5. All biomass formed is metabolically active
6. The continuous stirred tank bioreactor is operated at a steady state, meaning that flow rates and the concentrations in streams are time invariant over the sampling period.

As a result of Assumptions 1 and 2, the steady state biomass concentration can be determined as shown in Equation 5:

$$C_x = \frac{r_{CO_2}}{D}$$ **Equation 5**

where:

C_x	amount of carbon (as biomass) in the system	[mmol/l]
r_{CO_2}	rate of carbon dioxide utilisation	[mmol/(l.hr)]
D	bioreactor dilution rate	[1/hr]

Using stoichiometry, a degree of reduction balance and Assumption 3, the ferrous oxidation rate can be determined from the rates of carbon dioxide and oxygen utilisation shown in Equation 6, (the full derivation for this is shown in Appendix C). It can also be determined by performing a material balance over the bioreactor with respect to the ferrous iron, as shown in Equation 7.

$$-r_{Fe^{2+}} = -4r_{O_2} - 4.2r_{CO_2}$$ **Equation 6**

where:

$r_{Fe^{2+}}$	rate of ferrous iron oxidation	[mmol/(l.hr)]
r_{O_2}	rate of oxygen utilisation	[mmol/(l.hr)]
r_{CO_2}	rate of carbon dioxide utilisation	[mmol/(l.hr)]

$$-r_{Fe^{2+}} = D \cdot ([Fe^{2+}]_{inlet} - [Fe^{2+}]_{outlet})$$ **Equation 7**

where:

$r_{Fe^{2+}}$	rate of ferrous iron oxidation	[mmol/(l.hr)]
D	bioreactor dilution rate	[1/hr]
$[Fe^{2+}]_{inlet}$	concentration of ferrous iron in inlet	[mmol/l]
$[Fe^{2+}]_{outlet}$	concentration of ferrous iron in outlet	[mmol/l]

The substrate, carbon dioxide, is used for biomass growth and cell maintenance. The details of carbon utilisation are outlined in Section 2.9. The specific ferrous oxidation rate, defined as the rate of iron oxidation per mole of biomass (Equation 8), standardises the ferrous oxidation rate by quantifying it per unit of biomass and thus allows comparison across different culture conditions.

$$q_{Fe^{2+}} = \frac{-r_{Fe^{2+}}}{C_x}$$ **Equation 8**

where:

$q_{Fe^{2+}}$	specific iron utilisation rate	[mmolFe^{2+}/(mmolC.hr)]
$r_{Fe^{2+}}$	rate of ferrous iron oxidation	[mmol/(l.hr)]
C_x	amount of carbon (as biomass) in the system	[mmol/l]

The Monod Equation, proposed by Monod in 1949 and shown in Equation 9, relates the specific microbial growth rate to the concentration of limiting substrate. In this case, the limiting substrate is expected to be the ferrous iron concentration and thereby the provision of energy.

$$\mu = \frac{\mu_{max}[Fe^{2+}]}{K_{Fe^{2+}} + [Fe^{2+}]} \qquad \textbf{Equation 9}$$

where:

μ	specific microbial growth rate	[1/hr]
μ_{max}	maximum specific microbial growth rate	[1/hr]
$[Fe^{2+}]$	concentration of ferrous iron	[mmol/L]
$K_{Fe^{2+}}$	Monod constant (or affinity constant)	[mmol/L]

Pirt (1965) extended our understanding of microbial growth yields by modifying the simple yield relationships to include terms to account for endogenous respiration or energy used by cells. The rate of change of biomass in the system with respect to time, r_x, is given by μC_x assuming that cell death is negligible. The basic relationship is shown in Equation 10.

$$r_{Fe^{2+}} = \frac{1}{Y^{max}_{Fe^{2+}}} r_x + m_{Fe^{2+}} C_x \qquad \textbf{Equation 10}$$

where:

$r_{Fe^{2+}}$	rate of ferrous iron oxidation	[mmol/(l.hr)]
$Y^{max}_{Fe^{2+}}$	maximum growth yield on the ferrous iron	[mmolC/mmol Fe^{2+}]
r_x	rate of change of amount of carbon (as biomass) in the system over time	[mmol/(l.hr)]
$m_{Fe^{2+}}$	maintenance term	[mmolFe^{2+}/(mmolC.hr)]
C_x	amount of carbon (as biomass) in the system	[mmol/l]

The Pirt Equation is used to develop a new relationship for the specific ferrous oxidation rate according to Boon (1996) and Boon and Hansford (1997) to give Equation 11.

$$q_{Fe^{2+}} = \frac{\mu}{Y^{max}_{Fe^{2+}}} + m_{Fe^{2+}} \qquad \textbf{Equation 11}$$

where:

$q_{Fe^{2+}}$	specific iron utilisation rate	[mmolFe^{2+}/(mmolC.hr)]
μ	microbial growth rate	[1/hr]
$Y^{max}_{Fe^{2+}}$	maximum growth yield on the ferrous iron	[mmolC/mmol Fe^{2+}]
$m_{Fe^{2+}}$	maintenance term	[mmolFe^{2+}/(mmolC.hr)]

Using Equation 11, a plot of the specific ferrous oxidation rate as a function of the microbial growth rate is expected to give a linear correlation from which to determine the $Y_{Fe^{2+}}^{max}$ and the $m_{Fe^{2+}}$. The maintenance term is the metabolic energy needed to function without any growth and additional metabolic processes, derived from the specific rate of iron oxidation.

The rate of ferrous oxidation has been shown to be a function of the relative availability of ferrous iron and the oxidised ferrous iron. Hansford, with a number of co-workers (Boon et al., 1995; Breed & Hansford, 1999; Hansford, 1997; Hansford & Vargas, 2001) proposed that the specific ferrous oxidation rate can be described by the modified Michaelis-Menten kinetics where ferrous iron is the substrate and ferric iron the inhibitor. This is shown in Equation 12 in terms of the ferric: ferrous ratio, related to the redox potential.

$$q_{Fe^{2+}} = \frac{q_{Fe^{2+}}^{max}}{1+K'_{Fe^{2+}}\frac{[Fe^{3+}]}{[Fe^{2+}]}}$$ **Equation 12**

where:

$q_{Fe^{2+}}$	specific iron utilisation rate	[mmolFe^{2+}/(mmolC.hr)]
$q_{Fe^{2+}}^{max}$	maximum specific ferrous oxidation rate	[mmolFe^{2+}/(mmolC.hr)]
$K'_{Fe^{2+}}$	apparent affinity constant (modified by inhibition constant)	[-]
$\frac{[Fe^{3+}]}{[Fe^{2+}]}$	ratio of the concentration of ferric iron to ferrous	[-]

The $q_{Fe^{2+}}^{max}$ and the $K'_{Fe^{2+}}$ can be determined using a Lineweaver-Burke plot, or the Hanes plot. It is well recognised that the former is biased by overemphasising data collected at very low substrate concentrations leading to increased error. The latter is more appropriate as it keeps the substrate concentration in the numerator. A square error minimisation technique which reduces bias was used by Ojumu (2008) to calculate the same parameters. The ratio of ferric: ferrous iron is a very important measured parameter in ferrous oxidation rate studies. It is closely linked to the redox potential and is discussed in Section 2.6.

2.6 Reduction-oxidation potential and ionic strength

The rate laws given in Section 2.5 predict that the rate of microbial ferrous oxidation is a function of the ratio of ferrous iron concentration (energy source) to the ferric iron concentration (inhibitor) in the system. The solution potential, or redox potential, is indicative of this ratio.

Redox potential is "the tendency of a chemical species to acquire electrons and therefore be reduced" (Ebbing, 1993). In aqueous solutions, a more positive redox potential means that the solution will have a tendency to gain electrons from the new species introduced (i.e. to be oxidised by reducing the new species). In this way, it is expected that ferric iron (aq) will have a higher solution potential than ferrous iron (aq). Standard solution potential is measured in volts (V) and is defined relative to a standard

hydrogen electrode as Eh. In experimental work, it is often more convenient to choose a silver-silver chloride electrode as a reference electrode, resulting in a redox potential measurement according to the scheme below Shiers *et al.* (2005):

Ag | AgCl(satKCL) || H_2SO_4 (pH 1.50) || Fe^{3+}/Fe^{2+}(pH1.50) | Pt

In the above system, the redox potential for a ferric: ferrous iron ratio of 1000 and 1 are 670 and 490 mV respectively. To obtain the values for the solution potential relative to a standard hydrogen electrode, the value is increased by 222 mV (the solution potential of the silver-silver chloride system relative to a standard hydrogen electrode). The oxidation ability of the micro-organisms is dependent on the reduction potential of its environment (Boon, 1996). Strictly aerobic micro-organisms can only be active at positive redox potentials. Changes in the ratio of the concentration of ferrous iron to ferric iron and thus, changes in the solution potential are used to measure the level of oxidation by the microorganisms.

In industrial bioleaching operations, the redox measurements taken are chiefly used as an indication of the ferric: ferrous iron ratio even though this is also affected slightly by the molalities of other ions in solution. This is shown in Equation 13, the Nernst Equation:

$$E = E_0 + \frac{RT}{nF} ln\left(\frac{\prod_i a_i}{\prod_i a_i}\right) \qquad \textbf{Equation 13}$$

$$E_0 = \frac{\Delta G^0}{nF} \qquad \textbf{Equation 14}$$

where:

E	solution potential	[mV]
E_0	solution potential at standard state	[mV]
ΔG^0	change in Gibbs free energy, std conditions	[J/mol]
n	number of electrons transferred	[-]
F	Faraday constant	[9.649 C/mol]
$\boldsymbol{R}$	universal gas constant	[8.3145 J/(mol.K)]
T	temperature	[K]
a_i	chemical activity of relevant species *i*	[mol/dm^3]

Equation 13 shows that the solution potential is dependent upon both temperature and the ionic strength through the chemical activity. In a ferrous iron feed solution, iron is the major contributor towards the ionic strength. However, in typical bioleaching operations, other ions are also liberated from the gangue during the acid leaching stage and subsequent stages, and recycled through the metal extraction phase. These may affect the activity of the bioleaching micro-organisms as well as the solution potential. Dissolution of the gangue minerals, such as dissolution of aluminium and magnesium as they are major

constituents of gangue, increases the ionic strength of the solution. The ionic strength of a solution can be calculated assuming ideal behaviour using Equation 15.

$$I_m = \frac{1}{2}\sum_{i=1}^{n} c_i \cdot z_i^2 \qquad \text{Equation 15}$$

where;

I_m	ionic strength	[mol/dm^3]
c_i	concentration of species *i*	[mol/dm^3]
z_i	ionic charge of species *i*	[-]

The concentration of ions in the solution has been shown to affect the activity of micro-organisms (Shiers *et al.*, 2005; Ojumu *et al.*, 2008). In addressing the mechanism of action, one hypothesis is that the micro-organisms use energy to make organic compounds (i.e. proteins) which counteract the increased ionic strength and hence osmotic pressure in the solution. Hence, less carbon is converted to active biomass and a lower microbial growth rate results (Ojumu *et al.*, 2008). Active transport of specific metals out of the cells may also occur. To date it has been suggested that the quality of the process water is the industrial process limitation on cell growth and thus productivity (Blight & Ralph, 2003). However, the influence of ionic strength on the bio-oxidation process is not yet fully understood. It has been hypothesised that the ionic strength has an inhibitory effect on the growth and therefore oxidation ability of these cultures. This implies that high concentrations of metal ion impurities may limit the bioleaching process and a better understanding of the inhibiting effects may lead to an improvement in the process. The effect of chloride ions has been shown to improve the dissolution of chalcopyrite at mesophilic temperatures, but inhibit dissolution at lower (but still mesophilic) temperatures (Kinnunen and Puhakka, 2004). Shiers et al. (2005) showed that although it may improve dissolution, chloride ions are inhibitory to microbial growth and concentrations of 7 g/L NaCl reduced cell replication by up to 50%.

2.7 Energetics of bioleaching micro-organisms

Bioenergetics of bioleaching has been investigated since the early 1980's, at which time, *Acidithiobacillus ferrooxidans* (formerly known as *Thiobacillus ferrooxidans*) was considered the key micro-organism in bioleaching. Ingledew (1982) developed the Mitchell model of electron transfer (developed in 1966), and applied it to *At. ferrooxidans*. This model is applicable to other ferrous oxidising bacteria and archaea including the obligate ferrous oxidiser, *Leptospirillum ferriphilum* (Levicán *et al.*, 2008). The simplified reaction is shown in Equation 16:

$$2\,Fe^{2+} + \tfrac{1}{2}\,O_2 + 2\,H^+ \rightarrow 2\,Fe^{3+} + H_2O + Energy \qquad \text{Equation 16}$$

The energy released can be calculated using the Nernst Equation (Equation 13) and an E^0 value of -350 mV (in Equation 14). The very electropositive reduction potential of the Fe^{3+}/Fe^{2+} couple (+770 mV at pH 2) makes it a tangible energy source. This is the energy source that ferrous oxidising micro-organisms tap

into using an electron transport system to transfer energy and eventually store it as adenosine triphosphate (ATP). ATP is a universal energy carrier and used as measure of energy in all living organisms.

Thermodynamically, it was estimated by Ingledew (1982) that:

$ADP + P^i \rightarrow ATP$	$\Delta G = -8.1$ kcal/mol	Equation 17
$Fe^{2+} \rightarrow Fe^{3+} + e^-$	$\Delta G = +16$ kcal/mol	Equation 18
$NAD(P)^+ + H_2 \rightarrow NAD(P)H + H^+$	$\Delta G = +25$ kcal/mol	Equation 19

It was estimated that approximately 2 moles of Fe^{2+} must be oxidised to produce the energy required to form 1 mol of ATP.

It has been found that in such ferrous oxidising bioleach micro-organisms, the respiratory chain contains cytochromes of the *c* and *a* type and a periplasmic copper containing protein called rusticyanin (Cavazza *et al.*, 1995) involved in the energy harnessing process. The primary electron acceptor is the protein *Cyc2* in the outer membrane which passes the electron to rusticyanin as shown in Figure 2-5. It is accepted that rusticyanin plays an essential role in the electron transfer pathway from Fe^{2+} (Bonnefoy *et al.*, 2003). Furthermore, the presence or absence of iron has been proposed to closely regulate the levels of rusticyanin inside the cell (Rawlings, 2005).

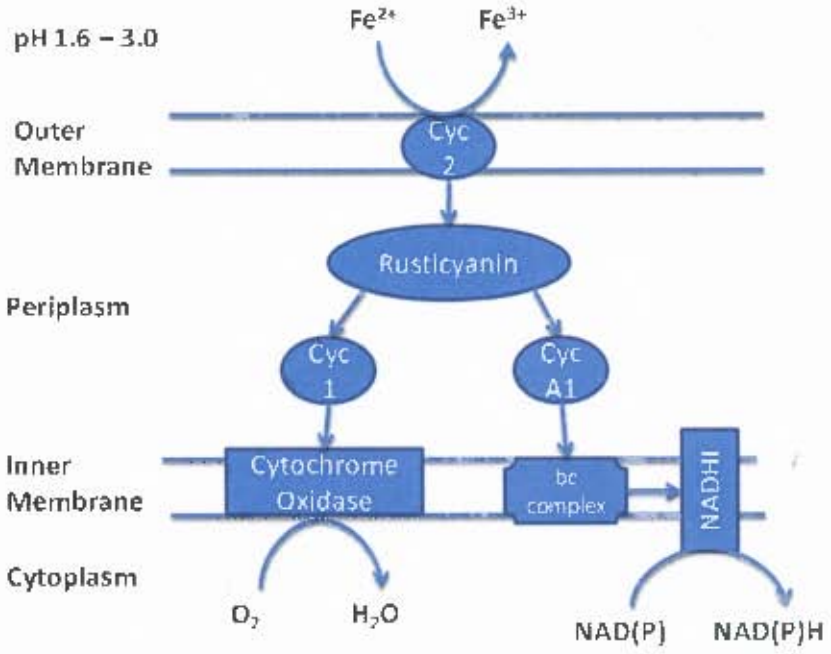

Figure 2-5. Forward and reverse electron transport chain in *At. ferrooxidans* (adapted from Appia-Ayme *et al.*, 2006a)

Figure 2-5 shows that there are two possible pathways for electron transport. Primarily, forward electron transport chain via cytochrome oxidase (an inner membrane protein), ultimately transfers the electron, combined with a proton to oxygen to form a water molecule. The route of electron transfer to water is short, passing the electron from rusticyanin to cytochrome oxidase via *Cyc1* in the periplasm (Rawlings, 2005). The influx of protons from the extracellular environment to bind to the oxygen molecule takes place through the ATP pump, generating energy stored as ATP. Since the external pH (typically between 1.6 and 3.0) is much lower than the internal pH (typically between 6.5 and 7.0), there is a natural proton gradient. The consumption of these protons within the cell also maintains this gradient. Thus, in the presence of ferrous iron and the electron transfer proteins, ATP synthesis can occur largely by the proton motor force.

There also exists the reverse electron transport chain which is used to form NAD(P)H (usually a substrate in the electron transport chain) via Ubiquinone (a small lipid-soluble compound). The necessity of the reverse electron transport chain results from the fact that NAD(P)H is a widely required substrate in anabolic metabolic processes. NAD(P)H can also enter a process known as oxidative phosphorylation cycle to transfer energy and store it as ATP.

The ATP produced is used in metabolic processes, such as carbon dioxide fixation and cell maintenance. Carbon dioxide is fixed using RuBisCO in the Calvin cycle. It is important to note that the reverse electron transport chain generates the NAD(P)H necessary for CO_2 uptake via the reverse electron transport chain. The fixation of 1 mole of CO_2 requires 3 mol of ATP and 2 moles of NAD(P)H (Ingledew, 1981). Thermodynamically, it can be calculated that 22.4 moles of ferrous iron are needed to fix 1 mole of carbon dioxide, corresponding to a maximum theoretical yield is 0.54 g carbon/mol Fe^{2+} (Ingledew, 1982). Measured values have been about half of the maximum theoretical value as the energy produced is also used for maintenance and other metabolic processes (Tuovinen and Kelly, 1972; Beck 1960). The details of the Calvin cycle, carbon dioxide fixation and the carbon use in bioleaching micro-organisms are discussed in Section 2.8.

2.8 Carbon uptake and utilisation in bioleaching micro-organisms

Obligate chemolithoautotrophic micro-organisms use atmospheric carbon dioxide as their carbon source. In the case of bioleaching of sulphide minerals, the micro-organisms utilise the energy and the reducing power derived from the oxidation of iron or sulphur oxidation or both for the carbon dioxide fixation, among other metabolic processes (Levicán *et al.*, 2008). Most genetic and metabolic pathway studies have been performed on *At. ferroxidans*. It is only recently that focus has been shifted to *Leptospirillum*. Since *At. ferrooxidans* has been the most widely researched and documented, research has mostly continued with this strain. In *At. ferrooxidans* and *At. thiooxidans*, the CO_2 fixation occurs via the Calvin cycle. While *L. ferriphilum* grows autotrophically, the molecular mechanisms involved in carbon fixation remain obscure (Valdes *et al.*, 2008).

The Calvin cycle is composed of 13 enzymatic reactions, 12 of which are involved in regeneration on ribulose 1,5-bisphosphate (RuBP) and one which is responsible for the CO_2 fixation catalysed by ribulose 1,5 bisphosphate carboxylase/oxygenase (RuBisCO). The processes in the Calvin cycle in *At. ferrooxidans* are outlined in Figure 2.6. As can be seen, the carbon fixing process utilises the ATP generated from the forward electron transport chain, as well as the NADPH generated via the reverse electron transport chain.

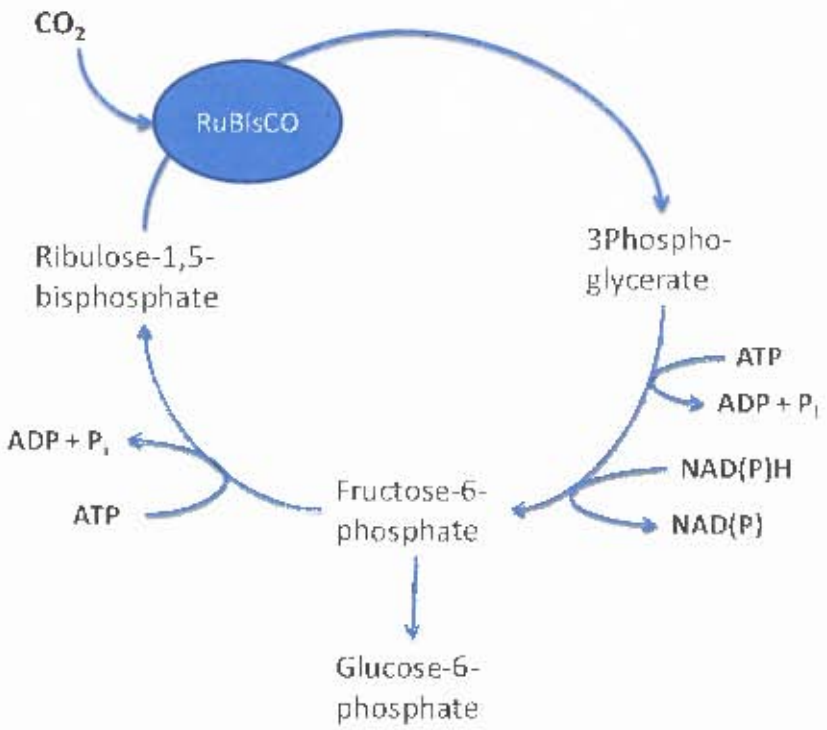

Figure 2.6. Carbon pathway in the Calvin cycle in *At. ferrooxidans* (adapted from Appia-Ayme *et al.*, 2006b)

The genes encoding for the key enzymes were identified in *Acidithiobacillus* (Levicán *et al.*, 2008) but not in *Leptospirillum* species. The absence of canonical enzymes of the Calvin cycle in *Leptospirillum* suggested the existence of an alternate mechanism for CO_2 fixation. The reductive tricarboxilic acid (RTCA) cycle is essentially the TCA cycle running in reverse. This also leads to the fixation of two molecules of carbon dioxide and the production of acetyl-CoA, which in turn is reduced by carboxylation to pyruvate (Levicán *et al.*, 2008). The key enzymes needed for the RTCA cycle are all present in the *Leptospirillum* genome and the presence of such is indicative of this being the carbon fixation mechanism for *L. ferriphilum*. The tricarboxilic acid (TCA) cycle moving in the forward direction in an oxidative manner is more commonly known as the Citric Acid cycle or the Krebs cycle. It is unlikely that the oxidative cycle takes place as the genes coding for 2-oxoglutarate dehydrogenase, a key enzyme in the oxidative cycle were not found in the gene search by Levicán *et al.*, (2008).

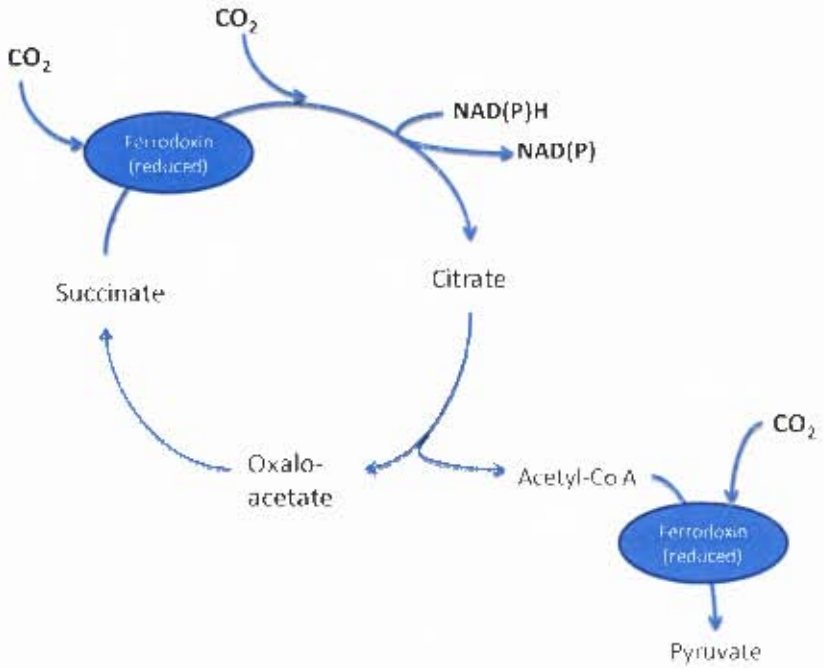

Figure 2-7. Carbon pathway in the reductive tricarboxilic acid cycle in *L. ferriphillum* (adapted from Levicán *et al.*, 2008)

Although less common, there are also other CO_2 fixation mechanisms besides the Calvin cycle and the RTCA, namely the 3-hydroxypionate cycle and the reductive acetyl-CoA cycle (Hügler *et al.*, 2003). These mechanisms are more commonly found in archaea and no genes coding for the key enzymes in either of these two cycles were found in *L. ferriphilum* (Levicán *et al.*, 2008). The study by Levicán *et al.* in 2008 was the first evidence of the RTCA cycle being the autotrophic carbon fixation mechanism found in *L. ferriphilum*. Until then it was assumed that *Leptospirillum* used the same Calvin Cycle found in *Acidithiobacilli*.

In acidic bioleaching environments, dissolved inorganic carbon can reach levels below the atmospheric concentration average. Therefore, it is not surprising that CO_2 concentrating mechanisms have been identified in autotrophic prokaryotes present in such environments (Dobrinski *et al.*, 2005). Carbon concentrating mechanisms (CCM's) can facilitate the rapid autotrophic growth in environments where the CO_2/HCO_3^- concentrations are chronically or episodically low, by using active HCO_3^- transport (Omata *et al.*, 1999) or CO_2 traps (Shibata *et al.*, 2002). Carboxysomal carbonic anhydrase converts intracellular HCO_3^- to CO_2 which is fixed by RuBisCO. The elevated intracellular concentrations of dissolved inorganic carbon resulting from active transport expedite the carbon fixation by RuBisCO by enhancing substrate availability and mitigating the RuBisCO oxygenase reaction (Dobrinski *et al.*, 2005). There is also the possibility for carbon to be provided from carbonate ions (leached from ore) in the aqueous environment. These phenomena are outside the scope of this research project. The carbon absorbed is channeled into biomass growth extracellular organic compounds and cell maintenance. The carbon partitioning in

bioleach micro-organisms is further discussed in Section 2.11. Further insight into carbon dioxide provision in related studies is provided in Section 2.9.

2.9 The effect of carbon dioxide provision and availability on bioleaching

Carbon dioxide has a low solubility in aqueous solution. This is further reduced by an increase in acidity and an increase in temperature. Reduction in solubility with temperature is common for all gases, but the significance of pH is not a universal trend. Carbon dioxide reacts with water to form several ionic and non-ionic species, in the following way:

$$CO_{2\,(aq)} + H_2O \Leftrightarrow H_2CO_3 \Leftrightarrow HCO_3^- + H^+ \Leftrightarrow CO_3^{2-} + 2H^+$$

Table 2-2 shows the solubility of carbon dioxide as a function of pH. The data is calculated based on pK_a values at 25°C and 1 atmosphere, and is a function of the Henry's Law solubility and the partial pressure of CO_2 in the air above the water. Due to a low solubility of oxygen and carbon dioxide, gas-liquid transfer limitation has been identified as a key limiting factor in bioleaching efficiency (d'Hughes *et al.*, 2002), especially in a rapidly operating bio-oxidation system. For this reason, carbon dioxide enrichment has been practiced in some tank leaching operations to improve bioleaching performance, especially at elevated temperature where gas solubilities are further reduced. Understanding the solubility and the equilibrium (based on thermodynamics and experimental data) between the gas and liquid phase are important since the solubility of carbon dioxide may become the rate limiting step in microbial growth dynamics. The solubility is relatively constant between pH 1 and pH 3, which are typical bioleaching operating conditions.

Table 2-2. Effect of pH on carbon dioxide solubility

pH []	dissolved CO_2 concentration [moles/L]
1	1.20×10^{-5}
2	1.20×10^{-5}
3	1.20×10^{-5}
4	1.21×10^{-5}
5	1.25×10^{-5}
6	1.73×10^{-5}
7	6.54×10^{-5}
8	5.49×10^{-4}
9	5.60×10^{-3}
10	7.85×10^{-2}
11	3.04×10^{0}

Work has been done to date by Crundwell (1997), du Plessis *et al.* (2001), Lizama et al. (2002) and de Kock *et al.* (2004) on respirometric methods, carbon dioxide and oxygen kinetic challenges and the assimilation, but limited work is reported to date on the effect of carbon dioxide concentration on the growth and activity of the *L. ferriphillum* which is accepted as the dominant mesophile in tank leaching in South Africa. In 1992, Haddadin *et al.* performed experiments at mesophilic temperatures on three different microbial populations in batch culture. They showed that there was an optimum carbon dioxide concentration in

the sparge gas for the growth of the one particular microbial population but did not give details of the microbial populations used, but later acknowledged as *Thiobacillus spp.* responsible for the ferrous iron and pyrite oxidation, and found this to be 2%, in two different media. Previously, in 1987, Holuige *et al.* showed that the growth and activity of *At. ferrooxidans* increased fourfold with an increase of CO_2 concentration from 0.03% to 0.06 % in the feed gas, with no further increase in growth with an increase to 0.35%. Beyond this point, there was even a decrease in the growth rate when the CO_2 concentrations reached 5.4%. Baron and Lucking (1990) investigated a different range of concentrations, but also reported an optimum concentration of 7% to 8% in the gas phase for a *Thiobacillus sp.* after which the effect became inhibitory. The differences in the optimum gaseous concentrations reported can be attributed to differences in the mass transfer approaches used and may also be a function of the microbial species used, which were incompletely classified.

Witne & Philips (2000) performed a study in leaching tanks with mixed mesophilic cultures. They increased the carbon dioxide concentration in the sparge gas and found an increase in leaching performance of between 10% and 15%. Since the study was focused on leaching performance, the microbial population was not monitored. It was assumed that in increase in carbon dioxide meant an increase in microbial population, but this assumption was not verified. Bouffard and Dixon (2002) ran a set of columns at 0.03% carbon dioxide enrichment in the air inlet. They found no improvement in leaching performance and no increase in biomass (measured by planktonic cell counts). They theorized that the carbon dioxide concentration was thus not relevant in their particular study at ambient conditions but might become important under other operating conditions.

2.10 Mass transfer in bioleaching

There are obvious mass and heat transfer profiles in heap and tank leaching. Tank leaching provides a better mixed system to overcome some of the mass transfer limitations encountered by irrigation-type leaching (Rawlings, 1997). Energy transport within the heap determines temperature profiles and affects the dominance of certain populations of microbes. Mass transport encompasses the transport of ferrous iron to microbes at the mineral surface, the gas-liquid mass transfer of oxygen and carbon dioxide, and the dissolution and transport of the leach solution out of the heap. The key processes and sub-processes in bioleaching which highlight the importance of mass transfer on the corresponding scales are shown in Table 2-3.

In heap leaching, gas-liquid mass transfer appears on the aggregate scale and is usually the rate limiting step in all systems. Boon and Heijnen (1997) examined whether gas-liquid mass transfer of oxygen or carbon dioxide has determined the bacterial oxidation rate of sulphide minerals. The maximum oxygen and carbon dioxide transfer rates were estimated for reported kinetic experiments with pyrite and compared with estimated maximum oxygen and carbon dioxide consumption rates reported in these experiments. It was concluded that carbon dioxide mass transfer limitation and exhaustion of carbon dioxide in the gas phase often occurred (Boon and Heijnen, 1997). It was then postulated that the decrease of bacterial oxidation at increasing slurry densities was probably caused by carbon dioxide limitation.

Table 2-3. Schematic representation of sub-processes in heap bioleaching (adapted from Dixon and Petersen, 2003)

Level	Sub-Processes	Illustration
Heap Scale	Solution Flow Through Packed Bed Gas Advection Water Vapour Transport Heat Balance	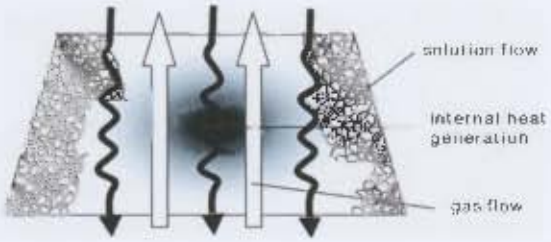
Aggregate Scale	Gas Absorption Particle Diffusion Microbial Growth Microbial Attachment Microbial Oxidation	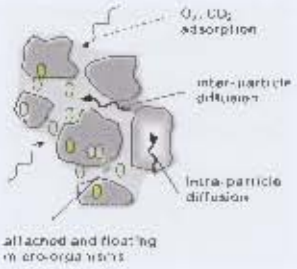
Particle Scale	Topological Effects Intra-particle Diffusion Particle and Grain Size Distribution	
Grain Scale	Ferric/Ferrous Reduction Mineral Oxidation Sulphur Oxidation Surface Processes	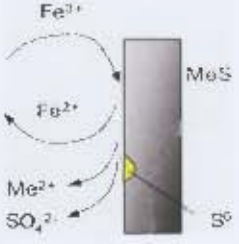

The product of the saturation concentration and volumetric mass transfer coefficient, K_La, quantifies the rate of gas-liquid mass transfer (Bailey & Ollis, 1986). In stirred tank biooxidation, K_La is affected by many parameters. Increasing gas flow rate and mixing intensity increase the K_La. Increase in the partial pressure of the gas through either increasing total pressure or gas enrichment, increases the saturation concentration. Increasing salt concentration has the opposite effect on both the K_La and the saturation concentration. The K_La for oxygen transfer increases with an increase in temperature even though the solubility of oxygen in aqueous systems and the saturation concentration decrease with an increase in temperature (Kaskila, 2005). Although there is an obvious need to improve gas-liquid mass transfer, the heap leaching system is largely pre-defined and leaves little scope for modifying K_La. Work has been done by Petersen (2010) on the gas-liquid mass transfer of oxygen in heap leaching systems. Even in tank leaching systems, increasing agitation and gas flow becomes energy intensive. Hence, most typically, gas

enrichment Is proposed to overcome gas-liquid mass transfer limitations in these systems. A novel approach was introduced with the advent of sono-bioleaching which claimed to improve mass transfer by assisting the dispersion of gas passing through the slurry and liquid phase turbulence near the surface of the gas bubble (Swamy *et al.*, 2004). It was also claimed that there would be increase in solid-liquid transport of nutrients to the cells.

2.11 Carbon partitioning in bioleaching micro-organism

It has been established that most carbon taken up by bioleaching microbes is used in the formation of new active biomass, either in growth or in production of new cells. Some organic compounds, especially EPS (extracellular polymeric substances) which serve as a microenvironment in which the ferric iron concentration is much higher than in the bulk solution, are also produced by *L. ferriphilum* (Crundwell, 1996, Florian *et al.*, 2010) and facilitate the attachment of micro-organisms to solid surfaces. Chemical analysis of the EPS of *At. ferrooxidans*, *At. thiooxidans* and *L. ferriphilum* indicate neutral sugars, fatty acids and uronic acids the composition of which changes with strain and growth substrate (Harneit et al., 2006). However, the production of EPS is not expected to be significant in planktonic micro-organisms as there is no solid surface to attach to and therefore no biofilm needed for attachment. *At. ferrooxidans* is also known to produce extracellular organic monomers, such as pyruvate (Valdês *et al.*, 2008)) and it is postulated that *L. ferriphilum* produce similar extracellular organic monomers (EOM). It is expected that the carbon utilisation and therefore, the partitioning of carbon flux in the cells changes depending on the conditions to which they are subjected e.g. the presence or absence of a solid phase. Under stressful conditions, microbes may modify the spectrum and levels of proteins expressed in response to conditions imposed. There are two approaches to this phenomenon outlined as follows:

- The first states that proteins are induced as they are needed, thus carbon concentrating proteins may be expressed when the carbon dioxide availability is limited. This prevents the unnecessary expenditure of energy.
- The second approach suggests that there a general stress response protein produced by cells.

These both remain to be investigated and qualified.

2.12 A comparison of planktonic and sessile populations

Micro-organisms involved in bioleaching form biofilms when they attach to solid surfaces (typically mineral). It is hypothesised that these biofilms are tailored to increase ferrous oxidation rate by concentrating the ferric iron through complexation (Kinzler *et al.*, 2003). Cells in the biofilm are referred to as attached or sessile. However, in microbial kinetic studies to date, cells have been suspended in an aqueous solution containing nutrients. These are referred to as planktonic populations and are thought to perform at much higher oxidation rates since there is a reduction of mass transfer limitations in the type of system and an increased supply of substrates (Kinnunen and Puhakka, 2005). The activity of planktonic and sessile cells has not been directly compared and contrasted in bioleaching operations. Kinnunen and Puhakka have shown that micro-organisms can attach to a non-mineral surface and form a biofilm. They used this to provide high rate ferrous iron oxidation, in the presence of activated carbon as a solid support.

2.13 Key issues raised

The following points highlight the gaps in knowledge identified through the review of the literature presented and pose the key questions on which this study is focused.

- In the analysis of biokinetic data, it is assumed that the carbon dioxide uptake rate is proportional to the microbial growth rate and the ferrous iron oxidation rate under ideal growth conditions. The following questions arise:
    - with respect to the ferrous oxidation rate and the carbon dioxide uptake rate:
        1. Is this relationship between the ferrous iron oxidation rate and the carbon dioxide uptake rate always in the same ratio?
        2. Is there a concentration of carbon dioxide at which the relationship breaks down and what would be the cause of it?
    - with respect to the ferrous oxidation rate and the microbial growth rate:
        3. Is this relationship between the activity (specific ferrous iron oxidation rate) and the growth rate constant across a broad range of carbon dioxide concentrations, including very low concentrations?
    - and with respect to the carbon dioxide uptake and utilisation:
        4. Is the carbon dioxide uptake rate proportional to biomass formed (active or inactive)?
        5. Is the carbon assimilation converted to active biomass or does the proportion converted to extracellular organic material vary?
        6. Is there a minimum concentration of carbon dioxide below which the growth is hampered and the biomass yield is affected?

- There is limited comparison between the activity of sessile populations and planktonic populations. Some of the questions which arise include:
    1. Is the sessile population as active as the planktonic population?
    2. How does the carbon utilisation differ between the two populations?
    3. Can the activity, growth and carbon dioxide uptake rates of the sessile population be accurately quantified and qualified by the same experiments as performed on the planktonic population?

3. Experimental Approach

In summation of Section 2.13, three key questions are raised with the following hypotheses:

- Firstly, what is the relationship between the ferrous oxidation rate as a function of the carbon dioxide concentration? It is hypothesised that the relationship will vary as a function of physical conditions, in this case, the range of carbon dioxide concentrations as long as the carbon dioxide taken up is used in the formation of active biomass.
- Secondly, what is the effect of the carbon dioxide concentration on the activity of sessile and planktonic bacterial populations? It is hypothesised that the effects will be the same on both populations; a decrease in availability of carbon dioxide arises in an increase in the specific ferrous oxidation rate.
- Thirdly, what is the carbon partitioning within these different populations under these different conditions? It is hypothesised that the carbon partitioning changes across the range of carbon dioxide concentrations with the possibility of the production of stress proteins or carbon concentrating proteins at lower carbon dioxide availability. It is also theorised that there will be more carbon used for the production of extracellular organic substances with the introduction of a sessile population.

The most direct way to address these is to perform a continuous culture rate study, to determine the ferrous oxidation rates and microbial oxidation rates at various dilution rates and carbon dioxide concentrations in the sparge gas. A continuous stirred tank reactor is the most apt apparatus to measure these rates over a period of time owing to the ability to develop steady state or pseudo-steady state environments. Using a ferrous iron feed in the absence of mineral, the ferrous oxidation rate can be calculated by performing an iron balance over the reactor. Similarly, gaseous uptake rates can be calculated by the mass balance approach.

L. ferriphilum has been identified as a dominant mesophile in tank leaching operations and an important organism in the mesophilic stage of heap leaching. It is also an obligate ferrous iron oxidiser, meaning that energetic calculations are simplified as the sulphur reactions can be ignored. *L. ferriphilum* is therefore a most suitable and obvious choice for this novel study.

The system is designed to better understand the behaviour of micro-organisms in heap and tank bioleaching operations. Under typical heap leaching conditions, the carbon dioxide concentration is at atmospheric concentration and below (unless the systems are enriched in the air supply or contain carbonate in the ore). The atmospheric carbon dioxide is circa 390 ppm, and so the gaseous carbon dioxide range used is 0 ppm to 500 ppm. Concentrations lower than 390 ppm provide insight into carbon dioxide starved areas, and those higher indicate the potential benefit of carbon dioxide enrichment. Typical heap leaching operations have a soluble total iron concentration of 2 to 3 g/L in the effluent (Watling, 2008). Accounting for precipitation at higher pH values, the system was supplied with a soluble ferrous iron concentration of 5 g/l to ensure that the system was not ferrous iron limited. This concentration was also chosen for comparison of bio-oxidation experiments performed by Ojumu *et al.* (2008). Washout in the CSTR for the *L. ferriphilum* culture at 5 g/l occurs at a residence time of 14 hrs. Therefore the residence times investigated were in the range of 15 hrs to 55 hrs. The gas entering the CSTR was scrubbed with various concentrations of NaOH(aq) to lower the carbon dioxide concentration below atmospheric concentrations.

To create a sessile population, there was the need for an inert solid support which would not affect the iron balance or the carbon balance over the reactor. Ceramic saddles were used as a support in this study and were arranged in a packed bed column reactor coupled to the CSTR with very rapid liquid recycle between these. Other materials used for this investigation and the set-up of the experiments are discussed below.

3.1 Materials used in experimental set-up

A diagrammatic representation of the basic experimental rig used is shown in Figure 3-1 and schematically in Figure 3-4. Two litre jacketed Applikon® autoclavable bioreactors with a working volume of 1L were used for chemostat culture of *L. ferriphilum*. Water, pre-warmed to 37 °C in a Grant constant temperature bath, was circulated in the jacket, maintaining a constant temperature of 37 °C in the reactor. The contents of the reactor were agitated by a pitched 45° four blade turbine impeller connected to a P100 (ADI 1032) stirrer controller rotating at 400 rpm. Pumping is performed by a Masterflex® consol drive, using L/S™ 7013/20 standard pump heads and L/S™ 13 Norprene® food tubing for the feed, and L/S™ 7014/20 standard pump heads and L/S™ 14 Norprene® food tubing for the effluent.

Sparge gas is supplied by a Peak Scientific OAG2000DA gas compressor, and controlled by a Brooks Model 5505 mass flow controller and Brooks model 0154 microprocessor. A reflux condenser circulating ethylene glycol from a low temperature bath was attached to the bioreactor to dry the off-gas by cooling to 2°C before entering the gas analysers (Hartmann & Braun, Magnos 6G and Uras 4).

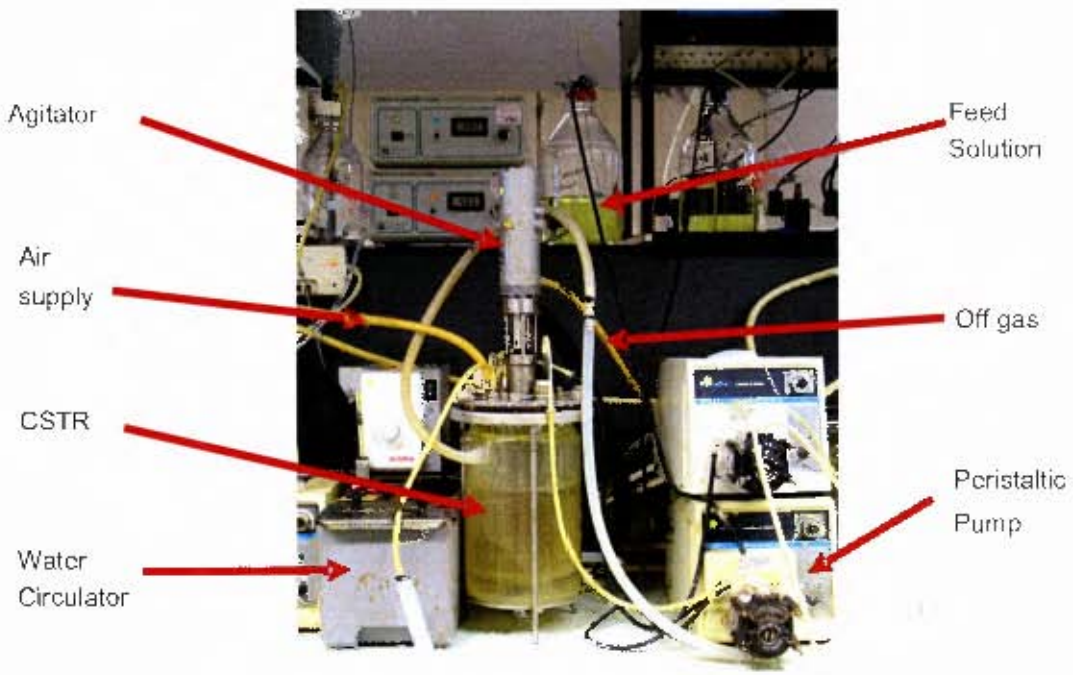

Figure 3-1. Photographic representation of reactor setup

3.2 Microbial culture

3.2.1 Choice of microbial culture

Although there have been many studies on pure cultures, it is well known that all industrial operations involve mixed cultures. Investigations into pure culture systems are done to determine the properties of a particular micro-organism and relate it to the bioleaching operation as a sub-process. Through characterisation of pure cultures and typical operating conditions, the mixed culture dynamics may be better predicted. For this study, *L. ferriphilum* was the micro-organism of choice. The reasons for this choice are outlined below.

L. ferriphilum is naturally occurring, most commonly associated with pyrite. More recent studies (Kinnunen & Puhakka, 2005; Dopson *et al.*, 2003; Okibe *et al.*, 2003) have shown that *Leptospirillum* is clearly more dominant in certain bioleach operations than its *At. ferrooxidans* counterpart. The species *Leptospirillum ferriphilum* sp. nov. was identified to be the dominant ferrous iron oxidising species after isolation of all ferrous iron oxidising species in a biooxidation plant in Barberton, South Africa (Coram & Rawlings, 2002). It is least inhibited by the high ferric: ferrous iron ratio and consequently a high redox potential, commonly found in tank leaching environments and certain irrigation-type systems (Rawlings *et al.*, 1999). Experimentally, this is advantageous as investigations can be carried out in continuous stirred tank reactors (CSTRs). The conditions in the CSTR are the same as the conditions of the outlet stream. In this case, the outlet stream has an extremely high ferric iron concentration as the iron oxidizing micro organisms convert ferrous iron to ferric iron by Equation 2. CSTRs are also best suited to maintaining steady state conditions allowing the generation of kinetic data under clearly specified conditions.

L. ferriphilum is an obligate chemolithotroph, using CO_2 as its carbon source and only ferrous iron as its energy source. It does not oxidise inorganic sulphur, or depend on the presence of sulphur for its growth. The ferrous iron is the electron donor and the electron acceptor is O_2. Experimentally, measuring the CO_2 uptake rate gives an indication of the metabolic growth rate, and measuring the oxygen uptake rate gives an indication of the ferrous oxidation rate.

3.2.2 Microbial culture used

The microbial species used was originally obtained from a vat-type two-stage (2x20 dm^3) continuous bioleaching mini plant treating a pyrite arsenopyrite concentrate, from Fairview, Barberton, South Africa. Prolonged exposure to leaching at elevated redox potential resulted in selection for *L. ferriphilum*. The stock culture was maintained on 5 g/L ferrous feed at a residence time of 72 hours.

No solutions were sterilised (either by filtration or autoclaving). Morphology checks of bacterial culture were done with each cell count, to ensure that the culture was dominantly spirilla (i.e. *Leptospirillum*) and any data from runs where rods (possibly *At. ferrooxidans*) were copious was not used. Visual checks for fungus in the reactor feed and effluent were performed. Before the commencement of experiments, DNA was extracted from a sample of the culture. The 16s rRNA gene was amplified using universal

primers and sequenced to confirm homology. The strain was found to have a >98% sequence homology to *Leptospirillum ferriphilum*.

3.3 Growth medium

All experiments were conducted with analytical grade reagents. The ferrous iron feed solution was prepared at 5 g/L with $FeSO_4.7H_2O$. The salt was added to a basal salts media consisting of 1.11 g/l of K_2SO_4, 0.53 g/L $(NH_4)_2HPO_4$, 1.83 g/L of $(NH_4)_2SO_4$ and 10 mL/L of Vishniac Trace Elements Solution (Vishniac & Santer,1957).

The Vishniac solution is prepared by dissolving 15 g/L EDTA in 6% KOH solution and adding 1 g/L $ZnSO_4.2H_2O$, 1.0 g/L $CoCl_2.6H_2O$, 1.0 g/L $MnCl_2.4H_2O$, 0.5 g/L $CuSO_4.2H_2O$, 5.0 g/L $FeSO_4.7H_2O$, 0.5 g/L $Na_2MoO_4.2H_2O$ and 0.5 g/L $CaCl_2.2H_2O$ one at a time.

The same growth medium was used for all experiments. The medium was prepared with de-ionised H_2O in 25 L batches and was kept chilled in a 4 °C refrigerator until needed. The medium was removed in 1 to 2 litre aliquots and pH adjusted before use as fresh feed.

The pH of the final solution is adjusted by adding conc. H_2SO_4. Usually, approximately 4 ml H_2SO_4 (conc.)/L solution is added to achieve a pH of 1.1, the starting pH of the feed for all runs.

3.4 Feed gas preparation

3.4.1 Previous work on feed gas preparation

To reduce the amount of carbon dioxide entering the bioreactor, the carbon dioxide was scrubbed out of the compressed air. There have been some studies where the carbon dioxide concentration had been enriched (Witne and Phillips, 2000; Bouffard and Dixon, 2002). The enrichment system is shown in Figure 3-2.

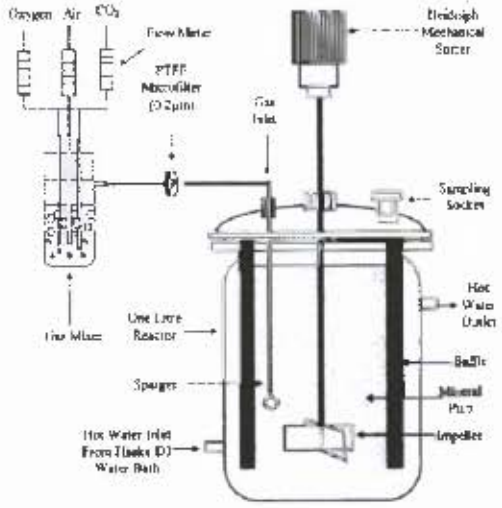

Figure 3-2. System for carbon dioxide enrichment to a bioreactor (taken from Witne and Phillips, 2000)

This was the principle on which the carbon dioxide scrubbing as based. Instead of having water in the gas mixer, the gas mixer was filled with NaOH (aq) and the extra carbon dioxide and oxygen lines to it were dropped. The gas mixer was now a gas scrubber.

3.4.2 Method for feed gas preparation

The initial feed gas is compressed air, characterised as 79% N_2, 20.6% O_2 and circa 400 ppm CO_2 at 2 bar. In the first set of experiments, normal compressed air was used, but for other runs, the CO_2 concentration was reduced by scrubbing the compressed air stream using aqueous sodium hydroxide (NaOH (aq)) at the concentrations shown in Table 3-1. The air was bubbled through the NaOH (aq) and sparged thought a glass sinter used in fish tanks. The off gas exited the scrubber and was transferred to the Applikon bioreactor. An air filter was placed in line between the scrubber and the bioreactor. For longer residence times, the solution was pumped out and fresh solution was added to a larger Schott bottle every 40 hours. The carbon dioxide concentration of the air stream after scrubbing is that entering the bioreactor.

Table 3-1. Concentration of carbon dioxide in air after scrubbing with sodium hydroxide

[NaOH] (Molar Solution)	[CO_2] (ppm after scrubbing)
0	360
1	300
3.5	120
5	70
7	45
10	<2

For every gaseous concentration of carbon dioxide used, a complete set of residence times was analysed. Since the reactors were run as CSTRs, the gas concentration in the outlet of the reactor can be assumed to be the gas concentration inside the reactor. The outlet concentration also varied over the residence times analysed. A midway value of the outlet concentrations, rounded to the nearest 10, was chosen to refer to the set of runs at the same inlet concentration. The carbon dioxide concentrations entering the reactor, the range of outlet concentrations as well as the concentration nominally used to represent each dataset are shown in Table 3-2. For the 450 ppm concentration, a standard gas mixture with a concentration of 500 ppm was used as the feed gas, which exited the system at approximately 450 ppm carbon dioxide. Each of these carbon dioxide concentrations was investigated across the following residence times: 16, 24, 32, 48, 54.5 hr.

Table 3-2. Inlet and outlet carbon dioxide concentrations from the bioreactor and reference concentrations

$[CO_2]$ inlet into bioreactor (ppm)	$[CO_2]$ outlet from bioreactor (ppm)	Referred to as $[CO_2]$ (ppm)
<2	<2	<2
45	25-37	30
70	42-52	50
120	82-102	100
300	242-274	270
360	347-348	340
500	448 470	450

3.5 Effect of carbon dioxide concentration on continuous culture planktonic experiments

3.5.1 Previous work on investigating ferrous iron oxidation rates

In order to understand and improve bioleaching, laboratory scale studies in micro-scale heaps i.e. columns or shake-flasks containing mineral or mineral ore have been undertaken extensively. Studies carried out in columns with ore are usually concerned with the overall rate of bioleaching and the effect of certain parameters on them, e.g. inoculation time, ferrous iron concentration, ferric: ferrous ratio etc. Microbial community are increasingly studied using molecular analyses on the various micro systems. Rate studies are typically carried out in stirred tank bioreactors in the absence of ore to measure the ferrous oxidation rate.

Even though it is accepted that cultures in industrial operations are seldom pure, the most direct way to attribute kinetics to a micro-organism is by pure culture study.

Ferrous iron oxidation rates have been determined previously in continuous culture using *L. ferriphilum* with a ferrous iron feed (Ojumu, 2006). The ferric: ferrous iron concentration in the CSTR was controlled by changing the dilution rate (D) in the reactor and therefore changing the microbial growth rate. This phenomenon of controlling the ferrous:ferric ratio by changing the dilution rate only holds under steady state conditions in a CSTR with aqueous ferrous feed and no alternate ferrous iron source. Figure 3-3 shows the resultant specific oxidation rate as a function of ferric: ferrous iron ratio. The experimental data points are plotted against the commonly used Hansford Model (Ojumu *et al.*, 2006).

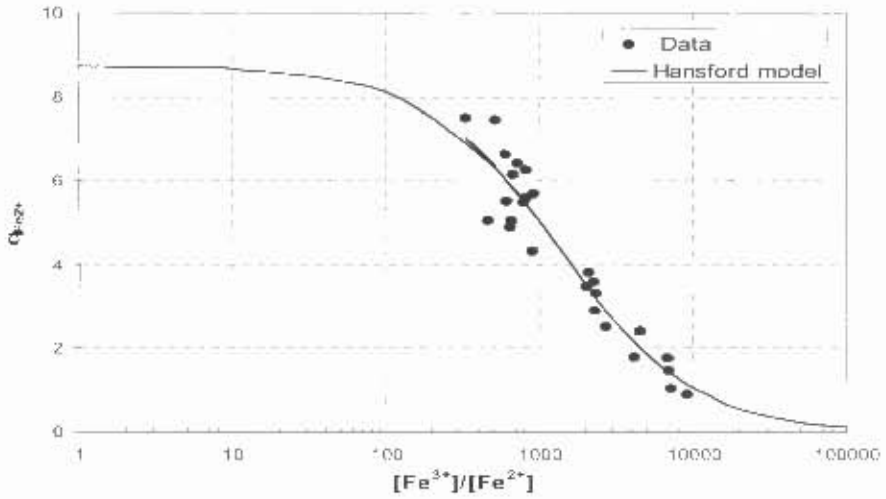

Figure 3-3. Specific ferrous-iron utilization rate as a function of ferric: ferrous ratio in a chemostat culture at 42°C and 5 g/L total Fe concentration for a *L. ferriphilum* culture.
(taken from Ojumu *et al.*, 2006)

The behaviour of *L. ferriphilum* with respect to bio oxidation and microbial growth rate, under the effects of physicochemical changes has been studied extensively by Ojumu *et al.* (2008). The effect of changes in temperature, pH, ferrous iron concentration and ionic strength (by magnesium and aluminium) were studied at different residence times. These studies were essentially an extension and expansion of the study carried out by Breed in 1999, which focused on the effects of pH on the mesophilic ferrous oxidation kinetics in a culture identified as a *Leptospirillum ferrooxidans*, but later typed as *L. ferriphilum*. The same system was adopted for this study.

3.5.2 Methods for start-up and running of planktonic experiments

The 2 litre Applikon reactor as inoculated by combining 500 ml culture from the stock reactor with 500 ml fresh feed. The reactor was operated in batch mode at 37°C and the redox potential was monitored until it exceeded 600 mV (relative to the $Ag/AgCl_2$ reference). At this point it was switched to continuous mode. The feed rate was controlled over the pump calibration range 1.3 to 2.5 to achieve the dilution rates across the range of 0.0183 hr^{-1} to 0.0675 hr^{-1} respectively. Throughout the experiment, the conditions were maintained at 37 °C agitation at 400 rpm and the aeration at 350 ml/min. The exit air from the reactor was passed through a condenser to reduce humidity, whereafter it passed through off gas analysis to measure residual oxygen and carbon dioxide (Figure 3-4). These were compared to the reference concentrations to calculate oxygen and carbon dioxide uptake rates.

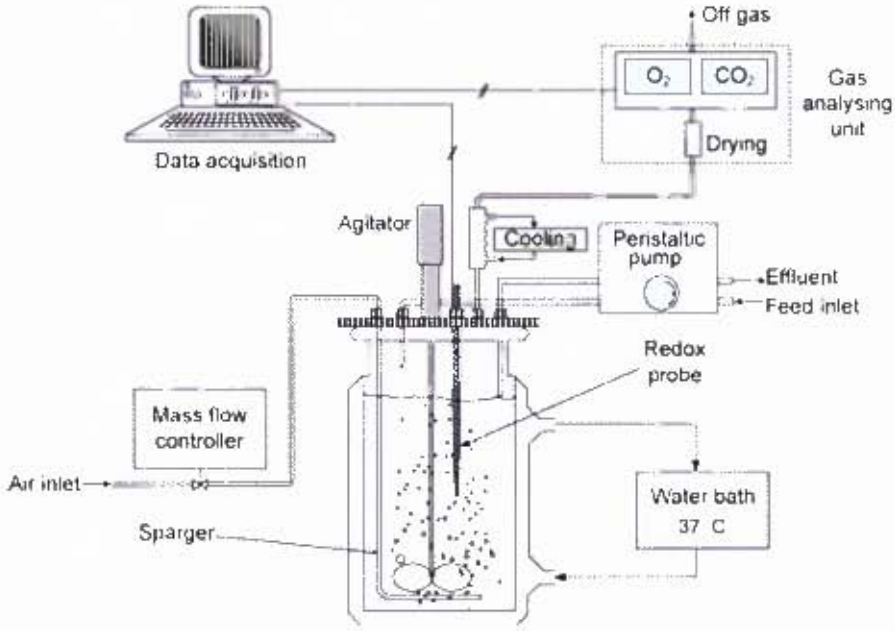

Figure 3-4. Basic schematic of experimental setup (taken from Ojumu *et al.*, 2008)

After a minimum of three residence times, steady state measurements were made. Constant CO_2 and O_2 concentrations were checked before taking sample data for calculations. Measured values included the carbon dioxide and oxygen concentrations entering and leaving the reactor, the concentration of ferrous iron in the feed and exit stream, the total iron concentration, the redox potential relative to the $Ag/AgCl_2$ electrode. A sample was taken for offline measurement of cell counts, total organic carbon and organic acids present measured by HPLC analysis.

3.6 The effect of carbon dioxide concentration on continuous culture planktonic & sessile experiments

3.6.1 Previous work on the incorporation of a non-mineral solid phase

In the work of Puhakka and co-workers, a *Leptospirillum* dominated culture has been retained on a solid phase in a fluidised bed system with high recycle ratio attached to a settling tank. The schematic is shown in Figure 3-5. The system was used by Kinnunen & Puhakka in 2005 to test the effect on the high rate oxidation process of low pH's at high Cu^{2+} concentrations. It was assumed that the ferrous oxidation was performed only by the attached (sessile) population in the fluidised bed. While it was claimed that the sessile phase was the only active population, no tests to check the absence of a planktonic phase was conducted. Ozkaya *et al.* (2007) extended this study to test whether the sessile population, referred to in this study as the "biofilm", performed at extremely high ferrous iron oxidation rates, by an order of magnitude higher than previously reported studies. They went on to conclude that the limiting factor in the high rate oxidation system was the mass transfer of oxygen to the liquid phase. In the study, the biofilm reactor was proposed as a ferric generating system for bioleaching.

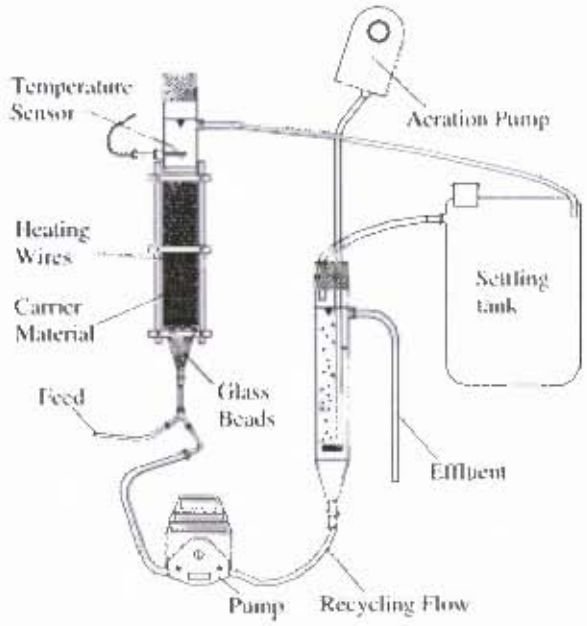

Figure 3-5. Schematic of solid phase inclusion in pure culture ferrous oxidation rate study (taken from Kinnunen & Puhakka, 2005)

There was no study or analysis on carbon utilization. In the Kinnunen and Puhakka study, the solid support used was activated carbon. Activated carbon could not be used in the current work as the support as it would interfere with the carbon balance proposed for this study. The packed bed column with a high recycle ratio as adopted from this study, but a different inert solid support was needed. Testing was done with sponge and ceramic saddles. Results from initial test work by Maas and Paxton (2007) showed that the sponge was not suitable as it entrained liquid. The ceramic saddles were shown to be pH resistant and to allow cell attachment; hence they were adopted as the solid support for this study.

3.6.2 Methods for start-up and running of planktonic & sessile experiments

The batch reactor was inoculated as described in Section 3.5.2. When the redox potential exceeded 600 mV (relative to the $Ag/AgCl_2$ reference), the reactor was switched to continuous mode and a packed column coupled to the CSTR, as shown in Figure 3-6. An air-tight glass column packed with 180 g of ceramic saddle packing was connected to the reactor via L/S™ 14 Norprene® food tubing, and pumped through the column at 390 ml/hr, the maximum speed on the Masterflex console. Since the flow rate of the fresh feed to the STR varied between experimental runs, the ratio of the flow rate through the packed bed: the flow rate of the fresh feed varied.

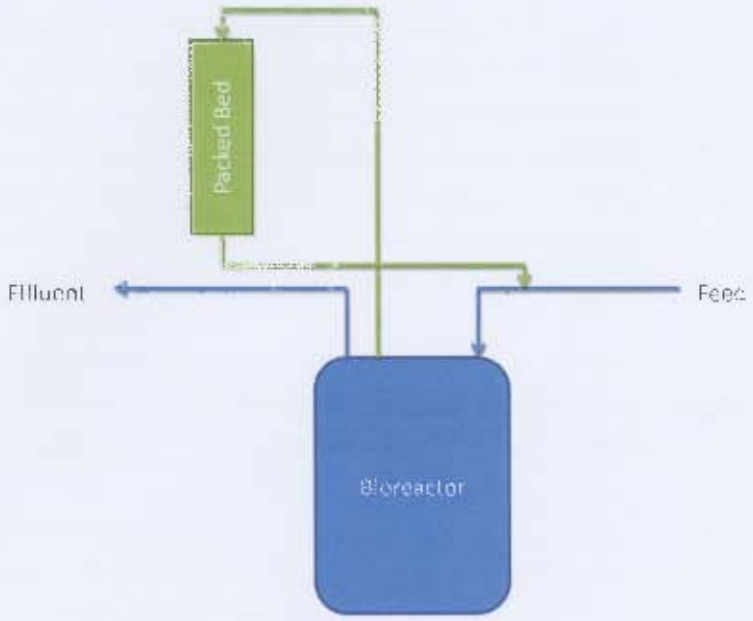

Figure 3-6. Schematic of experimental setup for the inclusion of the solid phase in a packed bed

Again, the system was left for three residence times before taking any measurements. In these set of experiments it took 3 to 7 residence times to reach steady gaseous uptake rates. Reasons for this are discussed in Section 5.1. Measured values during the experiment included the gaseous carbon dioxide and oxygen concentrations entering and leaving the reactor, the concentration of ferrous iron in the feed and exit stream, the total iron concentration, the redox potential relative to the $Ag/AgCl_2$ electrode. Samples were taken for microscopic cell count, total organic carbon analysis and analysis of organic acids by HPLC. When the column was sacrificed at the end of each residence time at each carbon dioxide concentration, the cells were washed off the packing with Tris buffer (0.1%), in two consecutive washes of 500 ml each to determine the number of cells on the solid support. As it was already identified in the planktonic cell studies conducted that the most significant changes were observed below a carbon dioxide concentration of 100 ppm, the sessile and planktonic study was carried out with compressed air to provide base case data, where after it was focused on carbon dioxide concentrations of 100 ppm and less. The carbon dioxide concentrations investigated, and residence times used are shown in Table 3-3.

Table 3-3. Carbon dioxide availability and residence times investigated in sessile & planktonic experiments

$[CO_2]$ (ppm)	Residence time (hr)
30	16
50	24
100	32
340	48
	54.5

3.6.3 Methods for start-up and running of the decoupling study

After completion of the experimental runs outlined in Sections 3.5 and 3.6, it was found that the activity of the sessile population could not be determined independently as the observed ferrous oxidation rate of a planktonic system and the planktonic and sessile system at the same carbon dioxide concentration were too similar as there was near complete oxidation of ferrous iron in both cases. The decoupling study was designed to determine whether sessile cells are capable of higher ferrous oxidation rates. The motivation for having the Decoupling Study is further discussed in Section 5.2.

In this set-up, a system with sessile and planktonic phase was separated as show in Figure 3-7. A reactor at steady state with respect to both planktonic and sessile populations was separated into the separate planktonic and sessile phases. The combined system reached a steady state under the following conditions:

- 32 hour residence time
- Sparge gas is compressed air at 400 ml/min (system at 340ppm)
- Ferrous feed contains 5 g/l Ferrous iron
- pH = 1.3 (in reactor)
- *Leptospirillum ferriphilum* pure culture

The separated planktonic phase (CSTR) was operated with fresh feed at a 32 hour residence time. The sessile phase was attached to a CSTR already running abiotically, at a 32 hour residence time at steady state. The dynamic oxygen and carbon dioxide uptake rates were monitored until both new systems reached steady state independently. The key differences in this study compared to the normal planktonic or the sessile & planktonic studies were that:

- the system was dynamic when the measurements were taken, and the measurements were taken until a steady state was reached
- the sessile phase was introduced to an unpopulated aqueous system as opposed to a planktonic culture being exposed to a solid support.

The measured values in this study are only the carbon dioxide and oxygen concentration entering and leaving the reactor. It was not possible to take any other measurements in real time.

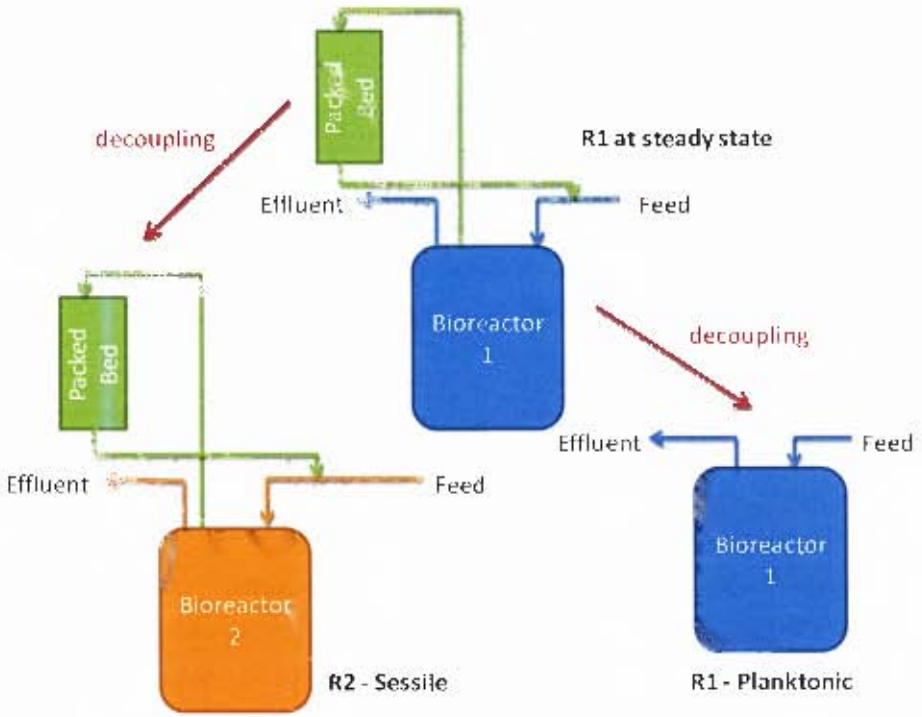

Figure 3-7. Schematic of the decoupling process in the decoupling study

3.7 Analytical methods used

The analytical methods used, and their principle of operation is provided in the section. A full analytical method with sample calibration curves is presented in Appendix D.

3.7.1 Weighing of feed and density

The feed reservoir was weighed in a 2 litre Schott bottle on a Denver ® Instrument XP-600 Scale. This was used to confirm the residence time of the system.

3.7.2 pH

The pH was measured with a Metrohm®, 691 pH Meter. The pH meter was calibrated between pH 1 and pH 4 daily.

3.7.3 Atomic absorption spectrum (AAS)

A Varian Spectra AA-200 Atomic absorption spectrophotometer incorporating Spectra AA 100/200 version 1.1 software was used to measure the total iron concentration, $[Fe_{total}]$ in the feed and the effluent streams. The analytical error was calculated to be < 1% for iron.

3.7.4 Ferrous iron analysis

The residual ferrous iron concentration was measured colorimetrically using the 1-10 phenanthroline method (Eaton *et al.*, 1998). A 2 ml aliquot of phenanthroline was added to 2 ml ammonium acetate and

made up to 5 ml with appropriately diluted sample. The ferrous iron is chelated by three phenanthroline molecules (a divalent ligand) to form $Fe(phen)_3^{2+}$, a magenta coloured compound with an absorbance maximum between 400 and 600 nm. The absorbance was measured on a Unicam ®, Helios, α.v4.04 spectrophotometer. A standard curve was generated with known concentrations of the ferrous iron and the concentration of the sample inferred from the curve. The method is detailed in Appendix D.3 and the sample calculation in Appendix F. Appropriate sample dilution was used to ensure within the calibration range.

3.7.5 Reduction–oxidation potential

The redox potential was measured with Mettler ®, P14805-SC-DPAS-K85/325 combination redox probe inserted into the reactor. The redox probe was calibrated between a ferric/ferrous iron ratio of 1.0 (typically ≈500mV) and 1000.0 (typically ≈ 700mV), at 36.5°C. Using the Nernst Equation (Section 2.6) a ferric: ferrous iron ratio can be informed from a measured redox potential. The method is outlined in detail in Appendix D.4 and the sample calculations are in Appendix F.

3.7.6 Microbial cell counts

Cell counts were performed on all the samples by direct counting under a phase contrast optical Olympus ® BX40 Microscope. A Thoma Haemocytometer with counting chambers at a depth of 0.02 mm was used at a magnification of 1000x. The cell concentration was then determined using the dilution, count and the dimensions of the haemocytometer.

$$[Cell] = \frac{Cells\ counted \times Dilution}{Volume \times Groups\ Counted}$$

The area of each square is $0.0025mm^2$ thus the volume of square counted is $5x10^{-8}$ ml. Typically, there is no dilution and four random groups of sixteen squares are counted. Thus the formula reduces to:

$$[Cell] = \frac{Cells\ counted \times 1}{0.00000005ml \times (16 \times 4)} = Cells\ Counted\ \times 312500 \text{ cells/ml}$$

Direct counting has been used by several researchers (Konishi *et al.*, 1995; Nemati *et al.*, 2000). Konishi *et al.* (1995) reported that the counting error of this method could be as high as 11% for bioleaching micro-organisms. Both planktonic cell concentration and cell numbers at the end of each run were measured by direct counting.

3.7.7 Solid support

To determine the cell numbers on the solid support, a washing procedure was used. After the column was sacrificed, the support was washed twice with two separate 500 ml washes of 0.1% Tris buffer. Cell counts for each solution were calculated separately.

3.7.8 *Dry weight analysis*

For the dry weight measurement, 1 litre of solution containing an active population of *L. ferriphilum* was centrifuged at 10 000 g. The supernatant was discarded and cells then resuspended in ddH2O and re-centrifuged. This was repeated three times. The cell dry weight was then measured after drying the sample in an oven at 80 °C until there was no further change in mass. Prior the harvesting of the cells, a microscopic cell count was performed, allowing mass per cell to be estimated.

3.7.9 *Total organic carbon*

Samples taken for total organic carbon (TOC) analysis must not contain sulphur or phosphorus compounds as it reduced the activity of the catalyst. Since the bioleach system contained a high concentration of sulphate, it was removed by precipitation with $BaCl_2$. Once the precipitate was filtered off, the sample was analysed using an ANATOC II Series ZO5-001 total organic carbon analyser. The analyser has a detection limit of 0.00 mg/L carbon, calibrated between 0.00 and 50 ppm of carbon and a typical error of <8% arose from readings. The sample was completely oxidised over a catalyst and the total amount of carbon dioxide produced is measured. From here, the concentration of organic carbon in the sample was calculated. More detail on this method is provided in Appendix D.1

3.7.10 *Off-gas data*

The off-gas analyser measured the carbon dioxide and oxygen concentration entering and leaving the system, $O_{2,inlet}$, $O_{2,outlet}$, $CO_{2,inlet}$ and $CO_{2,outlet}$. A mass flow controller was used to control adequate sparging of the bioreactor. The volumetric flow rate of air through the reactor, v_{gas}, was measured in ml/min with a bubble column and a stop watch, entering and leaving the system before the experiment is run. The volume between the points on the bubble column is 90 ml.

$$v_{gas} = \frac{90ml}{\Delta time\ (minutes)}$$

The oxygen and carbon dioxide uptake rates were calculated using material balances as follows:

$$-r_{O_2} = \frac{v_{gas,outlet} \cdot 60s/min}{V_{Rx} \cdot 22.406mol/dm^3} \times \left[\left(\frac{1 - \frac{O_{2,outlet}}{100} - \frac{CO_{2,outlet}}{10^6}}{1 - \frac{O_{2,inlet}}{100} - \frac{CO_{2,inlet}}{10^6}} \right) \times \frac{O_{2,inlet}}{100} - \frac{O_{2,outlet}}{100} \right]$$

$$-r_{CO_2} = \frac{v_{gas,outlet} \cdot 60s/min}{V_{Rx} \cdot 22.406mol/dm^3} \times \left[\left(\frac{1 - \frac{O_{2,outlet}}{100} - \frac{CO_{2,outlet}}{10^6}}{1 - \frac{O_{2,inlet}}{100} - \frac{CO_{2,inlet}}{10^6}} \right) \times \frac{CO_{2,inlet}}{10^6} - \frac{CO_{2,outlet}}{10^6} \right]$$

4. Results and Discussions I: Effect of Carbon Dioxide on Stoichiometry, Growth and Ferrous Iron Oxidation Rates of Planktonic Experiments

4.1 Aim and approach

The effect of carbon dioxide availability on the microbial growth rate and ferrous oxidation rate was investigated for a planktonic population in a continuous stirred tank reactor at a ferrous iron concentration of 5 g/L. The data analysis procedure used is presented, using the base case data set in Section 4.2. Thereafter, the complete dataset describing the effect of carbon dioxide in the planktonic system is presented and discussed in Section 4.3. Using the data collected there are several methods to calculate the ferrous iron oxidation rate and the specific ferrous iron oxidation rate. These are explained in Table 4-1. Methods 1, 2 and 3 are used for calculating the ferrous iron oxidation rate, while Methods A and B are used for calculating the specific ferrous oxidation rate.

Table 4-1. Summary of methods used to calculate ferrous oxidation rate and specific ferrous oxidation rate

	Method	Measured values used	Used to Calculate	Analytical Method
Ferrous Oxidation Rate	1	$[Fe_{total}]$	$[Fe^{2+}{}_{inlet}]$	A.A.S.
		$[Fe^{2+}]$	$[Fe^{2+}{}_{outlet}]$	Spectrophotometry
	2	$[Fe_{total}]$	$[Fe^{2+}{}_{inlet}]$	A.A.S.
		$[Fe^{3+}]/[Fe^{2+}]$	$[Fe^{2+}{}_{outlet}]$	Reduction-Oxidation Potential
	3	$[O_2]$, $[CO_2]$, $v_{gas,outlet}$	$-r_{O2}$	Off-Gas Analysis
		$[O_2]$, $[CO_2]$, $v_{gas,outlet}$	$-r_{CO2}$	Off-Gas Analysis
Specific Ferrous Oxidation Rate	A	$[Fe_{total}]$, $[Fe^{2+}]$	$-r_{Fe2+}$	Method 1
		Cell Count	[Cells]	Cell Counts
		$Cell_{Dry\ Weight}$	$Cell_{Carbon\ Equivalent}$	Dry Weight Analysis
	B	$[O_2]$, $[CO_2]$, $v_{gas,outlet}$	$-r_{Fe2+}$	Method 3
		$-r_{CO2}$	C_x	Off-Gas Analysis

4.2 Data analysis procedure

The base case data set was generated, using normal compressed air, at an approximate CO_2 concentration of 400 ppm and a liquid feed containing 5g/L ferrous iron. The air left the system at a carbon dioxide concentration of approximately 340 ppm. As the exit concentration in a well mixed system should represent that in the system, this is referred to as the 340 ppm run. A dataset at these conditions had been generated for a feed containing 5 g/L ferrous iron previously (Ojumu *et al.*, 2008). The comparison of these data sets is shown in Figure 4-1, and the method of calculation is outlined below.

4.2.1 *Ferrous iron oxidation rates determined through direct measurement of iron and biomass*

Atomic absorption spectroscopy (AAS) was used to measure the total iron concentration, $[Fe_{total}]$. For the base case, $[Fe_{total}]$ was 4.94 g/L. The ferrous feed used was from the same continuous stock for all the runs and the value obtained is the average of three separate measurements within 3% error. Knowing that the iron in the feed was provided as ferrous iron, the following hold:

$[Fe^{2+}]_{inlet} = [Fe_{total}]$ *from A.A.S*

$[Fe^{2+}]_{outlet} = [Fe^{2+}]_{reactor}$ *from Spectrophotomter*

From here, based on the assumptions that the system is at steady state and that there is no iron precipitation, the ferrous oxidation rate can be calculated using Equation 7.

$$-r_{Fe^{2+}} = \boldsymbol{D} \cdot ([\boldsymbol{Fe^{2+}}]_{inlet} - [\boldsymbol{Fe^{2+}}]_{outlet}) \qquad \textbf{Equation 7}$$

This is referred to as **Method 1** for the calculation of the ferrous oxidation rate. The results for the base case are shown in Table 4-2

Table 4-2. Ferrous iron oxidation rate in steady state culture sparged with air exiting at 340 ppm CO_2, calculated according to Method 1 (spectrophotometry and AAS)

Residence Time (hr)	Dilution Rate (1/hr)	$[Fe^{2+}_{inlet}]$ (g/L)	$[Fe^{2+}_{outlet}]$ (g/L)	$-r_{Fe2+}$ (g/hr)	$-r_{Fe2+}$ (mmol Fe/hr)
54.5	0.0183	4.94	0.0183	0.0904	1.62
48	0.0208	4.94	0.0175	0.103	1.84
32	0.0313	4.94	0.0247	0.154	2.75
24	0.0417	4.94	0.0915	0.202	3.62
16	0.0625	4.94	0.130	0.301	5.39

The redox potential, measured with the $Ag/AgCl_2$ electrode, was used to infer the ferric: ferrous iron ratio from a standard curve generated using the Nernst Equation. The redox potentials relative to the $Ag/AgCl_2$ electrode were measured for known concentrations and ratios of ferric: ferrous iron at a fixed temperature and used as a calibration curve. Given the total iron concentration (from AAS), the individual concentrations of ferrous ion and ferric iron were calculated. This approach was used in **Method 2**.

$[Fe^{2+}]_{inlet} = [Fe_{total}]$ *from A.A.S*

$\frac{Fe^{3+}}{Fe^{2+}} = Ratio$ *this 'Ratio' is inferred from the standard curve*

$[Fe^{2+}]_{outlet} = [Fe^{2+}] = \frac{[Fe_{total}]}{1+Ratio}$

$[Fe^{3+}] = [Fe^{2+}] \times Ratio$ *this is not used in any calculations*

For Method 2, the ferrous oxidation rate can now be calculated from these values and the dilution rate according to Equation 7. The results for the base case data set are shown in Table 4-3. Also, cell counts were performed on all the samples and the results for the base case are shown in Table 4-4. In addition, cell dry weight was determined gravimetrically following the centrifugation and used to calculate the dry mass of a typical *L. ferriphilum* cell as shown in Table 4-5.

Table 4-3. Ferrous iron oxidation rate in steady state culture sparged with air exiting at 340 ppm CO_2, calculated according to Method 2 (reduction-oxidation potential and A.A.S)

Residence Time (hr)	Dilution Rate (1/hr)	$[Fe^{2+}_{inlet}]$ (g/L)	Redox Potential (mV)	$[Fe^{3+}]/[Fe^{2+}]$	$[Fe^{2+}_{outlet}]$ (g/L)	$-r_{Fe2+}$ (g/hr)	$-r_{Fe2+}$ (mmol Fe/hr)
54.5	0.0183	4.94	709.6	3651	0.00135	0.0907	1.62
48	0.0208	4.94	708.0	3424	0.00144	0.103	1.84
32	0.0313	4.94	698.4	2374	0.00208	0.154	2.76
24	0.0417	4.94	663.1	619.7	0.00796	0.206	3.68
16	0.0625	4.94	653.2	424.0	0.0116	0.308	5.52

Table 4-4. Cell counts and cell concentration in steady state culture sparged with air exiting at 340 ppm CO_2

Residence Time (hr)	Dilution Rate (1/hr)	[Cells] ($x10^6$ cells/mL)
54.5	0.0183	25.3
48	0.0208	20.6
32	0.0313	23.4
24	0.0417	21.9
16	0.0625	24.7

Table 4-5. Calculation of the dry weight of *L. ferriphilum* cells in steady state culture sparged with air exiting at 340 ppm CO_2

[Cells] ($x10^6$ cells/mL)	Dry Weight (mg/L)	$Cell_{Dry\ Weight}$ (g/cell)	error (g/cell)
25.3	14.1	5.58E-13	2.51E-14

The mass of a typical *L. ferriphilum* cell was calculated to be $5.575x10^{-13}$g/cell. Biomass is typically 50% carbon by weight (Characklis & Marshall, 1990), and the carbon equivalent of an *L. ferriphilum* cell can be calculated:

$$Cell_{carbon\ equivalent} = 0.5 \times Cell_{dry\ weight} = 2.79 \cdot 10^{-13} g_{carbon}/cell = 2.32 \cdot 10^{-14} gmol_{carbon}/cell$$

This value can be used to calculate a specific ferrous oxidation rate, $q_{Fe^{2+}}$.

$$q_{Fe^{2+}} = \frac{-r_{Fe^{2+}}}{[Cells] \cdot \frac{Cell_{carbon\ equivalent}}{Mr_{Carbon}} \cdot 10^{12}} mmolFe/(mmolC.hr)$$

where the $-r_{Fe^{2+}}$ value used was that calculated from **Method 1** and the cell concentration was calculated through the combination of microscopic cell counts and dry mass, referred to as **Method A** for calculating the specific ferrous oxidation rate. The results for the base case data set are shown in Table 4-6.

Table 4-6. Specific ferrous iron oxidation rate in steady state culture sparged with air exiting at 340 ppm CO_2, calculated according to Method A (AAS, spectrophotometry, cell counts and dry weight analysis)

Residence Time (hr)	Dilution Rate (1/hr)	$-r_{Fe2+}$ (mmol Fe/hr)	[Cells] (x10^6 cells/mL)	Cx (mmol C/L)	q_{Fe2+} (mmolFe/mmolC.hr)
54.5	0.0183	1.62	25.3	0.588	2.75
48	0.0208	1.84	20.6	0.479	3.83
32	0.0313	2.75	23.4	0.544	5.05
24	0.0417	3.62	21.9	0.508	7.12
16	0.0625	5.39	24.7	0.573	9.39

4.2.2 Ferrous iron oxidation rates determined by respirometry

The established method for determining kinetic data through a combination of respirometry and microbial stoichiometry along with the assumptions which govern this process are outlined in Section 2.5. The measurements used from the off-gas analyser are: $O_{2,inlet}$, $O_{2,outlet}$, $CO_{2,inlet}$ and $CO_{2,outlet}$. The $[O_2]$ is recorded as a percentage of the air flow, and the $[CO_2]$ is recorded as parts per million (ppm) of the air flow. The raw data with these measurements is shown in Appendix C. The volumetric flow rate of air through the reactor, v_{gas} is used in conjunction with the volume of the reactor, V_{Rx} to calculate the oxygen uptake rate, $-r_{O_2}$, and the carbon dioxide uptake rate, $-r_{CO_2}$, in mmol/(l.hr) as described in Section 3.7.10.

These data have been compared to the equivalent study performed by Ojumu *et al.* (2008), shown in Figure 4-1. The results show that the data obtained is constant with the data generated by Ojumu *et al.* (2008) within the standard error of this study.

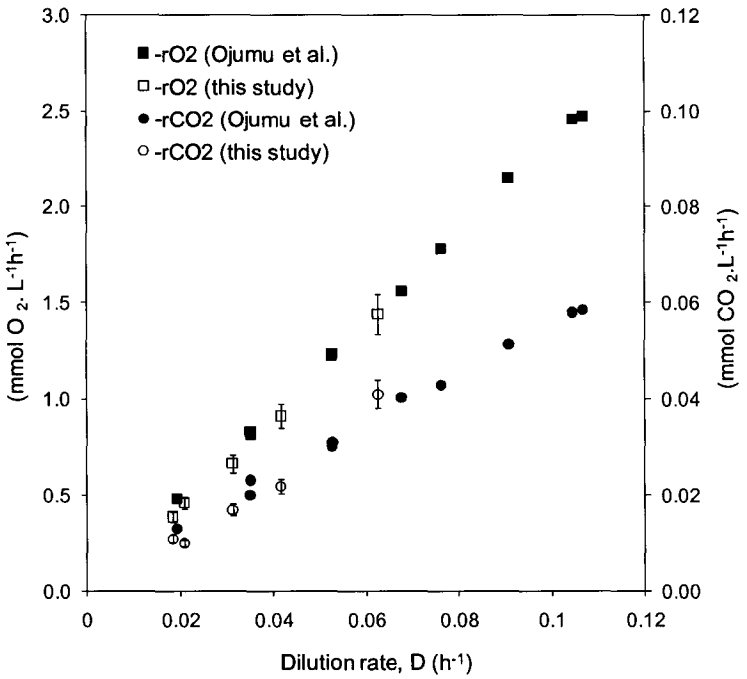

Figure 4-1. Comparison of off-gas data generated by this study to data from a previous study (Ojumu *et al.*, 2008)

The oxygen uptake rate, $-r_{O_2}$, and the carbon dioxide uptake rate, $-r_{CO_2}$, were used to calculate the ferrous oxidation rate based on the stoichiometric relationship between the ferrous iron oxidation rate and the carbon dioxide and oxygen uptake rates (Equation 6), proposed by Boon and Hansford (1996). This represents **Method 3**, used to calculate the ferrous iron oxidation rate.

$$-r_{Fe^{2+}} = -4r_{O_2} - 4.2r_{CO_2} \qquad \textbf{Equation 6}$$

The base case data is presented in Table 4-7. This method is based on the following underlying assumptions:

- The stoichiometric relationship between the ferrous oxidation rate and the carbon dioxide uptake rate presented in Equation 6 holds.
- All carbon assimilated is used to form active biomass.

Validation of these assumptions can be tested by comparing the ferrous iron oxidation rate calculated by this method to that calculated in Methods 1 and 2.

Table 4-7. Ferrous oxidation rate for 340 ppm run calculated by Method 3 (off-gas data)

Residence Time (hr)	Dilution Rate (1/hr)	$-r_{O2}$ mmol/hr	$-r_{CO2}$ mmole/hr	$-r_{Fe2+}$ (mmol Fe/hr)
54.5	0.0183	0.387	0.0109	1.59
48	0.0208	0.461	0.00997	1.89
32	0.0313	0.665	0.0169	2.73
24	0.0417	0.912	0.0219	3.74
16	0.0625	1.44	0.0410	5.93

Equation 5 can be used to calculate the "biomass" concentration in the CSTR as a carbon equivalent. From here, the specific ferrous iron oxidation rate can be calculated using Equation 8. This is referred to as **Method** B for calculating the specific ferrous iron oxidation rate, and the results for the base case are shown in Table 4-8. Hence, where the assumptions detailed in Section 2.5 and above are valid, a complete data set can be generated. It is valuable to determine the effect of the culture conditions on underlying assumptions using only the off-gas data.

$$C_x = \frac{r_{CO_2}}{D} \qquad \textbf{Equation 5}$$

$$q_{Fe^{2+}} = \frac{-r_{Fe^{2+}}}{C_x} \qquad \textbf{Equation 8}$$

Table 4-8. Specific ferrous iron oxidation rate in steady state culture sparged with air exiting at 340 ppm CO_2, calculated according to Method B (off-gas data)

Residence Time (hr)	Dilution Rate (1/hr)	$-r_{CO2}$ mmole/hr	C_x mmol C	$-r_{Fe2+}$ (mmol Fe/hr)	q_{Fe2+} (mmolFe/mmolC.hr)
54.5	0.0183	0.0109	0.592	1.59	2.69
48	0.0208	0.00997	0.479	1.89	3.94
32	0.0313	0.0169	0.542	2.73	5.04
24	0.0417	0.0219	0.526	3.74	7.10
16	0.0625	0.0410	0.656	5.93	9.04

4.2.3 Determining the growth yield, maintenance coefficients and carbon partitioning

The manipulated Pirt Equation (Equation 11) was then applied to calculate yield and maintenance coefficients. These provide a comparison between the different carbon dioxide concentrations. In a continuous stirred tank bioreactor at steady state, the microbial growth rate, μ is equal to the dilution rate, D where cell death is negligible.

$$q_{Fe^{2+}} = \frac{\mu}{Y^{max}_{Fe^{2+}}} + m_{Fe^{2+}} \qquad \textbf{Equation 11}$$

For the steady state culture sparged with air exiting at 340 ppm, the specific ferrous iron oxidation rate calculated by Method A was plotted against the dilution rate. The inverse of the yield was determined from the gradient and the maintenance coefficient was calculated from the y-intercept. The detailed calculation is given in Appendix F. The value for the maximum theoretical yield was calculated as 6.84×10^{-3} mmolC/mmolFe and the maintenance coefficient has the value of 0.524 mmolFe/mmolC for this particular set of experiments.

The $-r_{CO_2}$ value from off gas analysis and the $Cell_{carbon\ equivalent}$ calculated from dry weight analysis in Section 3.7.8 can be used to calculate a maximum theoretical biomass concentration according to the formula below. The maximum theoretical biomass is the maximum amount of biomass that can be formed from the measured amount of carbon dioxide taken up by the system. Mr_{Carbon} refers to the molecular mass of carbon (12 g/mol).

$$Biomass_{Maximum\ Theoretical} = \frac{-r_{CO_2} \times Mr_{Carbon} \times 10^{-12}}{D \times Cell_{carbon\ equivalent}} 10^6 cells/ml$$

From here, the percentage of carbon which is assimilated to form new biomass can be calculated for each run according to the following formula:

$$\%Carbon\ in\ New\ Biomass = \frac{[Cells]}{Biomass_{Maximum\ Theoretical}}$$

The results for the base case are shown in Table 4-9. The results suggest that for this planktonic population sparged with compressed air, the carbon which was removed from the air stream and is available to the micro-organisms in solution was mostly used for the production of biomass. This qualifies Equation 5 which assumes that all the carbon is assimilated to biomass.

Table 4-9. Percentage carbon in new biomass in steady state culture sparged with air exiting at 340 ppm CO_2

Residence Time (hr)	Dilution Rate (1/hr)	$-r_{CO2}$ mmole/hr	$Biomass_{Max.\ Theor.}$ ($x10^6$ cells/mL)	[Cells] ($x10^6$ cells/mL)	% carbon assimilated into new biomass
54.5	0.0183	0.0109	25.5	25.3	99.3
48	0.0208	0.00997	20.6	20.6	100
32	0.0313	0.0169	23.3	23.4	100
24	0.0417	0.0219	22.7	21.9	96.5
16	0.0625	0.0410	28.2	24.7	87.4

The methods compared well under planktonic conditions at residence times greater than 24 hrs and correlated well with the data generated by Ojumu (2008) under similar conditions. The microscopic cell counts also confirmed that the assumptions used to formulate Equation 5 held under these conditions. The study was then extended, repeating the same experiments and analyses over a range of carbon dioxide concentrations.

Under the most extreme NaOH scrubbing conditions used, the carbon dioxide concentration in the inlet gas measured by the off-gas analyser was undetectable (<2 ppm), yet some microbial growth occurred (as cell counts showed microbial concentrations between 0.63 $x10^6$ and $2.8x10^6$ cells/ml) . This suggested that the cells could scavenge trace concentrations or that trace CO_2 entered the reactor from elsewhere. For this reason, the results were not used in the comparative rate study. The results are presented in Table 4-11 for completeness. The ferrous oxidation rate calculated by Method 3 is therefore based solely on the oxygen uptake rate as the carbon dioxide uptake rate was not detectable. Methods 2 and 3 still yielded similar readings. This was explained by the fact that the stoichiometric relationship used in Method 3 depends very largely on the oxygen uptake rate and not on the carbon dioxide uptake rate (as the oxygen uptake rate was normally an order of magnitude greater than the carbon dioxide uptake rate and yet the coefficients in Equation 6 are 4 and 4.2 respectively). Results for Method 1 are up to 3 orders of magnitude greater than the other two methods. The analytical technique of measuring the ferrous iron concentration by spectrophotometry is very accurate over low (<100 ppm) ferrous iron concentrations. If the concentration of the sample is higher than 100 ppm (as they were for the <2 ppm experiment), serial dilutions were needed to have a sample within the range 0 - 100 ppm and error may have arisen in the process of serial dilution.

Table 4-11. Comparison of ferrous iron oxidation rates at a CO_2 concentration of < 2ppm of *L. ferriphilum* in continuous culture at steady state and 37°C using a ferrous iron feed concentration of 5 g/L

$[CO_2]$ ppm	Dilution Rate (hr^{-1})	Ferrous Iron Oxidation Rate (mmolFe/hr)		
		Method 1	Method 2	Method 3
<2 ppm	0.021	0.0889	0.000122	0.0327
	0.018	1.52	0.00152	0.00152
	0.031	2.37	0.00239	0.00239
	0.042	3.13	0.00316	0.00316
	0.063	-0.48	0.00017	0.0270

On inspection of Table 4-10, it is seen that the values obtained from the off-gas analysis (Method 3) were within 1% of the value from the Methods 1 and 2 at 450 ppm concentration, but elevated from Method 1 and 2 by up to 30% at lower concentrations (30 ppm and 50 ppm). Methods 1 and 2 yielded data within a 1% error consistently for all CO_2 concentrations.

The parity plot, given in Figure 4-2, is the graphical comparison of the ferrous oxidation rate calculated via off gas analysis using Method 3 and the ferrous oxidation rate calculated by Method 1. The deviation from the parity line at the lower CO_2 concentrations of 50 ppm and 30 ppm is observed for ferrous oxidation rates. The error bars suggest that all other values are in accordance with the parity line.

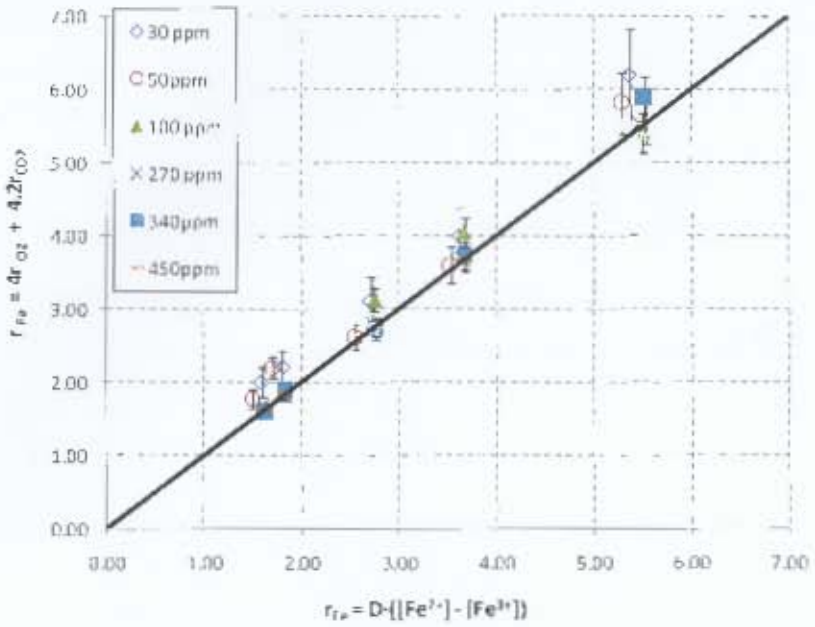

Figure 4-2. Parity plot for ferrous iron oxidation rates collected across a range of gaseous carbon dioxide concentrations

The assumption used to formulate Equation 6, forming the basis of Method 3, can be tested by using Methods 1 and 2.

$$-r_{Fe^{2+}} = 4r_{O_2} - 4.2r_{CO_2} \qquad \text{Equation 6}$$

The deviation from the parity line at higher ferrous oxidation rates was also observed by Ojumu *et al.* (2008). In order to bring the values to the parity line, the stoichiometric coefficient for CO_2 (-4.2) was varied. The values calculated are shown in Table 4-12. Between 100ppm and 450ppm, the coefficients are within 5% of theoretical coefficient value of -4.2. However, at lower CO_2 concentrations, the value of the coefficient increased. The physicochemical consequence of a higher coefficient is that a greater carbon dioxide uptake rate was associated with the same ferrous oxidation rate. This leads to the postulation that may imply that the cells are not only forming biomass for growth, but utilising the carbon differently.

Table 4-12. Calculated carbon dioxide coefficients for parity

$[CO_2]$	CO_2 Coefficient
30	-58.19
50	25.65
100	-4.368
270	-4.084
340	-4.136
450	-4.201

The specific ferrous oxidation rate can be calculated by Method A (using ferrous oxidation rate by redox probe inference, cell counts and the carbon equivalent) described in Section 4.2.1 and Method B (via off-gas data) as described in Section 4.2.2. The comparisons are first tabulated in Table 4-13 and then presented graphically in Figure 4-3 and Figure 4-4 respectively.

Table 4-13. Comparison of specific ferrous iron oxidation rates as a function of CO_2 concentration of *L. ferriphilum* in continuous culture at steady state and 37°C using a ferrous iron feed concentration of 5 g/L

$[CO_2]$ ppm	Dilution Rate (hr^{-1})	Sepcific Ferrous Iron Oxidation Rate mmolFe/(mmolC.hr)	
		Method A	Method B
30 ppm	0.021	6.72	5.71
	0.018	6.79	4.81
	0.031	11.0	8.55
	0.042	16.3	14.9
	0.063	25.5	23.0
50 ppm	0.021	6.68	5.30
	0.018	5.62	4.19
	0.031	9.50	8.51
	0.047	12.4	12.3
	0.063	18.2	17.2
100 ppm	0.021	3.17	3.06
	0.018	1.87	2.41
	0.031	5.32	4.77
	0.042	6.68	6.04
	0.063	9.33	9.43
270 ppm	0.021	3.99	3.95
	0.018	2.86	2.78
	0.031	4.92	4.92
	0.042	5.94	5.72
	0.063	10.0	9.18
340 ppm	0.021	3.95	3.83
	0.018	3.36	3.48
	0.031	5.22	5.27
	0.042	8.45	8.04
	0.063	12.2	11.4
450 ppm	0.021	3.27	3.28
	0.018	2.58	2.63
	0.031	4.94	5.02
	0.042	6.54	6.32
	0.063	7.54	8.10

Figure 4-3 and Figure 4-4 both show that the trend-lines for CO_2 concentrations between 100 ppm and 450 ppm were nearly parallel and overlapping. The increase in the slope for the 30 ppm and the 50 ppm runs indicated an increase in specific ferrous iron oxidation rate. This can be explained in one of two ways: either there was more ferrous iron oxidized for the same amount of biomass, or the same ferrous iron oxidation was performed by a smaller amount of biomass. Since, the ferrous iron was almost completely oxidized in all cases, and also, because there was less carbon dioxide available for cell formation, it is

postulated that the latter situation has occurred. This postulate was supported by the cell counts performed on the systems.

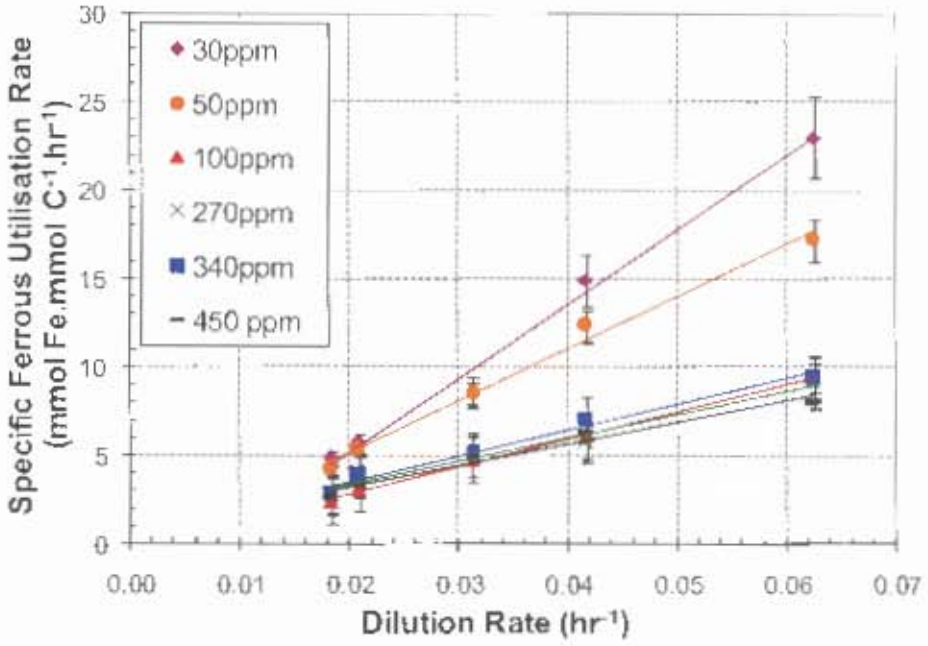

Figure 4-3. Specific ferrous iron utilisation rate vs dilution rate for carbon dioxide concentrations between 30 ppm and 450 ppm in steady state culture of *L. ferriphilum* calculated according to Method A (AAS, spectrophotometry, cell counts and dry weight analysis)

Although the trend lines are within experimental error of each other in both cases, it is apparent that the error associated with off-gas readings (Method B) was lower than those associated with Method A. This is possibly because the off-gas data rely on two measured values by one piece of equipment at steady state to calculate the specific oxidation rate, whereas Method A involved 3 measured values, each measurement performed separately on an individual piece of equipment with its own intrinsic error. Having acknowledged this, Figure 4-3 and Figure 4-4 both show the same values within experimental error.

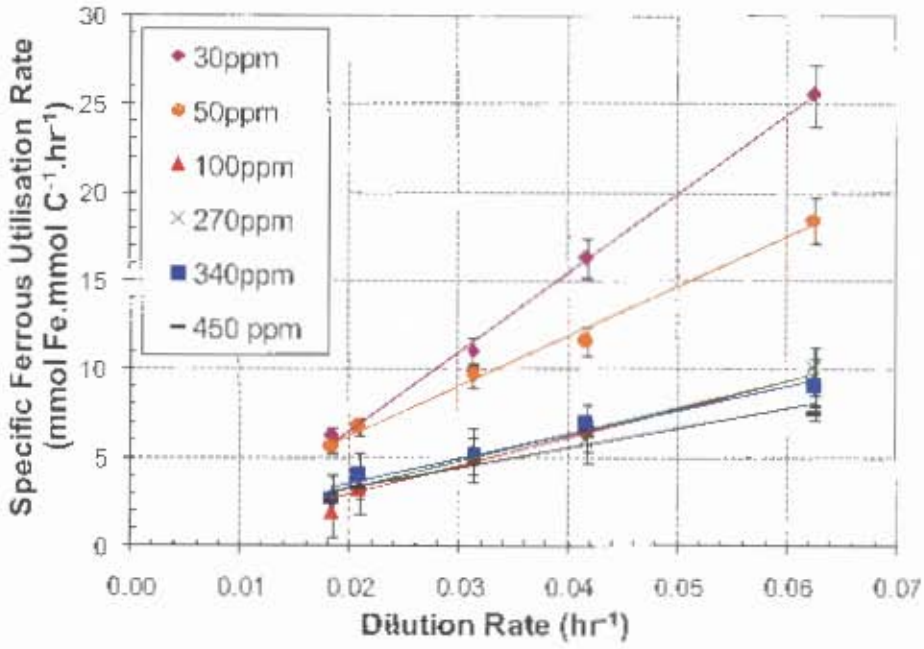

Figure 4-4. Specific ferrous iron utilisation rate vs dilution rate for carbon dioxide concentrations between 30 ppm and 450 ppm in steady state culture of *L. ferriphilum* calculated according to Method B (Off-gas Data)

As mentioned in Section 4.2.3, using the Pirt Equation, growth yield and maintenance can be determined for each experimental run. The maximum growth yield on ferrous iron, $Y_{X/Fe^{2+}}^{max}$ represents the biomass yield on the substrate and the maintenance term, $m_{Fe^{2+}}$ provides a measure of energy diverted to cell maintenance.

The maintenance terms and yield coefficients were calculated using the data generated by Method A and Method B and are shown in Table 4-14. On inspection of the plots of $q_{Fe^{2+}}$ as a function of μ (equivalent to D where cell death is negligible in the steady state chemostat), the gradient of the slope is equivalent to the inverse of the yield, and the y-axis intercept is equal to the maintenance coefficient. Since the gradient of the trend lines from 100 ppm to 450 ppm is relatively constant, it can be inferred that the yield was relatively constant.

Table 4-14. Rate analysis of CO_2 limitation experiments using Method A and Method B

	Method A		Method B	
$[CO_2]$ ppm	$Y^{max}_{Fe^{2+}}$ (x10^{-1}) (mmolC/mmolFe)	$m_{Fe^{2+}}$ (mmolFe/mmolC.hr)	$Y^{max}_{Fe^{2+}}$ (x10^{-1}) (mmolC/mmolFe)	$m_{Fe^{2+}}$ (mmolFe/mmolC.hr)
30	2.38	-3.27	2.25	-2.36
50	3.39	-0.806	3.56	0.617
100	6.45	-0.771	6.24	-0.321
270	7.52	0.667	6.59	0.227
340	6.84	0.528	7.24	0.736
450	8.19	0.805	8.91	1.05

The yield on ferrous iron decreased significantly at gaseous carbon dioxide concentrations below 100 ppm. This means that less biomass was formed, which resulted in a yield of up to 66% less than the reactor supplied with enriched air (450 ppm). Marginally negative maintenance coefficients are not uncommon in previous kinetic rate studies conducted in CSTRs (Ojumu *et al.*, 2008) and have been explained in the following way. The trend-lines drawn are best-fit trend-lines and should possibly be forced to present zero as the minimum value. Furthermore, the negative values are only a small percentage of the maximum ferrous oxidation rates at high dilution rate (i.e. $q_{Fe^{2+}}^{max}$) and are therefore within an acceptable range. The only values that are not only marginally negative are those that for 30 ppm. Breed and Hansford (1996) did not encounter negative maintenance coefficients but the Ojumu *et al.* (2008) deviated more significantly from near ideal conditions and did encounter them. Ojumu *et al.* went on to suggest that the data be forced through zero in certain instances. The validity of the assumptions underpinning the use of this form of the Pirt equation should be tested.

Cell counts and biomass equivalents are shown in Table 4-15. The biomass equivalent was calculated from a dry weight measurement and cell numbers from cell counts, with the assumption that 50% biomass in *Leptospirilla* is carbon (Characklis & Marshall, 1990). The percentage of carbon used in biomass formation was calculated as the ratio of cell counts and biomass equivalents. The values presented are averages across all dilution rates. The cell counts determined for the runs at CO_2 concentrations below 100 ppm were significantly lower than for 100 ppm and above ($\approx 13 \times 10^6$ cells/ml c.f. 26×10^6 cells/ml). However, the ferrous oxidation rate remained high which suggested that the micro-organisms in the system were using more energy to sustain less cells. This suggests that an increasing amount of energy was used in functions other than cell growth. The yield calculated by both Method A and Method B assumed that all carbon dioxide was assimilated into active biomass. The carbon utilisation is further discussed and compared in Chapter 5. The carbon used for biomass formation is within 5% of 100%. Since the error associated with the analytical techniques is 5 to 6% and that there may be a bit of variation in the mass per cell, it can be concluded that all the carbon taken up by the cells is used in the formation of new biomass.

Table 4-15. Cell concentration and biomass equivalents for carbon dioxide concentrations

$[CO_2]$ ppm	[Cells] ($x10^6$ cells/ml)	Biomass Equivalent ($x10^6$ cells/ml)	% Carbon used for Biomass
30	12.1	12.2	98.6
50	13.4	13.0	103
100	25.9	27.8	94.8
270	24.3	24.1	101
340	23.2	24.1	96.8
450	25.4	26.3	97.1

It is known that the carbon dioxide which is taken up by the micro-organisms is used for biomass, cell maintenance and the production of extracellular organic compounds (Ingeldew, 1981). There appeared to be a close correlation between the amount of carbon assimilated by the cells and the biomass formed, where almost 95-100% of the carbon dioxide used by the microbial population was used for the formation of new biomass in all cases. These results confirm the theory that all carbon assimilated Is used in biomass formation in the planktonic system under the conditions studied.

4.4 Conclusions from planktonic study

As carbon dioxide availability in the sparge gas decreased, there was no change in the specific ferrous iron oxidation rate between 100 ppm and 340 ppm. Below 100 ppm, the specific ferrous iron oxidation rate increased because, although the ferrous oxidation rate remained largely unchanged, the cell concentration decreased. In the system studied, the activity of the cells was shown to be generally unaffected by the carbon dioxide concentration and availability until a critical point (circa <100 ppm in the headspace of a well-mixed system). At lower carbon dioxide concentrations, the metabolic flux of carbon dioxide was changed such that the ratio of carbon dioxide assimilation to energy required from ferrous iron oxidation changed.

Since the ferrous iron oxidation approaches 99.9% in all the runs between 100 ppm and 450 ppm, the ferrous iron concentration may also be a limiting factor, however, the fact that the degree of oxidation was reduced at higher residence times and lower carbon dioxide availability indicates that the test conditions were sufficiently sensitive to detect changes in ferrous oxidation rates. Work by Ojumu *et al.* (2008) has shown that the ferrous iron is >99% oxidised from runs with $[Fe^{2+}]_{inlet}$ between 2 g/l and 12 g/l with only a slight increase in biomass, resulting in an increase in $q_{Fe^{2+}}$ at higher ferrous loading which indicate that there is a capacity for more ferrous oxidation.

The stoichiometric relationship proposed does not hold under non-ideal conditions. This also implies that the off-gas analysis methods to infer ferrous iron oxidation can be used only where it is validated that changes in stoichiometry do not occur (i.e. near ideal conditions). This work has provided insight into the suitability of the stoichiometric relationship used in ferrous iron oxidation rate calculations and shown that it must be validated in the range that they are used. It has also shown that the specific ferrous oxidation rates increase as the carbon availability is reduced as there is less biomass performing the same amount of oxidation. However, there remains a relationship between the amount of carbon dioxide assimilated and the total biomass formed; indicating that almost all the carbon fixed by the cells is used in the formation of new biomass. Further work on the exact fate of the carbon is needed to substantiate this claim. Therefore, the stoichiometric relationship can be used under near-ideal conditions, but as deviation from ideal behaviour is induced, the direct counting of cells and measurement of ferrous oxidation rate is the most reliable method to calculate the specific ferrous iron oxidation rate.

It is also apparent that since there is little change in the specific ferrous iron oxidation rate above 100 ppm, that ferrous iron may be starting to become a limiting substrate, especially at the higher carbon dioxide concentration (270 ppm, 340 ppm and 450 ppm).

5. Results and Discussions II: Comparison of Planktonic and Sessile Populations

5.1 Ferrous iron oxidation and carbon uptake in planktonic and sessile systems

It has been theorised that cells suspended in solution, i.e. a planktonic population, behave differently to those attached to mineral ore, i.e. a sessile population. As the sessile population continually re-seeds the solution phase, it is not possible to study the sessile population in isolation practically, so the differences are inferred from the comparison of planktonic and sessile system and the planktonic only system. To establish the sessile population, a column containing unsterilized ceramic saddles to provide a solid surface for the micro-organisms to attach was coupled to the bioreactor and the liquid circulated from a stirred tank through the column at a 70 to 80x recycle ratio as described in Section 3.6. The introduction of 180 g of 12mm ceramic saddles into a cylindrical column (4 cm diameter x 15 cm length) of volume 190 cm^3, provided 0.12 m^2 of surface area for the attachment of microbes (AceChemPack, 2010). No chemostatic attraction for attachment was provided, nor did the surface provide any nutrients or energy sources. Mineral ore was not used as it contains iron and possibly carbon which would interfere with the soluble iron concentration and the carbon balance across the system. It would be expected that the micro-organisms attached to the surface would use some of the carbon dioxide to produce EPS as well as for maintenance functions and possibly cell division. This would reduce the CO_2 available to the planktonic culture to form new biomass. The $[Cell]$ and the $Cell_{carbon\ equivalent}$ respirometry measurement can be used to test these theories. For convenience, the system containing dominantly planktonic cells is referred to as **System 1**, and the system with both planktonic and sessile microbes is referred to as **System 2**, as summarised in Table 5-1.

Table 5-1. Description of the planktonic and the sessile systems

System	Populations Present	Reactor Type	Reactor Volume (litres)	Ceramic Surface Area Provided (m^2)
System 1	Planktonic only	CSTR	1	-
System 2	Planktonic + Sessile	CSTR + Packed Column	1 + 0.19	0.12

While 2 to 4 residence times were required to reach steady state in System 1, between 5 and 9 residence times were required in System 2. This extension is expected to correlate with the time required for colonisation of the packing. Although it appeared that steady state was reached at the time of sampling, as gas measurements had levelled off to within 5%, it is possible that this was just a pseudo-steady state and that colonisation may have still been occuring on small scale in the column. As concluded from Chapter 4, the critical gas phase concentration at which the carbon dioxide concentration became limiting in the planktonic system was lower than 100 ppm, hence System 2 was only tested at the CO_2 concentrations of 340 ppm, 100 ppm, 50 ppm and 30 ppm. The solid phase was stripped of the sessile

residence time investigated at the respective carbon dioxide concentration used in order to quantify it. The solid phase was recolonised from the planktonic population at the new residence time and carbon dioxide supply rate.

5.1.1 Comparison of specific oxidation rate

System 2 was first investigated by supplying the oxygen and carbon dioxide requirement through normal compressed air, with an outlet CO_2 concentration of approximately 340 ppm. Respirometry data and the experimental spectrophotometry, AAS, cell counts and dry weight were used to calculate $q_{Fe^{2+}}$. The results were compared to its corresponding System 1 and the base case date for the ferrous oxidation rates is shown in Table 5-2. As the ferrous iron in System 1 was already largely oxidised (>98%), only a slight increase in ferrous iron oxidation rate was possible in System 2.

Table 5-2. Comparison of ferrous iron oxidation rates between System 1 (planktonic) and System 2 (planktonic +sessile) using Method 1 (spectrophotemtry and A.A.S), Method 2 (reduction-oxidation potential and A.A.S) and Method 3 (off-gas data) of *L. ferriphilum* in continuous culture at steady state and 37°C using a ferrous iron feed concentration of 5 g/L and air exiting the reactor with a carbon dioxide concentration of 340 ppm

Dilution Rate (hr^{-1})	Ferrous Iron Oxidation Rate (mmolFe/hr)					
	System 1			System 2		
	Method 1	Method 2	Method 3	Method 1	Method 2	Method 3
0.021	1.89	1.84	1.89	1.81	1.84	1.89
0.018	1.59	1.62	1.59	1.59	1.62	1.67
0.031	2.73	2.76	2.73	2.67	2.72	3.13
0.042	3.74	3.68	3.73	3.56	3.63	4.03
0.063	5.93	5.52	5.88	5.36	5.45	5.86

Looking at the values for the 340 ppm experiments at the lowest residence time of 16 hrs, corresponding to ***D*** at 0.063 hr^{-1} (where the effects are most significant), the increase in the ferrous iron oxidation rate of System 2 remained largely unchanged compared to System 1. However, there was an increase in the carbon dioxide uptake rate in the sessile system (0.0287 mmol/hr vs 0.0169 mmol/hr in the planktonic system using respirometry data). This was typically interpreted as an increase in microbial population in System 1, but is discussed further in the Section 5.1.2. Raw data for all the experiments are provided in Appendix E. The ferrous oxidation rates for the remaining experiments are shown in Table 5-3. These data show that the ferrous iron is near complete oxidation (in all instances). This fact, coupled with the increase in carbon dioxide uptake rate, indicating that carbon dioxide is probably not limiting and that there is a demand on ferrous iron which is not met by the current experimental set-up and the system may therefore be limited with respect to ferrous iron.

Table 5-3. Comparison of ferrous iron oxidation rates as a function of CO_2 concentration of *L. ferriphilum* in continuous culture at steady state and 37°C using a ferrous iron feed concentration of 5 g/L

$[CO_2]$ ppm	Dilution Rate (hr^{-1})	Ferrous Iron Oxidation Rate (mmolFe/hr) Method 1	Method 2	Method 3
30 ppm	0.021	1.84	1.82	1.82
	0.018	1.61	1.60	1.60
	0.031	2.74	2.71	2.72
	0.042	3.55	3.66	3.67
	0.063	5.34	5.50	5.51
50 ppm	0.021	1.81	1.84	1.84
	0.018	1.60	1.63	1.64
	0.031	2.73	2.78	2.79
	0.042	3.67	3.74	3.74
	0.063	5.51	5.60	5.62
100 ppm	0.021	1.78	1.87	1.87
	0.018	1.57	1.64	1.64
	0.031	2.66	2.79	2.79
	0.042	3.60	3.61	3.62
	0.063	5.40	5.44	5.44

Although there was little increase in the ferrous iron oxidation rate compared to System 1, the concomitant increase in biomass with the limited availability of ferrous iron resulted in a reduction of the specific oxidation rate. System 2 was also studied at gaseous phase carbon dioxide concentrations of 100 ppm, 50 ppm and 30 ppm. These data are shown in Tables 5-3 and 5-4, and then presented graphically in Figures 5-1 to 5-4 in terms of specific ferrous iron oxidation rate for 340 ppm, 100 ppm, 50 ppm, and 30 ppm respectively. The biomass present is further discussed in Section 5.1.2.

Table 5-4. Comparison of specific ferrous iron oxidation rates as a function of CO_2 concentration of *L. ferriphilum* in continuous culture at steady state and 37°C using a ferrous iron feed concentration of 5 g/L

$[CO_2]$ ppm	Dilution Rate (hr^{-1})	Specific Ferrous Iron Oxidation Rate mmolFe/(mmolC.hr) Method A	Method B
30 ppm	0.021	3.34	3.71
	0.018	3.01	3.12
	0.031	5.74	8.67
	0.042	8.16	13.0
	0.063	12.1	17.8
50 ppm	0.021	2.58	3.26
	0.018	2.47	2.81
	0.031	4.35	5.66
	0.042	5.72	7.98
	0.063	8.87	11.3
100 ppm	0.021	1.52	2.51
	0.018	1.22	2.01
	0.031	2.29	3.49
	0.042	3.24	4.61
	0.063	4.76	7.22
340 ppm	0.021	1.68	2.28
	0.018	1.52	1.60
	0.031	2.13	3.40
	0.042	2.67	4.53
	0.063	5.04	7.35

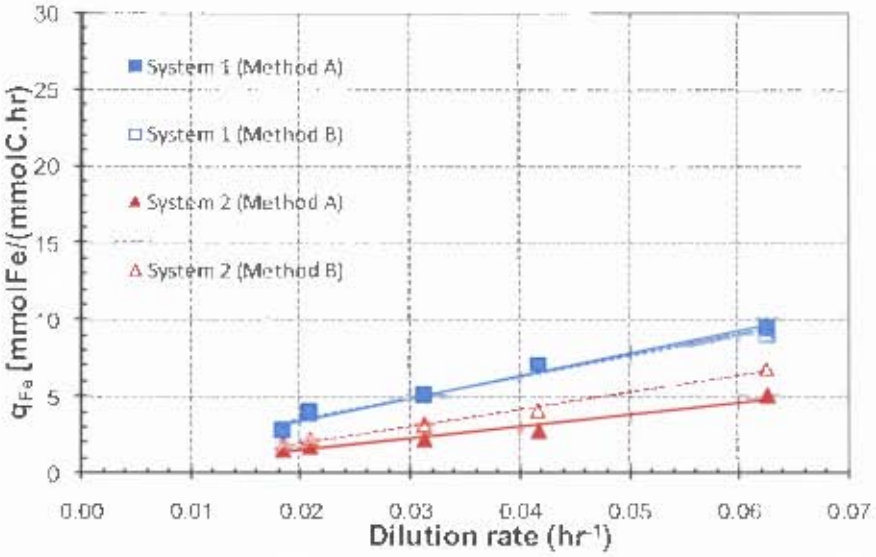

Figure 5-1. Specific ferrous iron utilisation vs dilution rate for System 1 (planktonic) and System 2 (sessile + planktonic) in steady state culture sparged with air exiting at 340 ppm CO_2. Closed symbols, solid lines calculated from wet chemistry and cell counts. Open symbols, dotted lines calculated from respirometry data.

In Figure 5-1, it appears that the specific oxidation rate of System 2 was lower than that in the planktonic System 1. For conformity, the closed symbols and solid trend-lines represent values calculated using data from spectrophotometry, A.A.S, cell counts and the dry weight analysis according to Method A. The open symbols and the dashed trend-lines depict values calculated from off-gas data according to Method B. To quantify biomass in the sessile system, sessile cells were removed from the solid support by washing twice with Tris buffer. Counting of these cells allowed the determination of total cells in System 2 (used in calculations for Method A).

It must be noted that the specific ferrous iron oxidation rate calculated for Method A and Method B now represented different quantities after the addition of a sessile population. In Method A, $q_{Fe^{2+}}$ represented the amount of ferrous iron oxidised per total biomass present, whereas in Method B, $q_{Fe^{2+}}$ represented the amount of ferrous iron oxidised per carbon assimilated, (assumed to represent the new biomas formed). In this way, these two values depict different quantities.

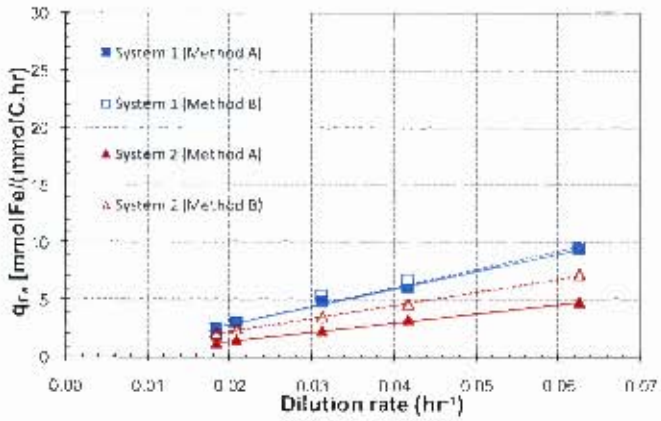

Figure 5-2. Specific ferrous iron utilisation vs dilution rate for System 1 (planktonic) and System 2 (sessile + planktonic) in steady state culture sparged with air exiting at 100 ppm CO_2.

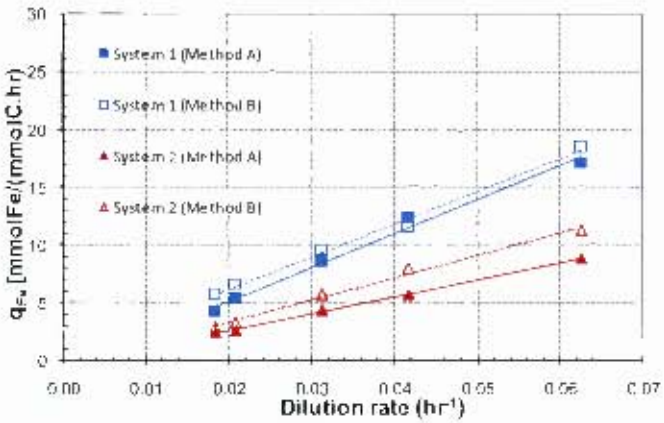

Figure 5-3. Specific ferrous iron utilisation vs dilution rate for System 1 (planktonic) and System 2 (sessile + planktonic) in steady state culture sparged with air exiting at 50 ppm CO_2.

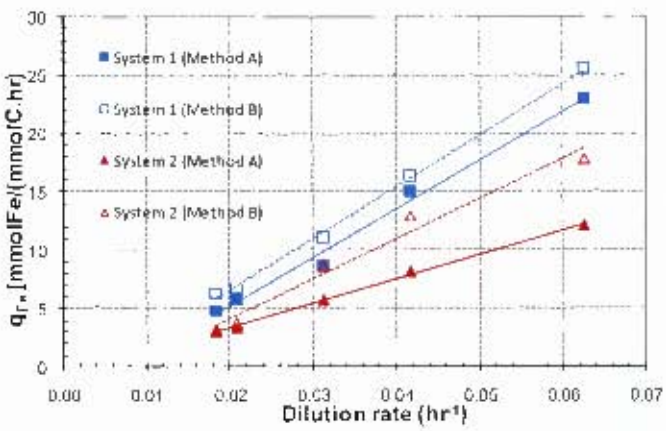

Figure 5-4. Specific ferrous iron utilisation vs dilution rate for System 1 (planktonic) and System 2 (sessile + planktonic) in steady state culture sparged with air exiting at 30 ppm CO_2. Closed symbols, solid lines calculated from wet chemistry and cell counts. Open symbols, dotted lines calculated from respirometry data.

For easy comparison, the results across the carbon dioxide concentrations for System 2 are presented in Figure 5-5 (note that the y axis maximum has been lowered to 20 mmolFe/(mmolC.hr) for clarity).

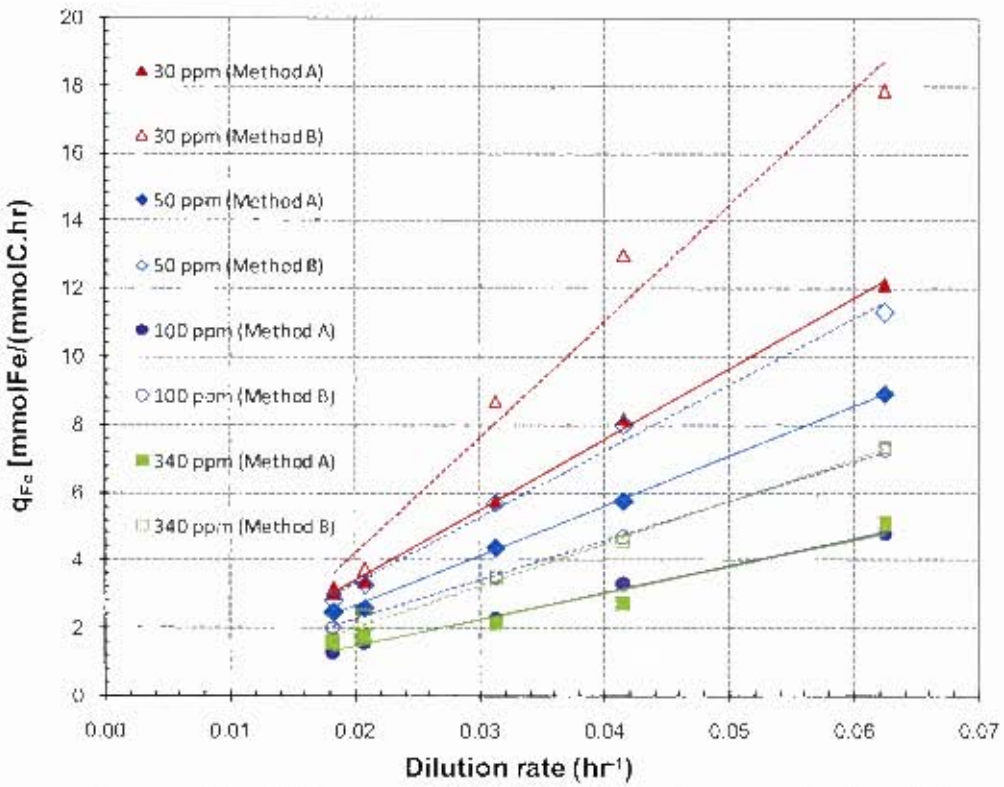

Figure 5-5. Summary of specific ferrous iron utilisation vs dilution rate for System 2 (sessile + planktonic) in steady state culture over a range of CO_2 concentrations. Closed symbols, solid lines calculated from wet chemistry and cell counts. Open symbols, dotted lines calculated from respirometry data.

The specific ferrous oxidation rates as a function of carbon dioxide concentration in System 1 have been discussed in Section 4.3. The trend from System 1, where there was an increase in specific ferrous iron oxidation rate with a decrease in carbon dioxide availability, was carried through into System 2 with the inclusion of a sessile population. It is also apparent that the specific oxidation rate for all the runs in System 2 were lower than its corresponding run in System 1. This resulted from the retained population, i.e. the sessile phase which are not lost from the reactor with flow, resulting in a larger biomass present. Figure 5-5 emphasises the phenomenon by which the specific ferrous iron oxidation rate calculated by Method A is lower than that calculated by Method B (especially under low carbon dioxide supply rates). It is postulated that the rate measured by off-gas analysis (Method B) yields a different value as the assumption on which these values are calculated (i.e. that all the carbon assimilated is used in the formation of active biomass) no longer holds. Method A, using direct quantification and wet chemistry analysis did not rely on this assumption. Furthermore, it took into account the total biomass present, not only the new biomass formed. This difference does not occur in the planktonic System 1 and the assumption holds under those conditions.

Table 5-5 (c.f. Table 4-9) also illustrated that the number of cells calculated to be formed from carbon dioxide taken up steady state was not equal to the actual number of cells present, as it was in the planktonic System 1. This can be attributed to the retained population which is not accounted for by the stoichiometric relationship in Equation 6. It is postulated that in the sessile population which remains attached to the surface, there exist cells that are less active than the normal biomass. Further, a long time was required to reach steady state owing to an accumulation of carbon in the system.

Table 5-5. Ratio of carbon fixed to produce biomass to carbon fixed in experiment at steady state in System 2

$[CO_2]$ ppm	Total Cells in System ($x10^9$ cells)	Biomass Equivalent ($x10^9$ cells)	(Carbon in system estimated based on cell number) / (Carbon fixed in experiment)
30	21.4	16.6	1.28
50	28.4	22.4	1.27
100	51.4	33.1	1.55
340	50.6	36.3	1.39

The biomass equivalent was calculated from respirometry data and cell mass assuming the stoichiometric ratio previously reported. As cells are retained, it was expected that the number of cells counted in the system would be more than the cell number calculated for the steady state uptake of carbon dioxide, equivalent to cells formed. Hence the ratios do not approximate 1 as they did for System 1 in Table 4-9. Cell counts were performed to determine the percentage of carbon dioxide used to form new biomass, as well as the amount used to form other organic compounds in solution. This is further discussed in Section 5.1.2.

5.1.2 Comparison of cell counts, biomass and organic carbon

In System 1, a cell count resulted directly in the cell concentration, $[Cell]$ as a number of cells/ml. In System 2, the cell concentration in the planktonic phase represented only a portion of cells in the system. Cells in the sessile phase were attached to or entrained in the solid support. This steady state cell number was measured at the end of each run on sacrificing the column and detaching the biomass. Therefore, at the end of each residence time at each carbon dioxide concentration, the cells were counted in the planktonic phase in the reactor. Furthermore, the sessile population was counted following detachment by washing twice with Tris buffer. The cells in the sessile phase were counted as a concentration of the wash solution. To allow for comparison, the basis of the 1 litre reactor was chosen. Therefore, using C_x in cells/ml and V in ml, the number of cells in the systems can be represented as follows:

In System 1:

$$N_{System1} = N_{Planktonic,System1} = C_{xPlanktonic,System1} \times V_{System1} = 1000 \cdot C_{xPlanktonic,System1}$$

In System 2:

$$N_{System2} = N_{Planktonic,System2} + N_{Sessile,System2}$$
$$= C_{xPlanktonic,System2} \times V_{System2} + C_{xSessile,System2} \times V_{washwater,System2}$$

The results from the reactor with a carbon dioxide outlet concentration of 340 ppm are shown in Figure 5-6. Although the total number of cells in System 2 was two to three times higher than in System 1, the number of planktonic cells in System 2 was slightly lower than that in System 1. The total number of planktonic cells was largely constant across all the dilution rates (20-25 x 10^9 cells in System 1 and 16-20 x 10^9 cells in System 2). The total number of cells in System 2 varied between 45x10^9 and 60x10^9 cells in the 1 litre system.

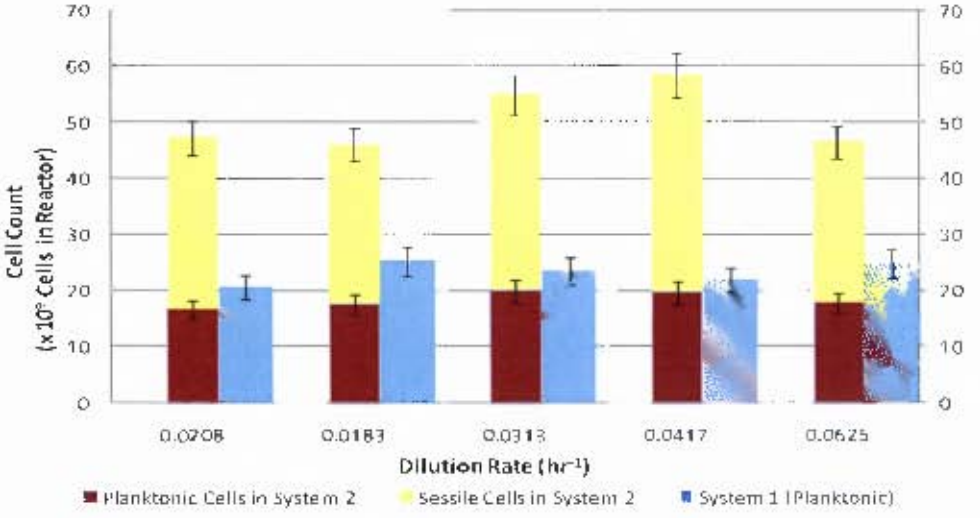

Figure 5-6. Cell counts for populations in System 1 and System 2 in steady state culture sparged with gas exiting at 340 ppm CO_2

This procedure was repeated for experiments run at 100, 50 and 30 ppm. The values compared were:

- the total number of cells in System 2 at different CO_2 concentrations
- the number of planktonic cells in System 2 compared to System 1
- the ratio of sessile cells to planktonic cells in System 2.

These trends are not consistent across all the CO_2 concentrations. The results for the experiments with System 2 at effective carbon dioxide concentrations of 100 ppm, 50 ppm and 30 ppm are shown in Figure 5-7, Figure 5-8 and Figure 5-9 respectively. Figure 5-7 shows that, at 100 ppm, the average number of cells in System 1 was similar to that in the experiment at 340 ppm carbon dioxide. The planktonic population in System 2 remained lower than that in System 1, and a similar two to three fold increase in the total number of cells in System 2 with respect to System 1 was observed, resulting in a total number of cells in System 2 of 45-60x10^9 on sparging at both 100 and 340 ppm CO_2. A repeat run was performed for the 340 ppm data set and the error associated was found to be 9.8%. This error was then used as a typical error and applied to the other data sets.

On sparging with a resulting CO_2 concentration of 50 ppm, the number of planktonic cells in System 1 again remained higher than that in System 2 as shown by Figure 5 8. However, the number of planktonic cells was approximately 50% of that reported at 100 ppm and 340 ppm CO_2 (9-12x10^9 cells at 50 ppm compared with 18-26x10^9 cells at 100 and 340 ppm CO_2). The ratio of total cells in System 2 compared to System 1 decreased from an average of 2.5 (at 100 and 340 ppm CO_2) to an average of 2 (at 50 ppm CO_2), however, this is not significant given that the error associated. The total cell number in System 2 decreased from 45-60x10^9 cells on sparging with air to 28-30x10^9 cells on sparging with 50 ppm carbon dioxide.

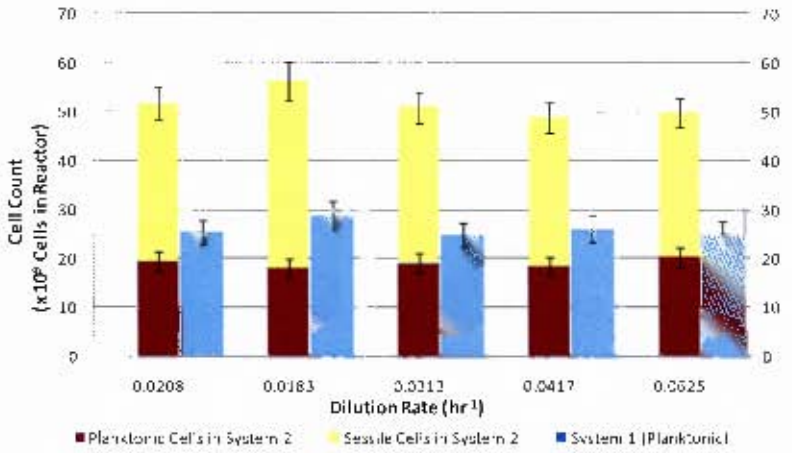

Figure 5-7. Cell counts for populations in System 1 and System 2 in steady state culture sparged with gas exiting at 100 ppm CO_2

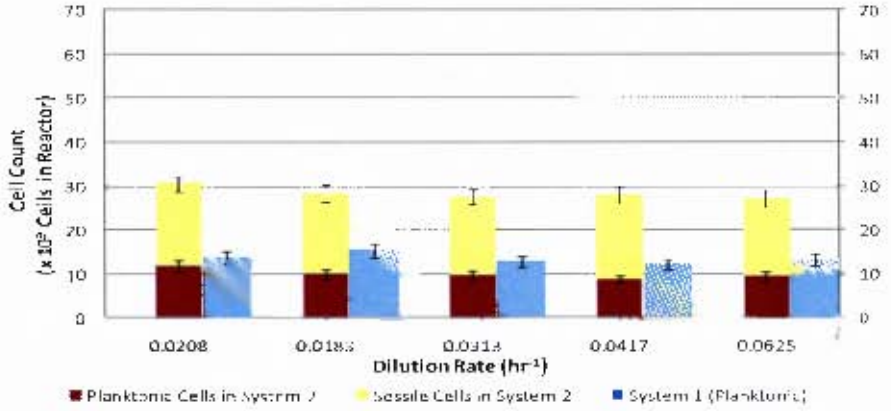

Figure 5-8. Cell counts for populations in System 1 and System 2 in steady state culture sparged with gas exiting at 50 ppm CO_2

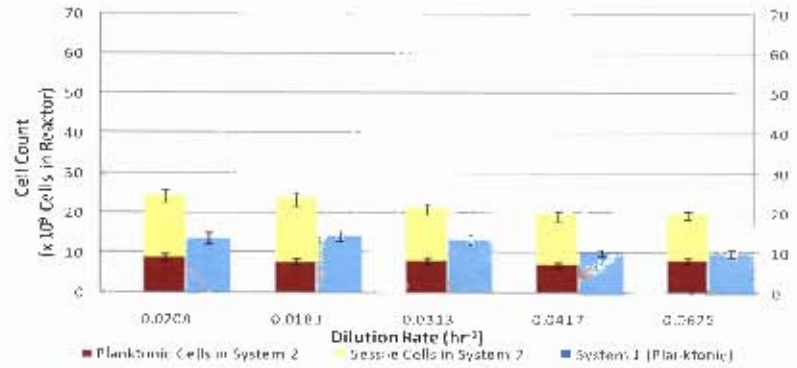

Figure 5-9. Cell counts for populations in System 1 and System 2 in steady state culture sparged with gas exiting at 30 ppm CO_2

Figure 5-9 shows that this trend was accentuated at a carbon dioxide concentration of 30 ppm. The total number of cells in the 1 litre system at 30 ppm CO_2 concentration was 20-25x10^6 cells while the ratio of total cells in System 2 compared to System 1 remained at approximately 2.0. The ratios between the total number of cells in each system and the number of sessile cells to planktonic cells in System 2 are summarised in Table 5-6 and Table 5-7 respectively. There do not appear to be any strong trends in these tables.

Table 5-6. Ratio of total cells in System 2 to total cells in System 1 in steady state culture over a range of CO_2 concentrations with *L. ferriphilum* at 37°C and 5 g/L ferrous iron in feed

[CO_2]	Dilution Rate (hr^{-1})				
ppm	0.021	0.018	0.031	0.042	0.063
30	1.79	1.67	1.60	1.91	2.00
50	2.23	1.86	2.15	2.31	2.07
100	2.04	1.96	2.06	1.88	1.99
340	2.29	1.81	2.35	2.67	1.89

Table 5-7. Ratio of sessile cells in System 2 to planktonic cells in System 2 in steady state culture over a range of CO_2 concentrations with *L. ferriphilum* at 37°C and 5 g/L ferrous iron in feed

[CO_2]	Dilution Rate (hr^{-1})				
ppm	0.021	0.018	0.031	0.042	0.063
30	1.75	2.13	1.68	1.77	1.48
50	1.58	1.84	1.84	2.21	1.90
100	1.66	2.10	1.67	1.64	1.45
340	1.85	1.63	1.75	1.97	1.61

Total organic carbon (TOC) in solution in the system was measured. The total organic carbon associated with the sessile population was measured as the concentration in the wash water (Tris buffer) and back-calculated to the amount in the 1 litre bioreactor as with the cell concentration, as the cells were dislodged. The suspensions from which the TOC measurements were taken was not hydrolysed to break down the organic carbon, nor was it treated in any way to cause cell disruption. The results for the run at

340 ppm CO_2 are shown in Figure 5-10. A three to fourfold increase in the amount of organic carbon in System 2 with respect to System 1 was observed. This is the consistent with the expectation of increased TOC owing to EPS production in the presence of the solid phase. The increase in TOC in the sessile environment was greater than the increase in cells in the sessile environment, supporting the production of EPS (equivalent to the extra TOC) by the presence of the solid phase. The error associated with TOC reading was calculated as less than 5% for the 340 ppm repeat data and this was applied as a typical error to the subsequent data sets.

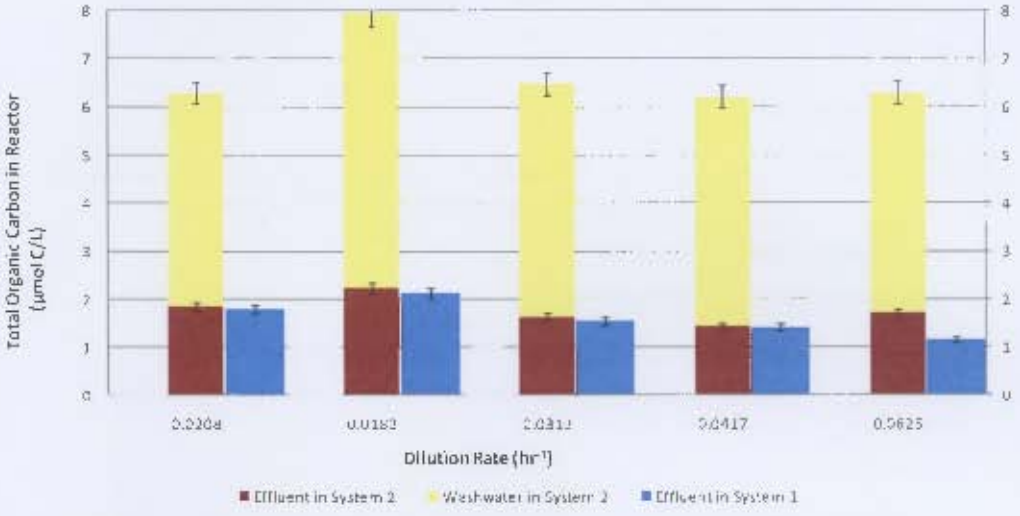

Figure 5-10. Total organic carbon for populations in System 1 and System 2 in steady state culture sparged with gas exiting at 340 ppm CO_2

The total organic carbon, measured for System 2 with carbon dioxide concentrations of 100 ppm, 50 ppm and 30 ppm in the exit gas, are shown in Figure 5-11, Figure 5-12 and Figure 5-13 respectively. The results measured from the planktonic system (System 1) are given for comparison. At 50 ppm and higher, there is clearly an increased amount of TOC in the sessile phase which can be attributed to the production of EPS by the sessile cells. The TOC in the overall System 2 decreased with decreasing carbon dioxide availability (3.5-5.0 μmolC/L at 50 ppm c.f. 4.0-8.0 μmolC/L at 340 ppm), however the TOC in the planktonic phase of System 2 remained lower than that of System 1. At 30 ppm, the TOC in the planktonic phase increased to 2.5 μmolC/L (c.f. 0.89 μmolC/L at 50 ppm). The TOC in the planktonic phase in System 2 was higher than that in System 1. Further, the TOC associated with the sessile cells was greatly reduced (≈ 1 μmolC/L c.f. 2.5-4.0 μmolC/L at 50 ppm) which was different to results from all other carbon dioxide concentrations and suggests a shift in carbon metabolism. It should be noted that despite the increase, in the overall carbon balance, TOC increased from an average of 0.4% to a maximum of 2.0% of the total carbon assimilated.

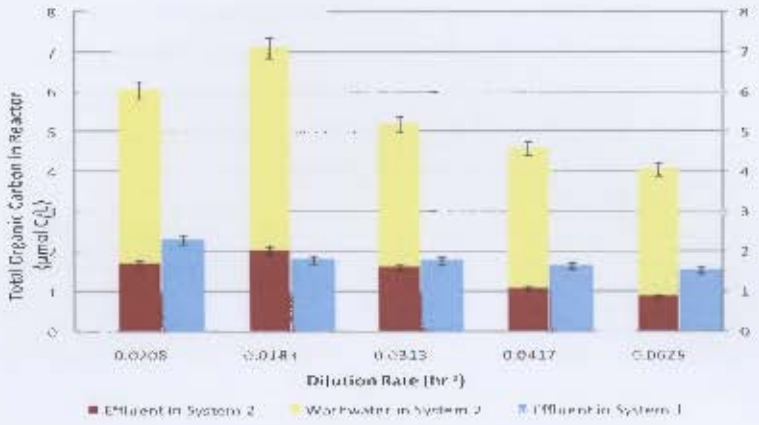

Figure 5-11. Total organic carbon for populations in System 1 and System 2 in steady state culture sparged with gas exiting at 100 ppm CO_2

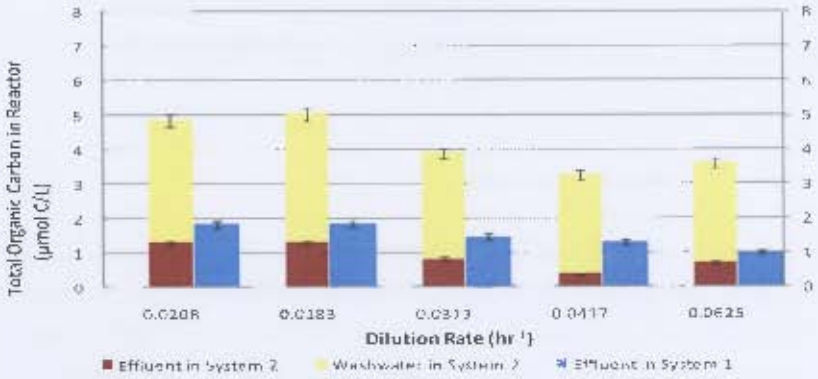

Figure 5-12. Total organic carbon for populations in System 1 and System 2 in steady state culture sparged with gas exiting at 50 ppm CO_2

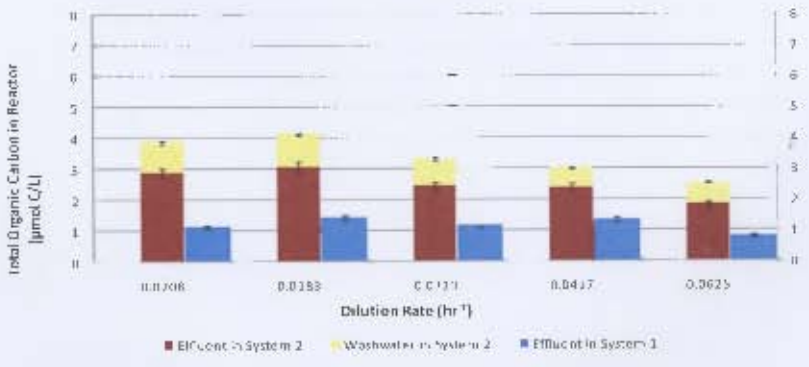

Figure 5-13. Total organic carbon for populations in System 1 and System 2 in steady state culture sparged with gas exiting at 30 ppm CO_2

In System 1 (planktonic), the TOC decreased with decreasing carbon dioxide availability from 1.1-2.0 μmolC/L at 340 ppm to 0.8-1.4 at 30 ppm. In the planktonic phase of System 2, there is an increase to above the levels of the planktonic System 1 with decreasing carbon dioxide availability, (2.0-3.0 μmolC/L at 30 ppm c.f. 1.4-2.2 μmolC/L at 340 ppm). In the sessile phase of System 2, there is a dramatic decrease in the TOC with a decrease in carbon dioxide availability at 30 ppm (0.6-1.0 μmolC/L at 30 ppm c.f. 4.0-6.0 μmolC/L at 340 ppm). At carbon dioxide concentrations of 50 ppm and higher, the TOC was clearly associated with the sessile phase and can therefore be attributed to the formation of EPS. At 30 ppm it was associated with the planktonic phase and not the sessile phase. This may most probably be attributed to the production of stress proteins or carbon concentrating proteins, while carbon dioxide limitation limited the formation of EPS. The relationship between cell numbers and extracellular total organic carbon is compared across the systems in Table 5-8. The values used are averages over the dilution rates investigated. It is apparent that the introduction of sessile population increased the amount of organic carbon in the systems.

Table 5-8. Total organic carbon per unit biomass for each system over the range of carbon dioxide concentrations

$[CO_2]$ ppm	**Total Organic Carbon present per Unit Biomass** (x 10^{-2} μmol C/cell)		
	Planktonic System 1	Planktonic System 2	Sessile System 2
30	12.2	32.6	6.25
50	11.0	6.65	17.49
100	6.91	7.59	12.19
340	6.90	9.61	15.11

The key ratios of populations and the concentrations of total organic carbon monitored are summarised in Figure 5-14. Again, averages across the dilution ranges were used as the data points. The figure shows that the ratios remain largely unchanged across the range of carbon dioxide concentrations except that there is significantly more TOC in the planktonic phase of System 2 compared to System 1. This supports the notion that the carbon utilisation changes at the lower carbon dioxide availability.

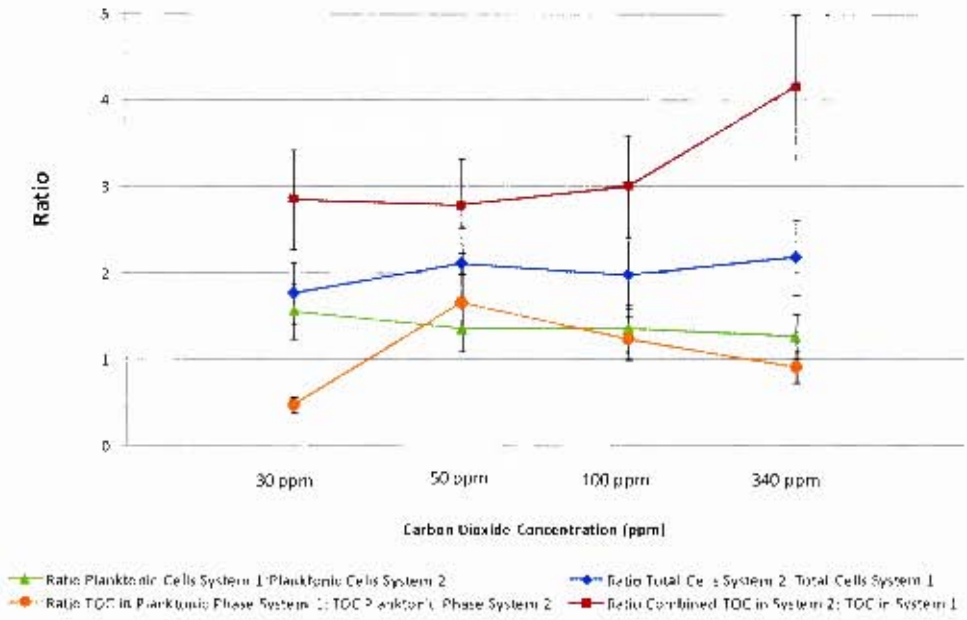

Figure 5-14. Comparison of ratios of total organic carbon in System 1 to total organic carbon in the planktonic phase and in the entire System 2, and ratios of cells in System 1 to planktonic and total cells in System 2, across the range of 30 to 340 ppm carbon dioxide

The organic carbon composition from both systems was also analysed using HPLC to detect organic acids. It must be noted that samples were not hydrolysed so complex carbohydrates would not be shown. The organic acids, namely acetate, lactate, propanoate and pyruvate were detected. A control was also performed with acidified ferric sulphate solution to find a baseline for integrating the curves. These results are shown in Table 5-9 from the 32 hr residence time at 340ppm.

Table 5-9. Organic acid concentration measured by HPLC in the TOC of System 1 and System 2 at 340 ppm CO_2 concentration and 5 g/L ferrous iron

	System 1		System 2		Ratio of concentration
Organic Acid	µmol/L	% of total	µmol/L	% of total	in Sytem 2: Sytem 1
acetate	0.117	14.2%	0.038	8.1%	0.326
lactate	0.327	39.5%	0.098	20.9%	0.301
propanoate	0.317	38.3%	0.048	10.1%	0.150
pyruvate	0.067	8.0%	0.287	60.9%	4.300
total organic acid detected	0.828		0.471		0.568

5.2 The decoupling study

In the presence of a solid phase, the amount of biomass in the system increased up to threefold under steady state conditions. However, the planktonic cell concentration in System 2 decreased by 20% with respect to the purely planktonic System 1. Owing to the limited availability of ferrous iron, the concomitant increase in the ferrous iron oxidation rate was small, hence the specific oxidation rate was reduced. The ferrous iron was >98% oxidised before the inclusion of the solid phase (and >99.8% oxidised with the inclusion of the solid phase). Hence, it is unclear whether the sessile cells were capable of functioning at a higher ferrous iron oxidation rate.

A decoupling study was undertaken to measure the performance of the sessile cells in an environment where they were not constrained by ferrous iron availability. This was carried out under dynamic conditions due to the constraints mentioned in Section 5.1.2. The method for the decoupling study is outlined in Section 3.6.3. **R1** refers to the reactor containing the planktonic population from which the column containing the sessile phase was removed at decoupling. **R2** refers to the sessile phase attached to the new abiotic reactor after decoupling.

Off gas analysis was used to determine the ferrous oxidation rate and the microbial growth rate. The redox potential and the number of planktonic cells were also monitored. The number of sessile cells in the system could only be quantified by sacrificing the packed bed column. While the carbon dioxide uptake rate has been shown to provide an estimation of growth rate, it could not be used to quantify the biomass equivalent of sessile cells in this study, owing to a bulk of biomass being introduced into the system independently of carbon dioxide uptake. Therefore, the biomass equivalent was not an accurate representation of the biomass in the decoupling study and is not reported.

The same decoupling experiment was repeated in a subsequent study; the colonized column was re-attached to a reactor with 5 g/L ferrous feed at a dilution rate of 16 hours (compared to 32 hours). The column containing the solid support washed out. Under normal planktonic conditions in a CSTR, washout of *L. ferriphilum* at 37°C was previously reported at a dilution rate of 14 hrs (Ojumu, 2008). It is likely that the bacteria, from the packed column moved into the planktonic phase and then washed out before they had a chance to adapt to the new culture environment and multiply at the required growth rate.

The actual specific oxidation rate, defined as the ferrous iron oxidation rate per unit biomass, cannot be measured through the course of the experiment as the sessile population was only quantified on sacrificing the column. This cannot therefore be quantified while taking measurements in a dynamic study. The ferrous iron oxidation rate per unit carbon assimilated could be calculated and provided some useful insights discussed in this section.

5.2.1 *The behaviour of the planktonic population (R1) in the decoupling study*

The off-gas data from the STR containing the planktonic cells following its decoupling from the packed column are shown in Figure 5-15. The system returned to steady state after 3 hours. This new steady state reached was comparable to the steady state of a standard CSTR reactor run in the absence of the packed column, as shown by the CO_2 and O_2 uptake rate and its comparison to System 1. The values for the $-r_{O_2}$ and the $-r_{CO_2}$ in the System 1 under steady state condition in the same reactor were reported as 0.665 mmol/(l.hr) and 0.0169 mmol/(l.hr) respectively and are shown on Figure 5-15.

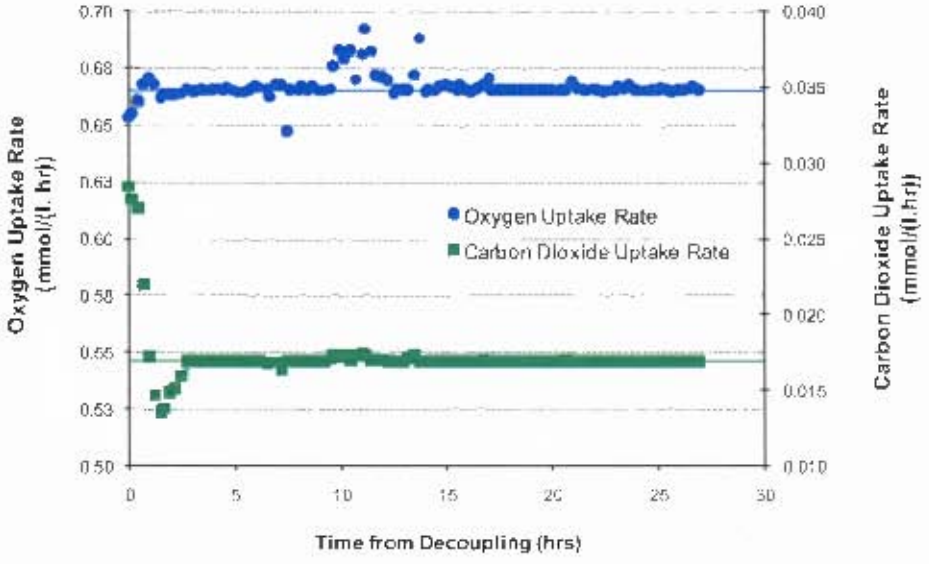

Figure 5-15. Gas uptake rates for planktonic system (R1) operated at a residence time of 32 hr and sparged compressed air, starting at the point of decoupling. The lines show the steady state readings for System 1.

The ferrous iron oxidation rate was inferred from off gas analysis. A steady state ferrous iron oxidation rate for System 1 has been reported as 2.73 mmolFe/hr, which is the same value calculated from respirometry data. This is not surprising as the measurements for the carbon dioxide uptake rate and the oxygen uptake rate are shown to be the same as the planktonic System 1 from Figure 5-15.

5.2.2 *The behaviour of the sessile population (R2) in the decoupling study*

Figure 5-16 shows the gas uptake rates for the sessile system (R2) from the point of decoupling. The oxygen uptake rate remained consistently high at approximately 0.65 mmol/(l.hr), while the carbon dioxide uptake rate increased slowly from approximately 0.016 mmol/(l.hr) following decoupling to a value of 0.025 mmol/(l.hr). It is likely that the system has not yet reached steady state as the former steady state (shown on Figure 5-16) has not yet been reached. Furthermore, the data for the oxygen uptake rate is still dynamic and values are not within 10% of each other. As mentioned in Section 5.1, when starting any new experiment set up as System 2, between 5 and 9 residence times were needed to reach steady state to accommodate the colonising, or recolonising, of the packed column. In this instance, the sessile population was first required to colonise the planktonic system, whereafter the population of

sessile cells would need to be re-established to former levels. The region of interest in this study is the initial dynamic period represented by the first few hours where the sessile population is acting independently of the planktonic systems.

The carbon dioxide uptake rate decreased from 0.028 to 0.016 mmol/(l.hr) in decoupling of the reactors, indicating that some 50% of the carbon dioxide assimilation capacity of the coupled reactor was resident in the packed column. For the first 4 hours the carbon dioxide uptake rate remained at an average of 0.016 mmol/(l.hr). This represented the sessile population largely without any planktonic cells present. The planktonic population built up slowly over the next 24 hours.

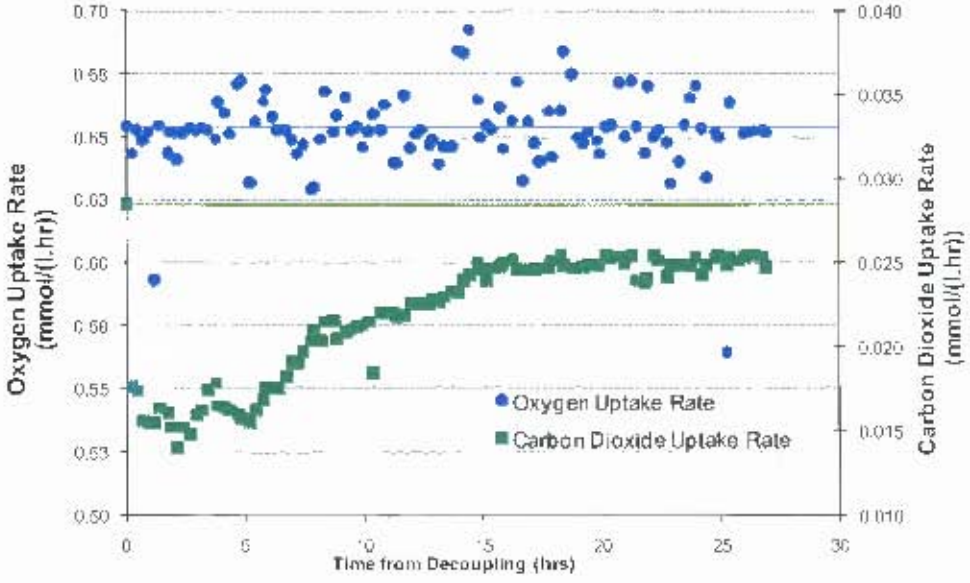

Figure 5 16. Gas uptake rates of sessile System (R2) operated at a residence time of 32 hr and sparged with compressed air, starting at the point of decoupling. The lines show the steady state readings for System 2

The oxygen uptake rate was an order of magnitude greater than the carbon dioxide uptake rate. This rate could be related to ferrous iron oxidation rate, meaning that the ferrous oxidation rate remained constantly high. The ferrous iron oxidation rate per unit carbon assimilated decreased as the carbon biomass increased in the planktonic phase.

The objective of these experiments was to determine whether the sessile population is capable of performing at a higher ferrous iron oxidation rate if supplied with additional ferrous iron. There was little change in the ferrous oxidation rate on removal of planktonic cells, illustrating the potential increase in the specific ferrous iron oxidation rate (as the carbon dioxide uptake remained lower than the coupled system while still achieving >95% oxidation of ferrous iron). The specific ferrous iron oxidation rate cannot be calculated directly without knowing the number of cells present in the sessile population and the planktonic population of System 2. This may require sacrificing the column as different points in the study. However, the $q_{Fe^{2+}}$ can be approximated using the ferrous iron oxidation rate calculated using

respirometry data to calculate the $-r_{Fe^{2+}}$ and using the microscopic cell counts from the sessile phase from the 32 hr residence time experiment in System 2 as an estimate for the biomass present. The resulting $q_{Fe^{2+}}$ is equal to 3.36 mmolFe/(mmolC.hr) compared to 5.05 mmolFe/(mmolC.hr) for the planktonic System 1 and 2.13 mmolFe/(mmolC.hr) for System 2 (by Method A). This shows that the sessile population is capable of higher oxidation rates that it is permitted in the experimental set-up of System 2.

This further suggests that the strong coupling between the ferrous iron oxidized and the carbon dioxide previously reported is not valid across a broad range of experimental conditions. Here, there occurred the same level of ferrous iron oxidation (2.70 mmol/hr) with almost half the carbon dioxide uptake rate (0.015 mmol/[l.hr] c.f. 0.027 mmol/[l.hr] in the coupled system). Thus, it appears that the biomass which is retained in the column, has the ability to perform at much higher oxidation rates than it does in the coupled system, and that the previous studies using System 2 were in fact ferrous iron limited.

5.3 Conclusion from sessile and planktonic studies

On the introduction of a solid phase, there is an increase in the cell concentration as a result of the retained population on the solid support. The rate of ferrous iron oxidation remains largely the same, and it has been suggested that the system has become ferrous limited as there was only a slight increase in the ferrous iron oxidation rate. The increase in biomass therefore results in a decrease in the specific ferrous iron oxidation rate. This suggested that the relationship between the ferrous iron oxidation rate and the carbon dioxide uptake rate is not fixed, nor is the relationship between the ferrous iron oxidation rate and the number of cells formed. It further suggested that cells use energy differently depending on whether they are in a sessile or planktonic phase.

The decoupling study was performed to address some of these issues. It suggested that the sessile population could oxidise ferrous iron at higher levels than it is permitted to in the experimental set up of System 2. Further work is needed to substantiate some of the hypotheses drawn from this section, but the dynamic data showed that in the sessile population, there can occur the same level of ferrous iron oxidation with a lower carbon dioxide uptake rate than the coupled system.

Total organic carbon increased with the introduction of a sessile population. The increase in TOC is thought to be associated with EPS production, further supported by the fact that it occurred mainly associated with the sessile population and that, under these conditions it was not composed predominantly of simple organic acids.

Sessile cells were also capable of colonising the planktonic phase faster than a planktonic system could colonise a solid support with sessile cells.

The study used a non-mineral solid support instead of the usual mineral support structure in order to ensure a consistent chemical environment. Although it was confirmed that the microbes did attach to the support structure, it is recognised that differences may be found in cell behaviour and excretion of organic compounds with a mineral support.

6. General Conclusions and Recommendations

In this novel study microbial growth and ferrous iron oxidation of *Leptospirillum ferriphilum* are investigated as a function of carbon dioxide concentration. Furthermore, the behaviour of planktonic and sessile populations were compared.

6.1 General conclusions

The following general conclusions can be drawn from this study:

- There existed a consistent stoichiometric relationship between the carbon dioxide uptake rate and the ferrous iron oxidation rate where carbon dioxide availability was sufficient, as found when provided by sparge gas at a carbon dioxide concentration of 100 ppm and above in planktonic cultures in the chemostat stirred tank reactor system used. Below 100 ppm, the stoichiometry of the relationship was changed. However, it was apparent that the carbon dioxide assimilated by the cells was all used in the production of active biomass in the planktonic system

- Below 100 ppm, there was an increase in the specific ferrous oxidation rate. This resulted from the ferrous iron oxidation rate remaining unchanged and a decrease in biomass concentration occuring.

- In the planktonic system, the carbon assimilated goes predominantly (>95% at residence times above 24 hrs) towards the formation of new biomass. This was confirmed by comparison of the cell counts, rate of carbon dioxide assimilation and the TOC readings and holds across the range of carbon dioxide availabilities and across all dilution rates investigated.

- Carbon dioxide enrichment to 450 ppm in this idealised planktonic system with good gas-liquid mass transfer did not yield an increase in the ferrous iron oxidation rate or the specific ferrous iron oxidation rate. Further work is needed to determine whether these results from a small scale idealised system will apply to the heap leach environment.

- A minimum concentration of carbon dioxide at which no microbial growth occurs was not observed, even at 30 ppm carbon dioxide availability. Below the detection limit of the carbon dioxide analyser, there was still a low level of microbial growth detectable by microscopic cell counts

- With the introduction of the sessile phase, there was a retained population of cells on the solid support resulting in an overall cell concentration of some 2 to 3 fold the normal planktonic system. Therefore, there was a decrease in the specific ferrous iron oxidation rate measured using direct measurements equivalent to overall biomass present. The data from off gas analysis

only accounted for the new biomass formed and its associated specific ferrous iron oxidation rate. This was and was closer (but not equal to) the planktonic system.

- Furthermore, there was a small change in the partitioning of carbon assimilated. This was reflected by the amount of total organic carbon produced (an average of 0.4 (for 340 ppm CO_2) to 1.6 % (for 30 ppm CO_2) of total carbon assimilated), the shift in organic acid profile, and the breakdown of the stoichiometric relationship previously upheld in planktonic cultures. Therefore, the use of the stoichiometric relationship to infer the ferrous iron oxidation rate needs to be validated within the range it is used.

- In System 2, a decrease in carbon dioxide availability resulted in support of a lower total population, as in System 1. The fate of carbon assimilated in System 2 changed with the introduction of a solid support. Analysis of the total organic carbon suggested that carbon was used for the production of EPS with the introduction of a sessile population (across all carbon dioxide concentrations). This is further supported by the results from HPLC. At the low concentrations of 30 ppm, there is a higher amount of TOC in the planktonic solution and reduction in potential EPS associated with the sessile cells. This needs further study to substantiate.

- The decoupling study has shown that the sessile population showed increased ferrous oxidation activity when ferrous iron limitation was removed.

- The decoupling study also showed that the planktonic phase can be colonised from established sessile populations, and that this colonisation has been shown to be faster in this instance than in the reverse case scenario.

These conclusions illustrate that the key questions raised in Section 2.13 have been addressed. Specifically, it has been shown that while, under ideal growth conditions, there existed a relationship between the ferrous oxidation rate and the carbon dioxide uptake rate, this relationship broke down when carbon dioxide availability was reduced. Concomitantly, the specific ferrous iron oxidation rate and biomass yield changed. The carbon dioxide assimilation rate was representative of the biomass formed under planktonic conditions in most instances.

On retaining a sessile population in the reactor, the biomass present was greatly increased. Owing to ferrous iron limitation, these populations showed a reduced specific ferrous iron oxidation rate. However, the sessile populations were shown to display similar oxidation activity to planktonic cells when not ferrous iron limited. It was also evident that the sessile populations had alternate paths for the carbon assimilated; hence not all carbon dioxide was converted to active biomass. Results so far suggest a greater portion of extracellular organic carbon in the presence of sessile cells consistent with some of the carbon being used in EPS formation. This partitioning of carbon away from the biomass formation was influenced by both the presence of solid support and the availability of carbon dioxide.

6.2 Significance of work

This study is significant because it addresses fundamental issues in understanding the behaviour of micro-organisms and the applicability of such measurements to industrial practice. Firstly, carbon dioxide provision is critical in heaps. Here demonstrated, is the ability of microbial populations to achieve growth and ferrous iron oxidation at low carbon dioxide concentrations. However, it must be noted that the population is compromised at very low carbon dioxide availability in terms of the amount of biomass supported. This is critical in terms of heap colonisation. The influence of carbon dioxide availability on the yield of biomass from ferrous iron oxidation has further impact on bioleaching efficiency.

While it is recognised that the planktonic STR data is useful for determining optimum conditions , it must be recognised that the kinetics in the planktonic system are restrictd to the demonstration of response to environmental conditions and are not representative of the whole heap system.

Data gathered has illustrated that the stoichiometric link between the carbon dioxide assimilated and the ferrous iron oxidised does not hold across all operating conditions. This implies that one is required to validate the relationship under the conditions where the respirometric method is used. Further, it may provide opportunity to improve understanding of this stoichiometric relationship to assist process design.

6.3 Recommendations

The following recommendations are suggested for future work. Firstly, to extend these experiments to get results to determine the affinity constant K_s specifically for carbon dioxide for *L. ferriphilum*. Also, running the experiments coupled with solid support in a reactor which controls the redox potential, (e.g. the Redostat™ used by Kamunga Kazadi and Petersen (2008)), thereby the availability of ferrous iron to determine the contribution of the sessile population toward ferrous iron oxidation.

Further understanding of the behaviour of the sessile population can be derived from isolating the solid support and treating it as a single system (packed bed reactor with catalyst) and then observing the ferrous oxidation rate of this system. One way to do this would be to establish the sessile population at steady state and then increase the dilution rate to force washout of the planktonic system, (at 5 g/L ferrous iron, washout occurs at $D \approx 14$ hrs). This will solve two questions. It will show whether the sessile population is attached or merely entrained in the solid support. Furthermore, once the planktonic population has been washed out, the sessile population can be investigated in its own capacity in the absence of ferrous iron limitation. To add to this, further analysis of TOC through hydrolysis of complex organics and through measurement of EPS would confirm the hypothesis that the carbon is being used for EPS production.

References

- Africa, C-J., Harrison, S.T.L., Becker, M., van Hille, R.P. (2010), ***In situ* investigation and visualization of microbial attachment in a heap leach environment: The novel biofilm reactor**, Minerals Engineering, **23(6)**, 486-491
- Akcil, A., Cifti, H. (2003), **Bacterial leaching of kure copper ore**, The Journal of The Chamber of Mining Engineers of Turkey, **42**, 15-25
- Akcil, A., Cifti, H., Deveci, H. (2006), **Role and contribution of pure and mixed cultures of mesophiles in bioleaching of a pyritic chalcopyrite concentrate**, Minerals Engineering, **20**, 310–318.
- Appia-Ayme, C., Quatrini, R., Denis, Y., Ratouchniak, J., Veloso, F., Valdes, J., Lefimil, C., Silver, S., Roberto, F., Orellana, O., Denizot, F., Jedlicki, E., Holmes, D., Bennefoy, V. (2006a), **Insights into the iron and sulphur energetic metabolism of *Acidithiobacillus ferrooxidans* by microarray transcriptone profiling**, Hydrometallurgy, **83**, 263 -272
- Appia-Ayme, C., Quatrini, R., Denis, Y., Ratouchniak, J., Veloso, F., Valdes, J., Lefimil, C., Silver, S., Roberto, F., Orellana, O., Denizot, F., Jedlicki, E., Holmes, D., Bennefoy, V. (2006b), **Microarray and Bioinformatics analyses suggest models for carbon metabolism in the autotroph *Acidithiobacillus ferrooxidans***, Hydrometallurgy, **83**, 273-280
- Bailey, A.D., Hansford, G.S. (1993), **Factors affecting the biooxidation of sulphide minerals at high concentrations of solids, A review,** Biotechnology and Bioengineering, **12**, 1164-1174
- Bailey, J.E., Ollis, D.F., (1986), **Biochemical engineering fundamentals**, 2nd Ed, McGraw-Hill International Editions, Singapore
- Barron, J.L., Lucking, D. R. (1990), **Growth and maintenance of *Thiobacillus ferrooxidans* cells**, Applied Environmental Microbiology, **56(9)**, 2801-2806.
- Battaglia-Burnett, F., d'Hughes, P, Cabral, T., Cezac, P., Garcia, J.L., Morin, D. (1998), **The mutual effect of *Thiobacilli* and *Leptospirilli* populations on pyrite bioleaching**, Minerals Engineering, **11**, 195-205
- Beck, J.V. (1960), Journal of Bacteriology, **79**, 502-509
- Bevilaqua, D., Leite, A.L.L.C., Garcia, O., Tuovinen, O.H. (2002), **Oxidation of chalcopyrite by *Acidithiobacillus ferrooxidans* and *Acidithiobacillus thiooxidans* in shake flasks**, Process Biochemistry, **38**, 587-592
- Blight, K.R., Ralph, D.E., (2008), **Aluminium sulphate and potassium nitrate on batch culture of iron oxidizing bacteria**, Hydrometallurgy, **92**, 130-134
- Boon, M., Heijnen, J.J., Hansford G.S., **Recent developments in the modeling of bio-oxidation kinetics and their implications in practices: Part I, measure methods in bio-oxidation kinetics**, in: D Holmes, Smith, R. (Eds) (1994), **Mineral Processing II**. The Minerals, Metals and Materials Society, Warrendale, PA, pp 41-51
- Boon, M., Hansford, G.S., Heijnen, J.J. (1995), **Recent developments in modelling biooxidation kinetics, Part II: Kinetic modelling of the bio-oxidation of sulphide minerals in terms of critical sub-**

processes involved, in, Holmes, D.S., Smith, R.W. (Eds.), Proceedings of Engineering Foundation Conference, July 1994, The Minerals, Metals and Materials Society, Salt Lake City, 63-68

- Boon, M. (1996), **Theoretical and experimental methods in the modelling of bio-oxidation kinetics of sulphide minerals**, PhD thesis, Technical University, Delft, The Netherlands
- Boon, M., Heijnen, J.J. (1997), **Gas-liquid mass transfer phenomena in biooxidation experiments of sulphide minerals: A critical review of literature data**, Hydrometallurgy, **48**, 187-204.
- Boon, M., Meeder, T.A., Thöne, C., Ras, C., Heijnen, J.J. (1999a), **The kinetic modelling of ferrous iron oxidation kinetics with *Thiobacillus ferrooxidans* in continuous cultures**, Applied Microbiology and Biotechnology, **51**, 193-201
- Boon, M., Brasser, H.J., Hansford, G.S., and Heijnen, J.J. (1999b), **Comparison of the oxidation of different pyrites in the presence of *Thiobacillus ferrooxidans* or *Leptospirillum ferrooxidans***, Hydrometallurgy, **53(1)**, 57-72
- Bouffard, S.C., Dixon, D.G. (2002), **On the rate-limiting steps of pyrite refractory gold ore heap leaching : Results from small and large column tests**, Minerals Engineering, **15**, 859-670
- Bosecker, K., (1997), **Bioleaching: metal solubilization by microorganisms**, FEMS Microbiology Reviews, **20**(3-4), 591-604
- Breed, A.W., (2000), **Studies in the mechanism and kinetics of bioleaching with special reference to the bioleaching of refractory gold-bearing arsenopyrite/pyrite concentrates**, PhD Thesis, University of Cape Town, South Africa
- Breed, A.W., Hansford (1999), G.S., **Effect of pH on ferrous-iron oxidation kinetics of a predominantly *Leptospirillum ferrooxidans* culture**, Biotechnology and Biochemical Engineering, **3**, 193-201
- Brierley, C.L. (1978), **Bacterial leaching, A critical review**, Microbiology, **6**, 207-262
- Brierley, C.L. (1982), **Microbiology mining**, Scientific America, **247(2)**, 42-51
- Brierley, C.L. (1997), **Mining biotechnology: Research into commercial development and beyond** in **biomining: Theory, bacteria and industrial processes**, Springer-Verlag, USA, 3-17
- Brierley, J.A., Brierley C.L. (1999), **Present and future application of biohydrometallurgy** in **Biohydrometallurgy and the environment towards the 21st century, Part A**, Amsterdam, Elsevier.
- Coram, N.J., Rawlings, D.E. (1999), ***Thiobacillus caldus* and *Leptospirillum ferrooxidans* are widely distributed in continuous flow biooxidation tanks used to treat a variety of metal containing ores and concentrates**, Process Metallurgy, **9(1)**, 777-786
- Coram, N.J., Rawlings, D.E. (2002), **Molecular relationships between two groups of *Leptospirillum***, Applied Environmental Microbiology, **68**, 838-845
- Coram-Uliana, N.J., van Hille, R.P., Kohr, W.J., Harrison S.T.L. (2006), **Development of a method to assay the microbial population in heap bioleaching**, Hydrometallurgy, **83**, 237-244
- Characklis, W.G., Marshall, K.C. (1990), **Biofilms: A basis for an Interdisciplinary approach**, 93-130, Wiley Interscience, New York
- Crundwell, F., (1996), **The formation of biofilms of iron-oxidizing bacteria on pyrite**, Minerals Engineering, **9(10)**, 1081-1089

- Crundwell, F., (1997), **The kinetics of the chemiosmotic proton circuit in the iron oxiding bacteria *Thiobacillus ferrooxidans***, Bioelctrochem. Bioenerg., **43**, 115-122
- Demergasso, C., Galleguillos, P.A., Escudero, L.V., Zepeda, V.J., Castillo, D., Casamayor, E. (2005), **Molecular characterisation of microbial populations in a low-grade copper ore bioleaching test heap**, Hydrometallurgy, **80(4)**, 241-253
- Dempers, C.J., Breed A.W. & Hansford, G.S. (2003), **The effect of maintenance on the ferrous oxidation kinetics of *Leptospirillum ferrooxidans***, International Biohydrometallurgy Symposium, September 2003
- Deveci, H. (2002), **Effect of solids on the viability of acidophilic bacteria**, Minerals Engineering, **15**, 1181-1189
- d'Hughes, P., Foucher, S., Galle-Cavalloni, P., Morin, D. (2002), **Continuous bioleaching of chacopyrite using a novel extremely thermophilic mixed culture**, International Journal of Mineral Processing, **66**, 107-119
- de Wulf-Durand, P., Bryant, L.J., Sly, L.L. (1997), Applied Environmental Microbiology, **63**, 2944-2948
- de Kock, S.H., Barnard, P., du Plessis, C.A., (2004), **Oxygen and carbon dioxide kinetic challenges for thermophilic mineral bioleaching processes**, Biochem. Soc. Trans., **32**, 273-275
- Dixon, D.G., Petersen, J. (2003), Dixon, D.G., Petersen, J. (Eds.) in: Roveros, P.A., Dixon, D.G., Dreisinger, D.B., Menacho, J., **Copper 2003, Hydrometallurgy of copper**, CIM, Montreal, Canada, pp. 493-516
- Dobrinski, K.P., Longlo, D.L., Scott K.M. (2005), **The carbon-concentrating mechanism of the hydrothermal vent chemolithoautotroph *Thiomicrospira crunogena,*** Journal Bacteriol, **187**, 5761-5766
- Dopson, M., Baker-Austin, C., Koppineedi, P.R., Bond, P.L. (2003), **Growth in the sulphidic mineral environments,: metal resistance mechanisms in acidophilic microorganisms**, Microbiology, **149**, 1859-1970
- du Plessis, C.A., Barnard, P., Naldrett, K., de Kock, S.H., (2001), **Developement of respirometry methods to assess the microbial activity of thermophilic bioleaching archaea**, J. Lof Microbbiol. Methods, **47**, 189-198
- Eaton, A.D., Clesceri, L.S., Greenberg, A.E. (1998), **Standard methods for the examination of water and wastewater**, Eds, American Public Health Association, Washington DC
- Ebbing, D. (1993), **General chemistry**, 4th Edition, Houghton Miffin Company, Boston, Toronto.
- Esner, A.A., Roels, J.A., Kossen, N.W., (1981), **Comments on the description of the maintenance metabolism during aerobic growth with product formation**, Biotechnology Letters, **3(1)**, 15-20
- Florian, B, Noël, E., Sand, W., **Visualisation of the initial attachment of bioleaching bacteria using combined atomic force and epiflourescence microscopy**, Minerals Engineering, **23(6)**, 532-535
- Gautier, V., Escobar, B., Vargas, T. (2008), **Cooperative action of attached and planktonic cells during bioleaching of chalcopyrite with *Sulfolobus Metallicus* at 70°C**, Hydrometallurgy, **94**, 121-126.
- Gericke, M., Pinches, A., van Rooyen, J.V. (2001), **Bioleaching of a chalcopyritic concentrate using an extremely thermophilic culture**, International Journal of Mineral Processing, **62**, 243-255.

- Ginsburg, M.A., Penev, K., Karamanev, D. (2008), **Immobilization and ferrous iron bio-oxidation studies of a *Leptospirillum* sp. mixed cell culture**, Minerals Engineering, **22(2)**, 140-148.
- Haddadin, J., Morin, D., Ollivier, P., Fick, M. (1993), **Effect of different carbon dioxide concentrations on ferrous iron and pyrite oxidation by a mixed culture of iron and/or sulphur-oxidzing bacteria,**
- Hallberg, K.B. (1995), **Role of arsenic toxicity to and arsenic resistance of thermophilic bioleaching organisms**, Microbiology, **140**, 3451-3456
- Harneit, K., Göksel, A., Kock, D., Klock, J.-H., Gehrke, T., Sand, W. (2006), **Adhesion to metal sulphide surfaces by cells of *Acidithiobacillus ferrooxidans*, *Acidithiobacillus thiooxidans* and *Leptospirillum ferrooxidans***, Hydrometallurgy, **83(1-4)**, 245-254
- Heijnen, J.J., van Dijken, J.P., **In search of a thermodynamic description of biomass yields for the chemotrophic growth of micro-organisms,** Biotechnology and Bioengineering, **39(8)**, 833-858
- Holuigue, L., Herrara, L., Phillips, O.M., Young, M., Allende, J.E. (1987), **CO_2 fixation by mineral leaching bacteria: characteristics of the ribulose bisphosphate carboxylase-oxygenase of *Thiobacillus ferrooxidans***, Biotechnology and Applied Biochemistry, **9**, 497-505
- Hügler, M, Huber, H., Stetter, K.O., Fuchs, G. (2003), **Autotrophic CO_2 fixation pathways in archaea (Crenarchaeorta)**, Archaea Microbiology, **179**, 160-173
- Ingledew, J. (1981), ***Thiobacillus ferrooxidans*: The bioenergetics of an acidophilic chemolithotroph**, Biochemica et Biophisica Acta, **683**, 89-117
- Johnson, D.B. (1998), **Biodiversity and the ecology of acidophilic microorganisms**, FEMS Microbiology Ecology, **27**, 307-317
- Jones, C.A., Kelly, D.P. (1983), **Growth of *Thiobacillus ferrooxidans* on ferrous iron in chemostat culture: influence of product and substrate inhibition**, Journal of Chemical technology and Biotechnology, **338**, 241-261
- Kamumnga Kazadi, T., Petersen, J., (2008), **Kineic measurement of biological oxidaition of ferrous iron at low farric-to-ferrous ratios in a controlled potential batch reactor**, Hydrometallurgy, **94**, 48-53
- Kaskiala, T. (2005), **Determination of mass transfer between gas and liquid in atmospheric leaching of sulphidic zinc concentrates**, Minerals Engineering, **18(12)**, 1200-1207
- Kinnunen, P.H-M., Puhakka, J.A. (2004), **Chloride promoted leaching of chalcopyrite concentrate by biologically produced ferric iron**, Journal of Chemical Technology, **79**, 830-834
- Kinnunen, P.H-M., Puhakka, J.A. (2005), **High rate iron oxidation at below pH 1 and at elevated Iron and copper concentrations by a *Leptospirillum ferriphilum* dominated biofilm**, Process Biochemistry, **40**, 3536-3541
- Kinzler, K., Gehrke, T., Telegdi, J., Sand, W. (2003), **Bioleaching – A result of interfacial processes caused by extracellular polymeric substances**, Hydrometallurgy, **71(1-2)**, 83-88
- Konishi, Y., Asai, S., Yoshida N. (1995), **Kinetics of *Thiobacillus thiooxidans* on the surface of elemental sulphur**, Applied and Environmental Microbiology, **61**, 3617-3622
- Levicán, G., Ugalde, J.A., Ehrenfeld, N., Maass, A., Parada, P. (2008), **Comparative genomic analysis of carbon and nitrogen assimilation mechanisms in three indigenous bioleaching bacteria: predictions and validations**, BMC Genomics 2008, **9**:581

- Llzama, H.M., Zielinski, P.A., Kerby, L.D., Abraham, C.C., (2002), **Comparison of biooxidation with carbon dioxide assimilation during bacterial growth on ferrous iron or elemental sulphur,** Biotechnolog. Bioeng., **5**, 111-117
- Madigan, M.T., Martinko, J.M., Parker, J. (2003), **Brock biology of microorganisms (international edition),** Pearson Education Inc., New Jersey,pp 151-152, 565-590, 669-674
- Maas, B., Paxton, J., (2007), **Ferrous oxidation rates of *L. ferriphilum* attached to an inorganic support,** Undergraduate project thesis, University of Cape Town, South Africa.
- Munoz, J.A., Gonzalez, F., Ballester, A., Blazquez, M.L. (2006), **Bioleaching of a Spanish uranium ore,** FEMS Microbiology Reviews, **11,** Issue 1-3, 109-119
- Nemati, M., Harrison, S.T.L., Hansford, G.S., Webb, C. (1998), **Biological oxidation of ferrous sulphate by *Thiobacillus ferrooxidans*: a review on the kinetic aspects,** Biochemical Engineering Journal, **1,** 171-190
- Norris, P.R. (1983), **Iron and mineral oxidation with *Leptospirillum*-like bacteria,** in Rossi, G., Torma, A.E. (Eds.), **Recent progress in biohydrometallurgy,** Associazone Mineraria Sardia, Iglesias, Italy, 83-96
- Norris, P.R., Barr, D.W., Hinson, D. (1988), **Iron and mineral oxidation by acidophilic bacteria,: affinities for iron and attachment to pyrite,** in Norris, P.R. & Kelly, D.P. (Eds.), Biohydrometallurgy, Proceedings of the International Symposium, 1987, Science and Technology Letters, Kew, Surrey, 43-59.
- Ojumu, T.V., Petersen, J., Searby, G.E., Hansford, G.S. (2006), **A review to rate equations proposed for microbial ferrous-iron oxidation with a view to application to heap bioleaching,** Hydrometallurgy, **83**, 21-28.
- Ojumu, T.V. (2008), **The effects of solution conditions on the kinetics of microbial ferrous iron oxidation by *Leptospirillum ferriphilum* in continuous culture,** PhD Thesis, University of Cape Town, South Africa.
- Ojumu, T.V., Petersen, J, Hansford, G. (2008), **The effect of dissolved cations on the microbial ferrous-iron oxidation by *Leptospirillum ferriphilum* in continuous culture,** Hydrometallurgy, **94**, 69-76
- Okibe, N., Gericke, M.,Hallberg, K.B., Johnson, D.B. (2003), **Enumeration and characterisation of acidophilic microorganisms isolated from a pilot plant stirred tank bioleaching operation,** Environmental Microbiology, **69**, 1936-1943
- Omata, T., Price, G.D., Badger, M.R., Okamura, M., Gohta, S., Ogawa, T. (1999), **Identification of an ATP-binding cassette transporter involved in bicarbonate uptake in the cyanobacterium *Synechococcus* sp. strain PCC 7924.,** Procedures of the National Academy of Science USA, **96**, 13571-13576
- Ozkaya, B., Sahinkaya, E., Nurmi. P., Kaksonen, A.H., Puhakka, J. (2007), **Iron oxidation and precipitation in a simulated heap leaching solution in a *Leptospirillum ferriphilum* dominated biofilm reactor,** Hydrometallurgy, **88**, 67-74
- Petersen, J., (2010), **Determination of the oxygen gas-liquid mass transfer rates in heap bioleach reactors,** Minerals Engineering, **23**(6), 504-510

- Petersen, J., Dixon, D.G. (2002), **Thermophilic heap leaching of a chalcopyrite concentrate**, Minerals Engineering, **15**, 777-785
- Petersen, J., Dixon, D.G. (2006), **Competitive bioleaching of pyrite and chalcopyrite**, Hydrometallurgy, **83**, 40-49
- Petersen, J., Dixon, D.G. (2007), **Principles, mechanisms and dynamics of heap bioleaching**, Microbiology of Bioleaching, in Donati, E., Sand, W. (eds.) (2007), **Microbial processing of metal sulfides**, Springer.
- Petersen, J., Minaaar, S.H., du Plessis, C.A., **Carbon dioxide and oxygen consumption during the bioleaching of a copper ore in a large isothermal column**, Hydrometallurgy, **104**, 356-362
- Petersen, J., Ojumu. T.V. (2006), **The effect of total iron speciation on the rate of ferrous iron oxidation kinetic of *L. ferriphilum* in continuous tank systems**, IBS conference paper.
- Rawlings, D.E. (1997), **Biomining: Theory, bacteria and industrial processes**, Springer-Verlag, USA
- Rawlings, D.E. (2002), **Heavy metal mining using micro-organisms**, Annual Review Microbiology, **56**, 65-91
- Rawlings, D.E., Tributch, H., Hansford, G.S. (1999), **Reasons why *'Leptospirillum'*-like species rather than *Thiobacillus ferrooxidans* are the dominant iron-oxidising bacteria in many commercial processed for the biooxidation of pyrite and related ores**, Microbiology, **145**, 5-13
- Rohwerder, T, Gherke, T., Kinzler, Sand, W. (2003), **Bioleaching review, Part A: Progress in bioleaching: Fundamentals and the mechanism of bacterial metal sulphide oxidation,** Applied Microbiology and Biotechnology, 63, 239-248
- Rubio, A., Garcia Frutos, F.J. (2002), **Bioleaching capacity of an extremely thermophilic culture for chalcopyrite materials**, Minerals Engineering, **15**(11), 689-694
- Sand, W., Gherke, T., Jozsa, P.G., Shippers, A. (2001) **(Bio)chemistry of bacterial leaching – direct vs. indirect bioleaching**, Hydrometallurgy, **59**, 159-175
- Schnell, H.A. (1997), **Bioleaching of copper** in Rawlings, D.E. (ed), **Biomining: Theory, bacteria and industrial processes,** Springer-Verlag, USA, 21-43
- Shibata, M., Ohkawa, H., Katoh, H., Shimoyama M., Ogawa, T. (2002), **Two CO_2 uptake systems in cyanobacteria: four systems for inorganic carbon acquisition in *Synechocystis* sp. strain PCC6803.** Functional Plant Biology, **29**, 123-129
- Stott, M.B., Watling, H.R., franzmann, P.D., Sutton, D.C. (2000), **The role of Iron-hydroxy precipitates in the passivation of chalcopyrite during bioleaching**, Minerals Engineering, **13** (10-1), 1117-1127
- Stott, M.B., Sutton, D.C., Watling, H.R., Franzmann, P.D. (2003), **Comparative leaching of chalcopyrite by selected acidophilic bacteria and archaea**, Geomicrobiology Journal, **20**, 215-230
- Swamy, K.M., Narayana, K.L., Misra, V.N. (2004), **Bioleaching with ultrasound**, Ultrasomnics Sonochemistry, **12(4)**, 301-306
- Tuovinen, O.H., Kelly, D.P. (1972), Z. Allg. Microbiol., **12**, 311-346
- Valdês, J., Pedroso, I., Quatrini, R., Holmes, D.S. (2008a), **Comparative genome analysis of *Acidithiobacillus ferrooxidans, A. thiooxidans* and *A. caldus*: Insight into their metabolism and ecophysiology**, Hydrometallurgy, **94**, 180-184

- Valdés, J., Pedroso, I., Quatrini, R., Dodson, R.J., Tettelin, H., Blake II, R., Eisen, J.A., Holmes, D.S. (2008b), ***Acidithiobacillus ferrooxidans* metabolism: from genome sequence to industrial applications**, BMC Genomics, **9**:597
- Van Aswegen, P.C., Godfrey, M.W, Miller, D.M., Heynes A.K. (1991), **Developments and innovations in bacterial oxidation of refractory ores**, Mineral & Metallurgical Processes, **8**, 188-192
- van Hille, R.P., Bromfield, L.V., Botha, S.S., Jones G. van Zyl, Harrison, S.T.L. (2009), **The effect of nutrient supplementation on growth and leaching performance of bioleaching bacteria**, Advanced Materials Research, **71-73**, 413-413
- Watling, H.R. (2006), **The bioleaching of sulphide minerals with emphasis on copper sulphides – A review,** Hydrometallurgy, **84**, 81-108
- Witne, J.Y., Phillips, C.V. (2001), **Bioleaching of Oktedi copper concentrate in oxygen- and carbon dioxide-enriched air**, Minerals Engineering, **14**, 25-48

AceChemPack (accessed 03/03/2010)
http://www.tower-packing.com/ceramic/ceramic_saddles_ring_chemical_packing.htm

Appendices

A. Media preparation

A standard ferrous iron solution prepared as described below.

A.1 Base salt media

The media for growth on ferrous-iron is prepared by weighing the following reagents accurately and diluting to desired volume with dH_2O (and 30 ml conc. H_2SO_4 to a 25 L volume)

Desired volume ⟶	**1 L**	**10 L**	**20 L**	**25 L**
$(NH_4)_2SO_4$ (grams)	1.83	18.3	36.6	45.75
K_2SO_4 (grams)	1.11	11.1	22.2	27.75
$(NH_4)_2HPO_4$ (grams)	0.53	5.3	10.6	13.25
Vishniac trace metal solution (ml)	10	100	200	250

A.2 Vishniac trace metal solution

The Vishniac trace metal solution required in the base salt media is prepared by accurately weighing the following reagents and then diluting to a 500ml volume with dH_2O. The following procedure below must be followed.

(a) Prepare 6% KOH by weighing 15g KOH and diluting to 250 ml with dH_2O.

(b) Dissolve 25g EDTA in 100 ml of 6% KOH on a magnetic stirrer.

(c) In a separate 250 ml beaker weigh the following reagents and dissolve then in 200ml dH_2O for 30 minutes on magnetic stirrer.

$ZnSO_4.7H_2O$.	11 g
$CaCl_4.2H_2O$	4.62 g
$MnC_{l2}.4H_2O$	2.53 g
$FeSO_4.7H_2O$	2.50 g
$(NH_4)_6Mo7O_{24}.4H_2O$	0.55 g
$CuSO_4.5H_2O$	0.79 g
$CoC_{l2}.6H_2O$	0.81 g

Transfer solution (c) quantitatively into (b) on a magnetic stirrer and make up to 500ml with dH_2O by rinsing the beaker containing solution (c) with 200 ml dH_2O (this will result in the formation of a deep greenish brown solution).

A.3 Ferrous iron solution

5 g/L Fe^{2+} solution: Dissolve 124.50 g of $FeSO_4.7H_2O$ in 5 L of solution in (1) above.

B. Sampling, culture maintenance and data logging

B.1 Sampling

Firstly, measure the mass of the feed solution and record the time of sampling. Check that the residence time of the system is correct by performing the calculation shown in Appendix F.1 using the change in feed mass and time.

A 15 ml sample is then taken from the effluent after two residence to three residence times, given that the readings from the off-gas analyser are within 10% of each other, and the redox probe measurements are within 5% of each other.. Samples will be taken from the effluent and not directly from the reactor so as not to perturb the steady state operation. The sample is still is representative of the conditions inside the reactor as it is a CSTR. The following measurements are then taken.

1. Measure the redox potential of the solution with the redox probe.
2. Measure the pH and ensure its 1.3 by adjusting the feed pH (add H_2SO_4 drop-wise).
3. Stop the pump in order to weigh the feed, note the time. Top up the feed to desired level and weigh. Note the time as the pump is started.
4. Measure the redox potential of the feed with the redox probe.
5. 5 ml of sample is sent for AAS analysis
6. 5 ml of sample is sent for TOC analysis
7. A spectrophotometric measurement of ferrous iron will also be performed (2ml).
8. The CO_2 and O_2 consumption is recorded by the lab computer.
9. A 1 cm^3 sample is kept for microbial work, (including microscopic cell counts)

B.2 Culture maintenance

The following checks should be performed every time a sample is taken to ensure good operation at steady state.

Feed

- Check that there is no white fungus in it
- Keep refrigerated if staying out for more than 5 days

Pumps

- Check that they are turning silently
- Calibration curve is on the side of the glass cabinet with sulphur reactors

Feed Flow

- If reactor is filling up, then clear exit feedline, possibly replacing tubing, and using thin wire through pipe, and then flushing
- If feed is not moving, then feed pipe is blocked, deal with in same fashion

Maintenance

- If the colour of the reactor gets lighter brown/goes green, stop reactor, and leave in batch mode until colour returns, possibly innocluating with old effluent
- Pressure can build up in reactor, check for pressure build up by sound and gas leaks on lid with soap bubbles. If there is a gas build up reconnect pipes to off gas analyser

General

- Refill feed containers before they run out
- Fill to about 3 litres and empty effluent container into acid waste

B.3 Off-gas logging and analysis

1) Start the data logger by typing **LOG6M** at **C:** prompt and press **ENTER**.
2) Follow instructions: enter filename to be used.

CAUTION! DOS only recognises filenames of 8 characters or less, longer names will be truncated.

For example, files will be saved as 27feb0.rec, 27feb1.rec, 27feb2.rec, 27feb3.rec, 27feb4.rec, ... etc. so if your filename is 7 characters long, you will save 9 files, and then repeatedly over write them, so restrict the name to 5 characters (you can then save up to 999 files, at 48/day, this should be vastly more than adequate.) E.g. **c:\linus\27feb ENTER**

3) Select channels according to those in use, generally all four channels will be in use.
4) Select O2 range **(B) 19-21%**

Getting files off the data logger

1) If data logger is already running, hit F10, computer will return to DOS prompt.
2) Make Folder under C:\linus : **md 27feb09**
3) Type **move 27feb*.rec 27feb09**
4) Count number of entries
5) type **cd** to return to the c: prompt
6) Type **cd progs** to change to the progs directory
7) Type **APPEND** enter, to run the program
8) Enter the information as requested
9) Note that while you are asked to enter a filename for the new file to be formed, the file will be saved as **27febOUT.rec**
10) You will now need to change the file format from a .rec file to a .txt file, this may be accomplished using the FILES program, also to be found in the **c:\progs** directory
11) Type **FILES** to run program
12) Enter the information requested
13) Type **move 27febout.txt A:** to copy to floppy
14) Restart logging

Working up data

1) The .txt file containing your data can be opened in Excel, and macros exist to re-distribute the data in a more meaningful format.

2) You will need TEMPLATE.XLS, LOGGINGMACROS.XLS (available G:\BIODATA\LOG) and your .txt file open in excel – for the text file, open as delimited, NEXT, change delimiters from tabs to commas, FINISH.

3) Copy data to Raw data sheet of template starting at A6

4) Fill in data on Run info sheet – crucial info required – Run Start time, and Gas Flow rates, these affect how the macro manipulates the data.

5) Click on Tools-> macro-> macros-> movedata-> edit-> change number of files to number of original .rec files produced -> Run, wait until macro finishes, save file as something other than Template.

6) Save the original .rec files and your final .xls file somewhere that can be backed up, and in an organised fashion.

C. The Stoichiometric Equation and the Degree of Reduction Balance

The stoichiometry of the Equation representing the growth of bacteria on ferrous iron substrate (Equation 6) was derived as follows (Boon et al., 1995): Given that the carbon source is CO_2, the nitrogen source is NH_4^+, oxygen is an electron acceptor and that the proton is essential for the microbial growth and substrate utilisation, the balanced equation for the aerobic oxidation microbial growth of biomass on ferrous-iron can be written as:

$$aCO_2 + bNH_4^+ + cO_2 + dFe^{2+} + eH^+ + 1.0CH_{1.8}O_{0.5}N_{0.2} + fFe^{3+} + gH_2O = 0$$

The rate biomass production can be related to the rate of substrate consumption of ferrous iron.

$$-r_{Fe^{2+}} = d.r_x$$

The elemental and charge (z) balances can be done as follows:

C: $a + 1 = 0$

H: $4b + e + 1.8 + 2g = 0$

O: $2a + 2c + 0.5 + g = 0$

N: $b + 0.2 = 0$

Fe: $d + f = 0$

Z: $b + 2d + e + 3f = 0$ **Equations C.1**

There are six balanced equations with seven unknown parameters, the values of these parameters in best expressed in terms of the coefficient of the limiting substrate (ferrous iron), d.

$$a = -1 \qquad e = d + 0.2$$
$$b = -0.2 \qquad f = -d$$
$$c = \frac{d+4.2}{4} \qquad g = -\left(0.6 + \frac{d}{2}\right)$$ **Equations C.2**

d can be determined from the yield of biomass on ferrous iron.

$$d = -\frac{r_{Fe^{2+}}}{r_x} = -\frac{1}{Y_{Fe^{2+}X}}$$

Therefore the stoichiometry in Equation 6 can be obtained by substituting for d the above system of equations.

$$a = -1 \qquad e = -\left(\frac{1}{Y_{Fe^{2+}X}} - 0.2\right)$$
$$b = -0.2 \qquad f = \frac{1}{Y_{Fe^{2+}X}}$$
$$c = -\left(\frac{1-4.2Y_{Fe^{2+}X}}{4Y_{Fe^{2+}X}}\right) \qquad g = -\left(0.6 - \frac{1}{2Y_{Fe^{2+}X}}\right)$$ **Equations C.3**

Using the stoichiometric parameters, the relative rates of the compounds can be written with respect to biomass production rate, r_x which follows from:

$$\frac{1}{a}\frac{d[CO_2]}{dt} = \frac{d[X]}{dt} \xrightarrow{yields} a = \frac{\frac{d[CO_2]}{dt}}{\frac{d[X]}{dt}}$$ **Equation C.4**

By substitution into the original equation, the equation for the degree of reduction balance for ferrous iron oxidation by can be written as:

$$CO_2 + 0.2\,NH_4^+ + \frac{1-4.2Y_{Fe^{2+}X}}{4Y_{Fe^{2+}X}}\,O_2 + \frac{1}{Y_{Fe^{2+}X}}\,Fe^{2+} + \left(\frac{1}{Y_{Fe^{2+}X}} - 0.2\right)H^+ \rightarrow CH_{1.8}O_{0.5}N_{0.2} + \frac{1}{Y_{Fe^{2+}X}}Fe^{3+} + \left(\frac{1}{2Y_{Fe^{2+}X}} - 0.6\right)H_2O \qquad \textbf{Equation C.5}$$

A simple method to achieve the above is making use of the concept of degree of reduction as described by Esner et al. (1981). The degree-of-reduction, of a C,H,O,N- containing compound, is the number of electrons that are liberated in a redox half-reaction where one C-mole of an organic compound or one mole of inorganic compound is converted to; H^+, CO_2, H_2O, N-source, N_2, SO_4^{2-} or Fe^{3+}.

Table B-1. Calculated stoichiometric parameters of Equation C.4 and Gibbs energy of formation obtained from thermodynamic references

Relative rate	*Compound*	*Stoichiometric constant*	*Value*	ΔG_f°	*From Equation B.4*
r_x/r_x	$CH_{1.8}O_{0.5}N_{0.2}$	1	1	-237.18	(i)
r_{CO_2}/r_x	CO_2	***a***	-1	-394.36	(ii)
r_x/r_x	NH_4^+	***b***	-0.2	-79.37	(iii)
r_x/r_x	O_2	***c***	$-\left(\frac{1-4.2Y_{Fe^{2+}X}}{4Y_{Fe^{2+}X}}\right)$	0	(iv)
r_x/r_x	Fe^{2+}	***d***	$-\frac{1}{Y_{Fe^{2+}X}}$	-78.87	(v)
r_x/r_x	H^+	***e***	$-\left(\frac{1}{Y_{Fe^{2+}X}} - 0.2\right)$	-39.87	(vi)
r_x/r_x	Fe^{3+}	***f***	$\frac{1}{Y_{Fe^{2+}X}}$	-4.6	(vii)
r_x/r_x	H_2O	***g***	$-\left(0.6 - \frac{1}{2Y_{Fe^{2+}X}}\right)$	-237.18	(viii)

It represents the electron content of a compound relative to these species. By definition, degree-of-reduction equals 0, ($\gamma = 0$), for H^+, CO_2, H_2O, N-source, N_2, SO_4^{2-} and Fe^{3+}, and the composition formula of the undissociated compound is normally used when calculating the degree-of-reduction.

Table C-2. Degree of reduction balance for stoichiometric parameters

Compound	*C*	*H*	*O*	*N*	*Fe^{2+}*	*Fe^{3+}*	*Charge*	*Degree-of-reduction*
$CH_{1.8}O_{0.5}N_{0.2}$	1	1.8	0.5	0.2				4.2
CO_2	1		2					0
NH_4^+		4		1			1+	0
O_2			2					-4
Fe^{2+}					1		2+	1
H^+		1					1+	0
Fe^{3+}						1	3+	0
H_2O		2	1					0

Equation C.5 can be split into two half reactions:

$$2Fe^{2+} + \frac{1}{2}O_2 + 2H^+ \xrightarrow{micro-organisms} 2Fe^{3+} + H_2O \qquad \textbf{Equation C.6}$$

The energy produced from Equation B.6. is used autotrophically to form biomass by assimilation of CO_2 as a carbon source and NH_4^+ as a N-source, which is represented by Equation B.7.

$$\mathbf{CO_2, H_2O, NH_4^+ \rightarrow CH_{1.8}O_{0.5}N_{0.2}} \qquad \textbf{Equation C.7}$$

The degree of reduction is an alternative way of expressing the conservation of electron in the system i.e.

$$\sum_{i=0}^{i} \gamma_i r_i = 0$$

Therefore the balance becomes:

$$-r_{Fe^{2+}} = -4r_{O_2} + 4.2r_x \qquad \textbf{Equation C.8}$$

$$-r_{Fe^{2+}} = -4r_{O_2} - 4.2r_{CO_2} \qquad \textbf{Equation 6}$$

The Gibbs free energy is equal to the energy dissipated per mole of biomass, and for systems with reverse electron transport mechanisms; the energy dissipated per mole biomass is equal to 3500kJ/molC (Heijnen & van Dijken, 1992).

$$\Delta G_R = \sum_{i=0}^{i} a_i \Delta G_{if}^{\circ} = -\left(\frac{D_s^{01}}{r_x}\right)_{growth} = -3500\ kJ/molC$$

where

ΔG_R	is the Gibbs free energy of reaction
ΔG_{if}°	is the Gibbs free energy of formation of component i at standard conditions
a_i	is the stoichiometric coefficient of component I

By solving Equation C.6 for $Y_{Fe^{2+}X}$ at standard conditions (i.e. at 25°C, liquid concentration of 1.0 M and 1.0 atm gas partial pressure), yields $Y_{Fe^{2+}X}^{max} = 0.011$ molC/molFe^{2+}

D. Analytical techniques and analytical reagent preparation

D.1 Total organic carbon analysis

Total Organic carbon is measured by a TOC analyser. It measures the total amount of organic carbon by combustion and analysis of the carbon dioxide concentration in the flue gas. The catalyst of oxidation is sensitive to phosphate and sulphate anions which affect the catalyst activity and interfere with readings.

Since microbial growth solution is made with ferrous sulphate and acidified with sulphuric acid, it has an extremely high sulphate ion concentration (approx 0.13 M in a 5g/L ferrous feed solution taking into account the ferrous sulphate and the sulphuric acid.). The sulphate is removed by precipitation with $BaCl_2$ followed by a two stage filtration.

Since stoichiometry of reaction of Ba^{2+} with SO_4^{2-} is 1:1, an equimolar solution of $BaCl_2$ at 0.15M should precipitate the SO_4^{2-}.

A 0.15 M solution is prepared by dissolving 36.642 g in 1 L de-ionised water. A two stage precipitation is done to ensure that the precipitation of sulphate is complete. 5 ml of sample is added to 5 ml of 0.15 M $BaCl_2$, the solution is mixed and filtered through a 0.45 micron filter. The process is then repeated, adding another 5ml, mixing and filtering. It is often necessary to filter again to remove all the precipitate. Note now that the sample is now at a 1/3 dilution. If the TOC concentration is below the detection limit (10 mg), then the samples must be concentrated in the rotor-evaporator.

D.2 High performance liquid chromatography analysis for organic acids

Acetate, propionate, butyrate, pyruvate and lactate concentrations can be estimated using high performance liquid chromatography (HPLC, Beckman, System Gold), with a UV detector (Detector no. 168) and a glass lined Wakosil column. Phosphoric acid (0.1%, pH 2.5) acts as the mobile phase at a flow rate of 0.5 ml/min. Prior to injection, acidify diluted samples using 4 N H_2SO_4 (if sulphide is present in the sample to be analysed) and filter using 0.22 m membranes. In the absence of sulphide in the sample solution filter only.

Prepare standard solutions 0.05, 0.1, 0.5 and 1.0 g/l by performing serial dilutions on HPLC grade solutions using deionised water.

D.3 Ferrous iron concentration by spectrophotometry

The following method was used to quantitatively determine the ferrous iron concentration in the effluent solution.

Reagents required

- Standard ferrous iron solution (100ppm),
- 1-10 Phenanthroline indicator solution
- Ammonium acetate buffer solution (pH 7)

Procedure is as follows:

1. Pipette 2ml of Acetate Buffer to 7 test-tubes
2. Pipette 2 ml of indicator solution to each test-tube
3. Pipette the following volumes into teach of the first 6 test tubes shown in Table D.1
4.

Table D.1. Pipette volumes for generation of standard curve for ferrous iron assay by spectrophotometry

test-tube	1	2	3	4	5	6
volume d. H_2O (µl)	1000	900	800	700	600	500
volume Fe^{2+} std. (µl)	0	100	200	300	400	500

5. To the last test-tube, pipette 1 ml of effluent solution
6. Set wavelength to 510nm on spectrophotometer
7. Use first test tube as blank to zero
8. Record absorbance of other 6 samples

Notes:

The first 6 test tubes are used to generate the standard curve from which the concentration in the effluent is determined. The process relies on the fact that one Fe^{2+} molecule and three molecules of 1-10 phenanthroline form an orange-red complex which has an absorbance maximum at 510 nm.

The first 6 samples will give absorbances for 0, 20, 40, 60, 80, 100 ppm respectively. If the effluent sample has a higher absorbance than the value for 100 ppm it is advisable to dilute sample until the value can be determined from the standard curve by interpolation rather than extrapolation. A sample of the standard curve is shown in Figure D.2.

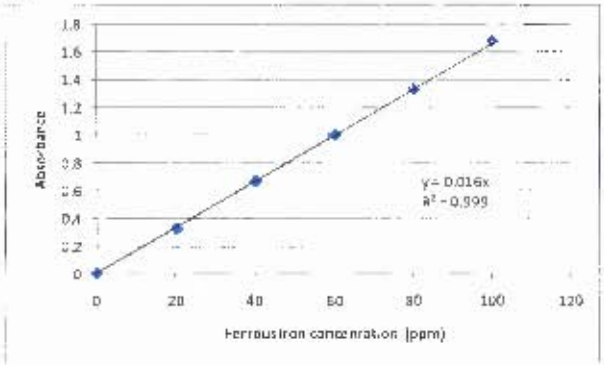

Figure D.2. Sample standard curve for ferrous iron analysis by spectrophotometry

The concentration of ferrous iron in the sample is then calculated from the standard curve using the standard curve generated.

Reagent preparation:

Standard Fe^{2+} stock solution (100ppm)

Slowly add 20ml of concentrated H_2SO_4 to 50ml of distilled water and then dissolve 497.6mg of $FeSO_4.7H_2O$. Dilute to 1l with distilled water and mix thoroughly.

1-10 phenanthroline indicator solution

Dissolve 2127.7mg of 1-10 phenanthroline ($C_{12}H_8N_2.H_2O$) in about 100ml of water. Dilute with more distilled water to 1l mark. (This gives a concentration of 1-10 phenanthroline in excess of the stoichiometric requirements.)

Ammonium acetate buffer solution

Dissolve 250g of ammonium acetate ($NH_4C_2H_3O_2$) in 150ml of distilled water. Add 700ml of concentrated glacial acetic acid

D.4 Redox probe calibration

Standard solutions of ferrous iron and ferric iron are prepared at pH 1.3 (adjusted with H_2SO_4). The ferric iron is submerged into a waterbath at the desired temperature at and a redc probe is inserted to take measurements. The ferrous iron solution is added in small increments shown in Table D.2 to obtain the following ratios of ferric:ferrous iron.

Table D.2. Volumes of ferrous and ferric iron used to make standard solution in redox probe calibration

VFe^{3+} (ml)	VFe^{2+}(ml)	V^T (ml)	$[Fe^{3+}]$ (mg/l)	$[Fe^{2+}]$ (mg/l)	$[Fe^{3+}]/[Fe^{2+}]$
200	0.2	200.2	999.00	0.999	1000.0
200	0.3	200.3	998.50	1.498	666.7
200	0.5	200.5	997.51	2.494	400.0
200	1.7	201.7	991.57	8.428	117.6
200	3.5	203.5	982.80	17.199	57.1
200	10	210	952.38	47.619	20.0
200	25	225	888.89	111.111	8.0
200	50	250	800.00	200.000	4.0
200	150	350	571.43	428.571	1.3
200	200	400	500.00	500.000	1.0

The redox probe is measured in triplicate at various concentrations to plot a standard curve of the redox probe reading vs the ratio (on a logarithmic scale. A standard curve is fitted and used to infer the ratio of ferric: ferrous iron for any ratio (given the total iron concentration [from AAS]). A sample of this curve is shown in Figure D.2.

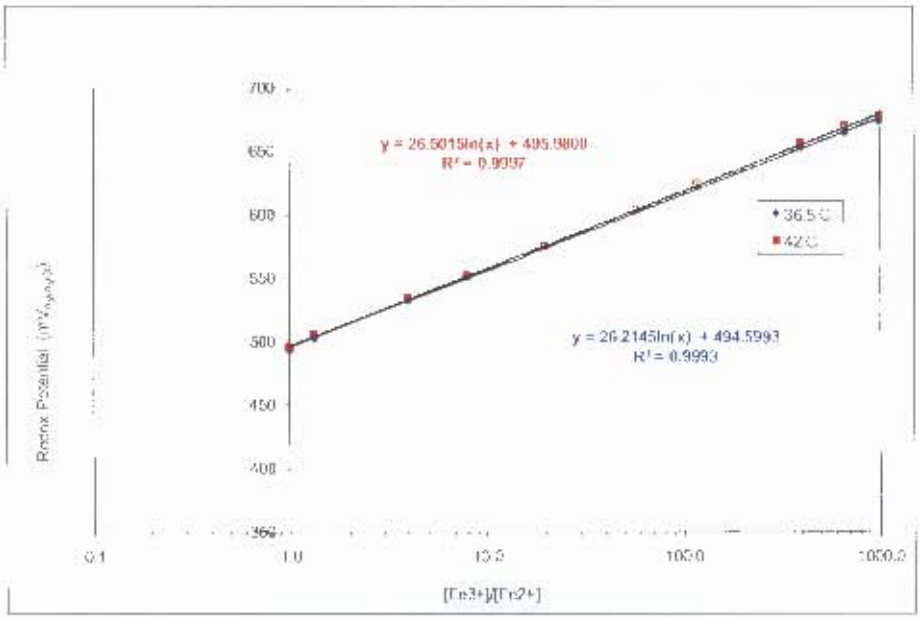

Figure D.2. Sample of redox probe calibration curve

Reagent preparation:

1.000 g/L ferrous iron solution

Add 1726 mg of $Fe(SO_4).7H_2O$ to 400ml dd. H_2O. Add H_2SO_4 conc. to dissolve and adjust to pH 1.3.

1.000g/L ferric iron solution

Add 1991 mg of $Fe_2(SO_4)_3$ to 400ml dd. H_2O. Add H_2SO_4 conc. to dissolve and adjust to pH 1.3.

E. Raw data

E.1 Measured data for System 1 and System 2

Table E.1 Raw data from System 1 (planktonic only) experiments

Technique **measurement** *units*	*set* **tau** *(hr)*	*set* **D** *(hr^{-1})*	*probe* **redox** *mV*	*offgas* **rO_2** *mmol /hr*	*offgas* **rCO_2** *mmole/(l.hr)*	*AAS* **Fe^{2+} (initial)** *g/L*	*spectro-photometry* **Fe^{2+} (residual)** *g/L*	*microscopic cell count* **number of** *cells* dil*	*total organic carbon* **TOC** *µ mol/L*
<2 ppm	48	0.0208	574	0.008	-	4.55	4.312	-	1.43
	54.5	0.0183	576	0.000	-	4.84	0.213	-	1.45
	32	0.0313	548	0.001	-	4.84	0.611	-	0.79
	24	0.0417	545	0.001	-	4.84	0.640	-	0.62
	16	0.0625	537	0.007	-	4.96	5.388	-	0.62
30 ppm	48	0.0208	664	0.546	0.00686	4.86	0.080	43	1.13
	54.5	0.0183	669	0.493	0.00582	4.86	0.075	45	1.43
	32	0.0313	651	0.769	0.00885	4.86	0.199	42	1.18
	24	0.0417	648	0.989	0.01024	4.86	0.210	32	1.37
	16	0.0625	645	1.533	0.01516	4.82	0.199	31	0.81
50 ppm	48	0.0208	682	0.542	0.00683	4.57	0.035	44	1.82
	54.5	0.0183	685	0.437	0.00571	4.57	0.035	49	1.83
	32	0.0313	679	0.645	0.00843	4.57	0.046	41	1.46
	24	0.0417	673	0.812	0.01185	4.74	0.057	39	1.31
	16	0.0625	671	1.455	0.01999	4.74	0.059	42	0.99
100 ppm	48	0.0208	707	0.454	0.01225	4.84	0.015	81	2.28
	54.5	0.0183	712	0.390	0.01599	4.91	0.019	92	1.78
	32	0.0313	682	0.761	0.01833	4.93	0.040	79	1.76
	24	0.0417	675	0.983	0.02520	4.93	0.054	83	1.63
	16	0.0625	687	1.314	0.03625	4.93	0.035	80	1.52
270 ppm	48	0.0208	710	0.452	0.00966	4.93	0.015	64	1.41
	54.5	0.0183	714	0.409	0.01095	4.93	0.016	80	2.19
	32	0.0313	676	0.679	0.01792	4.91	0.062	76	1.62
	24	0.0417	674	0.889	0.02574	4.91	0.065	87	1.03
	16	0.0625	661	1.346	0.03442	4.91	0.089	81	0.54
340 ppm	48	0.0208	708	0.461	0.00997	4.94	0.018	66	1.78
	54.5	0.0183	710	0.387	0.01086	4.94	0.018	81	2.12
	32	0.0313	698	0.665	0.01693	4.94	0.025	75	1.54
	24	0.0417	663	0.912	0.02194	4.94	0.092	70	1.41
	16	0.0625	653	1.440	0.04100	4.94	0.130	79	1.15
450 ppm	48	0.0208	710	0.449	0.01176	4.94	0.018	77	2.47
	54.5	0.0183	714	0.394	0.01157	4.94	0.002	85	2.33
	32	0.0313	678	0.673	0.01748	4.94	0.059	75	2.19
	24	0.0417	669	0.897	0.02349	4.94	0.084	79	1.94
	16	0.0625	651	1.338	0.04599	4.96	0.176	91	1.69

Table E.2 Raw data from System 2 (sessile + planktonic) experiments

								planktonic population		sessile population	
Technique **measurement** ***units***	*set* **tau** *(hr)*	*set* **D** *(hr^{-1})*	*probe* **redox** *mV*	*offgas* **rO_2** *mmol /hr*	*offgas* **rCO_2** *mmole/(l.hr)*	*AAS* **Fe^{2+} (initial)** *g/L*	*spectro-photometry* **Fe^{2+} (residual)** *g/L*	*microscopic cell count* **number of** *cells* dil*	*total organic carbon* **TOC** *µ mol/L*	*microscopic cell count* **number of** *cells* dil*	*total organic carbon* **TOC** *µ mol/L*
30 ppm	48	0.0208	725	0.457	0.0105	5.01	0.00077	28	2.88	49	1.00
	54.5	0.0183	738	0.400	0.0096	4.99	0.00046	24	3.08	51	1.05
	32	0.0313	714	0.687	0.0101	4.99	0.00116	25	2.45	42	0.88
	24	0.0417	707	0.891	0.0116	4.84	0.00146	22	2.39	39	0.63
	16	0.0625	703	1.340	0.0190	4.86	0.00174	25	1.84	37	0.70
50 ppm	48	0.0208	736	0.448	0.0118	4.93	0.00049	38	1.28	60	3.56
	54.5	0.0183	742	0.398	0.0107	4.97	0.00039	32	1.28	59	3.75
	32	0.0313	728	0.680	0.0153	4.97	0.00068	31	0.82	57	3.06
	24	0.0417	712	0.915	0.0195	5.01	0.00125	28	0.38	62	2.86
	16	0.0625	708	1.370	0.0310	5.01	0.00144	30	0.70	57	2.90
100 ppm	48	0.0208	751	0.439	0.0151	4.87	0.00027	62	1.69	103	4.35
	54.5	0.0183	764	0.386	0.0146	4.87	0.00017	58	2.02	122	5.09
	32	0.0313	761	0.653	0.0242	4.84	0.00019	61	1.59	102	3.59
	24	0.0417	721	0.884	0.0331	4.91	0.00086	59	1.07	97	3.51
	16	0.0625	712	1.328	0.0476	4.91	0.00122	65	0.87	94	3.18
340 ppm	48	0.0208	787	0.454	0.0173	4.93	0.00007	53	1.84	98	4.45
	54.5	0.0183	794	0.398	0.0191	4.93	0.00005	56	2.23	91	5.72
	32	0.0313	770	0.752	0.0287	4.86	0.00013	64	1.62	112	4.86
	24	0.0417	725	0.969	0.0371	4.86	0.00073	63	1.43	124	4.79
	16	0.0625	716	1.413	0.0499	4.87	0.00103	57	1.69	92	4.60

E.2 Typical off-gas data set

Table E.3. Off-gas data log for System 1 (planktonic only), at a CO_2 concentration of 270 ppm and a residence time of 32 hrs (complete data set available on CD)

Inlet Oxygen (%)	Outlet Oxygen (%)	Inlet Carbon Dioxide (ppm)	Outlet Carbon Dioxide (ppm)	Gas Flow Rate (ml/min)	$-r_{gO_2}$ (mmole/(l.hr))	$-r_{gCO_2}$ (mmole/(l.hr))	Feed Flow Rate (/hr)	C_x Bacterial Concentration (mmol C/l)	$q_{CO_2} = mu$ (mmolCO2/(l.hr.mmol C))	q_{gO_2} (mmolO2/(l.hr.mmol C))	r_{Fe2+} (mmole/(l.hr))	$Y_{Fe2+/X}$	q_{Fe2+} mmol Fe/mmol C/hr
20.680	20.632	276.69	261.20	378	0.68745	0.01786	0.03125	3.67119	0.03125	1.20349	2.82469	158.24732	4.84523
20.680	20.632	276.30	259.34	378	0.69422	0.01839	0.03125	3.76204	0.03125	1.11897	2.85825	147.42840	4.60714
20.680	20.631	276.31	262.40	378	0.70110	0.01680	0.03125	3.52155	0.03125	1.34419	2.87324	174.25652	5.50802
20.680	20.630	276.61	260.20	378	0.71462	0.01884	0.03125	3.80277	0.03125	1.16565	2.93755	155.54580	4.87343
20.680	20.632	276.59	259.34	378	0.69851	0.01908	0.03125	3.82976	0.03125	1.09456	2.83990	144.30310	4.56047
20.680	20.631	276.66	258.33	378	0.70236	0.02018	0.03125	3.98487	0.03125	1.05639	2.89671	139.41665	4.35677
20.687	20.630	276.58	261.49	378	0.61217	0.01747	0.03125	3.95809	0.03125	1.09464	2.52206	144.35210	4.51103
20.687	20.630	278.67	263.54	378	0.66827	0.01541	0.03125	3.49362	0.03125	1.39586	2.81754	182.87351	5.71480
20.686	20.629	278.56	259.34	378	0.75514	0.01962	0.03125	3.52936	0.03125	1.19867	3.09516	157.37422	4.91794
20.686	20.630	277.35	262.40	378	0.51158	0.01525	0.03125	3.45810	0.03125	1.25296	2.91540	164.56141	5.14317
20.686	20.629	278.65	256.26	378	0.72790	0.02085	0.03125	4.06705	0.03125	1.05123	2.99516	143.87775	4.49618
20.688	20.633	278.65	259.13	378	0.70216	0.01906	0.03125	3.68863	0.03125	1.09949	2.89248	144.99454	4.52920
20.686	20.629	278.69	260.02	378	0.72721	0.01819	0.03125	3.58215	0.03125	1.24918	2.98529	164.09456	5.12795
20.686	20.630	278.50	263.50	378	0.71366	0.01515	0.03125	2.98579	0.03125	1.40907	2.91841	192.24058	6.00752
20.687	20.630	278.31	264.74	378	0.72611	0.01304	0.03125	2.44605	0.03125	1.62788	2.96299	212.56630	6.64270
20.687	20.631	278.67	264.21	378	0.71357	0.01475	0.03125	2.47204	0.03125	1.50911	2.91633	197.36609	6.16765
20.686	20.631	278.55	261.19	378	0.70158	0.01760	0.03125	3.56961	0.03125	1.23159	2.88110	161.65686	5.05803
20.674	20.630	278.57	260.22	378	0.56136	0.01373	0.03125	2.59946	0.03125	0.93643	2.32410	124.26311	3.87697
20.675	20.632	278.56	261.34	378	0.54830	0.01759	0.03125	3.56273	0.03125	0.97436	2.26707	128.91759	4.02867
20.675	20.630	277.30	264.44	378	0.57547	0.01621	0.03125	3.51867	0.03125	1.10522	2.36107	145.66847	4.55214
20.673	20.632	278.65	260.65	378	0.54844	0.01617	0.03125	3.58153	0.03125	0.94370	2.27036	124.51722	3.90366
20.686	20.632	278.57	259.13	378	0.71489	0.01958	0.03125	3.68615	0.03125	1.12375	2.94335	148.04345	4.62636
20.686	20.632	278.56	260.02	378	0.68869	0.01805	0.03125	3.97760	0.03125	1.19268	2.83136	156.86315	4.90197
20.680	20.631	277.30	263.50	378	0.70064	0.01416	0.03125	2.45325	0.03125	1.64579	2.86203	202.06122	6.31441
20.687	20.630	278.65	264.74	378	0.61135	0.01428	0.03125	2.48605	0.03125	1.34045	2.50516	175.78197	5.49310
20.687	20.633	278.65	264.21	378	0.68826	0.01481	0.03125	2.47397	0.03125	1.45186	2.81440	190.03848	5.93870
20.688	20.629	278.69	261.19	378	0.76269	0.01793	0.03125	3.57363	0.03125	1.31214	3.08609	172.15402	5.37981
20.686	20.636	278.30	260.22	378	0.61242	0.01847	0.03125	3.59116	0.03125	1.03596	2.62725	136.80319	4.27510
20.686	20.629	278.41	258.35	378	0.72782	0.02051	0.03125	3.95637	0.03125	1.10880	2.99741	146.13239	4.56664
20.688	20.633	278.48	258.34	378	0.70259	0.02030	0.03125	3.69174	0.03125	1.20657	2.95108	154.32105	4.82753
20.686	20.629	278.40	261.50	378	0.72725	0.01832	0.03125	3.56638	0.03125	1.24029	2.98564	162.94564	5.09215
20.686	20.630	278.30	263.55	378	0.71394	0.01623	0.03125	3.51952	0.03125	1.13423	2.92364	180.10161	5.62818
20.687	20.630	278.38	260.35	378	0.72782	0.02048	0.03125	3.65540	0.03125	1.11049	2.99729	146.34333	4.57323
20.687	20.631	278.12	262.41	378	0.71391	0.01810	0.03125	3.51528	0.03125	1.38660	2.92328	181.64351	5.67321
20.686	20.631	278.47	258.27	378	0.70259	0.02166	0.03125	3.69308	0.03125	1.21372	2.89133	133.95558	4.18611
20.674	20.630	278.47	259.14	378	0.56188	0.02074	0.03125	3.65364	0.03125	0.84006	2.53401	112.67308	3.51791
Average					0.67902	0.01792							4.5401
Std Dev					0.06026	0.00227							0.7425

Table E.4. Off-gas data for R1 (planktonic system) in the decoupling study

time	$-r_{O2}$	$-r_{CO2}$	C_x	$-r_{Fe2+}$	$Y^{Fe2+/X}$	q_{Fe2+}
	mmol/(l.hr)	*mmol/(l.hr)*	*(mmol C/l)*			
00:00:00	0.653489912	0.028421097	0.909475116	2.733328	0.010398	3.005391
00:08:00	0.654329082	0.027563123	0.882019936	2.733081	0.010085	3.098662
00:26:00	0.659809103	0.026873764	0.859960455	2.752106	0.009765	3.200271
00:38:00	0.66791838	0.021891247	0.700519904	2.763617	0.007921	3.945094
00:56:00	0.669834907	0.017098124	0.547139978	2.751152	0.006215	5.028241
01:08:00	0.668091284	0.014592871	0.466971883	2.733655	0.005338	5.854004
01:26:00	0.661222314	0.013591861	0.434939552	2.701975	0.00503	6.2123
01:38:00	0.662989871	0.01377819	0.440902089	2.709828	0.005085	6.146099
01:56:00	0.662987187	0.014787123	0.473187949	2.714055	0.005448	5.73568
02:08:00	0.662912738	0.014990292	0.479689334	2.71461	0.005522	5.659101
02:26:00	0.663877184	0.01597128	0.511080954	2.722588	0.005866	5.327117
02:38:00	0.664901284	0.016745246	0.53584787	2.729935	0.006134	5.094609
02:56:00	0.664192313	0.016747487	0.535919591	2.727109	0.006141	5.088653
03:08:00	0.664281211	0.016761066	0.536354116	2.727521	0.006145	5.0853
03:26:00	0.664819813	0.016770404	0.536652918	2.729715	0.006144	5.086556
03:38:00	0.665190182	0.016765643	0.53650056	2.731176	0.006139	5.090724
03:56:00	0.665001332	0.016790503	0.537296094	2.730525	0.006149	5.081975
04:08:00	0.66598741	0.016773138	0.536740419	2.734397	0.006134	5.094449
04:27:00	0.665298641	0.016783786	0.537081149	2.731686	0.006144	5.086171
04:38:00	0.665720982	0.016768826	0.536602443	2.733313	0.006135	5.093739
04:56:00	0.665127618	0.016753324	0.536106373	2.730874	0.006135	5.093904
05:08:00	0.664512731	0.016753755	0.536120162	2.728417	0.00614	5.089189
05:27:00	0.664529823	0.016757721	0.536247072	2.728502	0.006142	5.088143
05:38:00	0.66468713	0.016797708	0.537526654	2.729299	0.006155	5.077514
05:57:00	0.666273192	0.016804992	0.537759757	2.735674	0.006143	5.087167
06:08:00	0.666562128	0.016761106	0.536355377	2.736645	0.006125	5.102298
06:27:00	0.664821376	0.016698918	0.534365372	2.729421	0.006118	5.10778
06:38:00	0.662354732	0.016819218	0.538214991	2.72006	0.006183	5.053853
06:57:00	0.667126398	0.016812788	0.538009212	2.739119	0.006138	5.091213
07:08:00	0.666871332	0.016303007	0.521696238	2.735958	0.005959	5.244351
07:27:00	0.64665113	0.016767406	0.536556976	2.657028	0.006311	4.951995
07:38:00	0.665071261	0.016765641	0.53650052	2.730701	0.00614	5.089838
07:57:00	0.665001282	0.016792869	0.537371794	2.730535	0.00615	5.081277
08:09:00	0.666081241	0.016768119	0.536579817	2.734751	0.006131	5.096634
08:27:00	0.665099573	0.016821486	0.53828754	2.731049	0.006159	5.073587
08:39:00	0.667216324	0.016773856	0.536763401	2.739315	0.006123	5.103395
08:57:00	0.665327128	0.016773604	0.53675533	2.731758	0.00614	5.089391
09:09:00	0.665317123	0.016790321	0.537290271	2.731788	0.006146	5.08438
09:27:00	0.665980193	0.017026104	0.54483534	2.73543	0.006224	5.020655
09:39:00	0.67533243	0.017198573	0.550354321	2.773564	0.006201	5.039597
09:57:00	0.682173298	0.01712317	0.547941424	2.800611	0.006114	5.111149
10:09:00	0.679182473	0.017204225	0.550535189	2.788988	0.006169	5.065957
10:27:00	0.682397487	0.016894696	0.540630283	2.800548	0.006033	5.180153
10:39:00	0.670120192	0.017175214	0.549606838	2.752617	0.00624	5.008338
10:57:00	0.681246781	0.01745499	0.558559683	2.798298	0.006238	5.009846
11:09:00	0.692343981	0.017209809	0.5507139	2.841657	0.006056	5.159952
11:27:00	0.682619003	0.016919218	0.541414976	2.801537	0.006039	5.174472
11:39:00	0.671092832	0.016897195	0.540710225	2.75534	0.006133	5.095779
11:57:00	0.670219281	0.016864622	0.53966791	2.751709	0.006129	5.098892
12:09:00	0.668927315	0.016738135	0.535620331	2.746009	0.006095	5.126783
12:27:00	0.663910273	0.016758508	0.536272243	2.726027	0.006148	5.083289
12:39:00	0.66471833	0.016761046	0.53635347	2.72927	0.006141	5.088565
12:57:00	0.664819012	0.016758532	0.536273015	2.729662	0.006139	5.09006
13:09:00	0.664719287	0.016947091	0.542306925	2.730055	0.006208	5.034151
13:27:00	0.672198418	0.017350079	0.555202537	2.761664	0.006282	4.974156
13:39:00	0.688182743	0.016743164	0.535781246	2.823052	0.005931	5.269039
13:57:00	0.664109731	0.016765936	0.53650996	2.726856	0.006148	5.082582
14:09:00	0.665012984	0.01677045	0.536654398	2.730488	0.006142	5.087982
14:27:00	0.665192017	0.016793966	0.537406904	2.731303	0.006149	5.082374
14:39:00	0.666124761	0.016819285	0.538217128	2.73514	0.006149	5.081852
14:57:00	0.667129047	0.016795664	0.537461255	2.739058	0.006132	5.096289
15:09:00	0.66619213	0.016766145	0.536516628	2.735186	0.00613	5.098046
15:27:00	0.665021249	0.01681918	0.538213775	2.730726	0.006159	5.073682
15:39:00	0.667124891	0.016761805	0.536377761	2.738899	0.00612	5.106288
15:57:00	0.664849121	0.016745903	0.535868894	2.729729	0.006135	5.094025

Table E.5. Off-gas data for R2 (sessile + planktonic system) in the decoupling study

time	$-r_{O2}$	$-r_{CO2}$	C_x	r_{Fe2+}	$Y^{Fe2+/X}$	q_{Fe2+}
00:00:00	0.65349	0.028421	0.909475	2.733328	0.010398	3.005391
00:13:00	0.643409	0.01758	0.562575	2.647476	0.00664	4.705998
00:25:00	0.652388	0.017411	0.557161	2.68268	0.00649	4.814908
00:45:00	0.648648	0.015642	0.500534	2.660287	0.00588	5.314901
00:55:00	0.651997	0.015392	0.492544	2.672634	0.005759	5.426184
01:13:00	0.592665	0.015392	0.49254	2.435304	0.00632	4.944378
01:25:00	0.654569	0.016444	0.526218	2.687343	0.006119	5.106902
01:45:00	0.643202	0.015979	0.511333	2.639921	0.006053	5.162817
01:55:00	0.651841	0.015268	0.488569	2.671491	0.005715	5.46799
02:13:00	0.640282	0.01394	0.446082	2.619677	0.005321	5.872631
02:25:00	0.650995	0.015243	0.487779	2.668003	0.005713	5.4697
02:45:00	0.652731	0.014725	0.471213	2.67277	0.005509	5.672104
02:55:00	0.652406	0.015872	0.507909	2.676287	0.005931	5.269227
03:13:00	0.652923	0.016235	0.519532	2.679881	0.006058	5.158265
03:25:00	0.652075	0.017365	0.55568	2.681231	0.006477	4.825133
03:45:00	0.649229	0.017905	0.572959	2.672118	0.006701	4.663719
03:55:00	0.663255	0.016523	0.52875	2.72242	0.006069	5.148782
04:13:00	0.659657	0.016445	0.526232	2.707695	0.006073	5.145435
04:25:00	0.65119	0.016235	0.519525	2.672948	0.006074	5.144988
04:45:00	0.67065	0.016045	0.51344	2.74999	0.005835	5.35601
04:55:00	0.671743	0.0157	0.502408	2.752914	0.005703	5.479438
05:14:00	0.631435	0.015484	0.495483	2.590773	0.005977	5.228782
05:25:00	0.655315	0.016188	0.518017	2.689248	0.00602	5.191433
05:46:00	0.664314	0.01677	0.536655	2.727693	0.006148	5.082765
05:56:00	0.668916	0.017439	0.558039	2.748906	0.006344	4.926014
06:14:00	0.657511	0.017431	0.557779	2.703252	0.006448	4.846459
06:25:00	0.652438	0.017446	0.558282	2.683028	0.006502	4.805868
06:46:00	0.652349	0.018157	0.581008	2.685652	0.006761	4.622399
06:56:00	0.648213	0.01902	0.608637	2.672737	0.007116	4.391346
07:14:00	0.643323	0.01902	0.608647	2.653177	0.007169	4.359139
07:26:00	0.646281	0.019614	0.627655	2.667504	0.007353	4.249954
07:46:00	0.629162	0.020341	0.650905	2.602079	0.007817	3.997636
07:56:00	0.629252	0.021026	0.67284	2.605317	0.008071	3.872118
08:14:00	0.649298	0.020324	0.650382	2.682556	0.007577	4.124584
08:26:00	0.668271	0.021534	0.689101	2.763528	0.007792	4.010339
08:46:00	0.651697	0.02146	0.686704	2.696917	0.007957	3.927334
08:56:00	0.65811	0.020558	0.657854	2.718784	0.007561	4.13281
09:14:00	0.665124	0.020778	0.664891	2.747764	0.007562	4.132651
09:26:00	0.652456	0.021041	0.673305	2.698197	0.007798	4.007393
09:46:00	0.653386	0.021198	0.678326	2.702575	0.007844	3.984182
09:56:00	0.646097	0.021317	0.682136	2.673918	0.007972	3.919919
10:14:00	0.651479	0.021511	0.688338	2.696258	0.007978	3.917058
10:26:00	0.658692	0.018437	0.589986	2.712202	0.006798	4.597059
10:46:00	0.652417	0.02197	0.703042	2.701944	0.008131	3.843219
10:56:00	0.663041	0.02197	0.703042	2.74444	0.008005	3.903664
11:14:00	0.639098	0.021962	0.702795	2.648636	0.008292	3.768716
11:26:00	0.639009	0.021762	0.696375	2.647437	0.00822	3.801742
11:46:00	0.666144	0.021932	0.701838	2.756691	0.007956	3.927818
11:56:00	0.645168	0.022574	0.722373	2.675484	0.008437	3.703745
12:14:00	0.651273	0.022536	0.721166	2.699746	0.008348	3.743588
12:26:00	0.652175	0.022558	0.721856	2.703443	0.008344	3.745126
12:46:00	0.646263	0.022544	0.721397	2.679736	0.008413	3.714645
12:56:00	0.648397	0.022761	0.728348	2.689185	0.008464	3.692171
13:14:00	0.639544	0.022698	0.72633	2.653507	0.008554	3.653308
13:26:00	0.645551	0.023	0.736005	2.678803	0.008586	3.639655
13:46:00	0.645518	0.023241	0.743718	2.679684	0.008673	3.603089
13:56:00	0.684586	0.023256	0.744189	2.83602	0.0082	3.810886
14:14:00	0.683037	0.02393	0.76576	2.832654	0.008448	3.69914
14:26:00	0.692948	0.024194	0.774192	2.873404	0.00842	3.711486
14:46:00	0.664982	0.024876	0.796034	2.764405	0.008999	3.472724
14:56:00	0.64991	0.024501	0.784023	2.702542	0.009066	3.44702
15:14:00	0.654067	0.023964	0.766847	2.716917	0.00882	3.542972
15:26:00	0.653146	0.024648	0.788739	2.716107	0.009075	3.443608
15:46:00	0.66124	0.024706	0.790608	2.748727	0.008988	3.476728
15:56:00	0.645478	0.024918	0.797362	2.686564	0.009275	3.369313

F. Sample calculations

F.1 Dilution rate

The dilution rate of the system is check by using the change in mass of the feed. The density if found by measuring the mass of 1 cm^3 of feed by pipette:

$$\tau = \frac{\Delta time \times \rho \times V_R}{\Delta mass\ of\ feed}$$

F.2 Ferrous iron concentration

Calculated from spectrophotometry with a standard curve:

Use equation of curve e.g. if curve of absorbance vs ferrous iron concentration is y = 0.016x (from Section D.3) and the absorbance of the sample is 0.856 then:

$$[Fe^{2+}] = \frac{0.856}{0.016} ppm$$

Calculated from redox potential and total ferrous iron

Using the equation of the curve e.g. if curve of redox potential vs ratio of ferric:ferrous iron is y=26.502ln(x)+495.98 (from Section D.4), the total ferrous iron concentration is 4.86 g/L (from AAS), and the redx measurement from the probe is 642.77 mV then:

$$\frac{[Fe^{3+}]}{[Fe^{2+}]} = e^{\frac{(643.77-495.98)}{26.502}} = 284.93$$

$$[Fe^{2+}] = \frac{4.86 g/L}{1 + \frac{[Fe^{3+}]}{[Fe^{2+}]}}$$

$$[Fe^{3+}] = \frac{[Fe^{3+}]}{[Fe^{2+}]} \times [Fe^{2+}]$$

F.3 Ferrous iron oxidation rate

Calculated from direct measurements (AAS, redox measurements and Spectrophotometry)

$$\frac{dFe^{2+}}{dt} = -r_{Fe^{2+}} = D \cdot ([Fe^{2+}]_{inlet} - [Fe^{2+}]_{outlet})$$

Calculated from off gas data (oxygen and carbon dioxide uptake rates calculated shown in Section 3.7.10):

$$-r_{Fe^{2+}} = -4r_{O_2} - 4.2r_{CO_2}$$

F.4 Specific ferrous iron oxidation rate

Calculated from direct measurements:

$$q_{Fe^{2+}} = \frac{-r_{Fe^{2+}}}{[Cells] \cdot \frac{Cell_{carbon\ equivalent}}{Mr_{Carbon}} \cdot 10^{12}}$$

Calculated from off gas data:

$$qFe = \frac{-r_{Fe} \cdot D}{-r_{CO_2}}$$

F.5 Error analysis

$$mean\ value\ of\ \boldsymbol{n}\ data\ points = \frac{\sum_{i=1}^{n} x_i}{n}$$

$$absolute\ error = |maximum\ value - mean\ value|$$

$$\%\ relative\ error = \frac{|maximum\ value - mean\ value|}{mean} \times 100\%$$

When adding and/or subtracting, absolute errors were added
When multiplying and/or dividing, relative errors were added

Standard deviations were calculated using the STDEV() function in MSExcel

G. Material Safety Data Sheets

The following hazards and safety measures for usage of key chemicals were sourced and summarised from http://www.jtbaker.com

Ammonium acetate

Hazards:

May be harmful if swallowed, impairs motor function affecting central nervous system

May cause irritation if it comes into contact with the skin, eyes and respiratory tract

Personal Protective Equipment:

Safety gloves, mask if working with extensively

Ammonium orthophosphate - $(NH_4)_2HPO_4$

Hazards:

May be harmful if swallowed

May cause irritation if it comes into contact with the skin, eyes and respiratory tract

Personal Protective Equipment:

Safety gloves

Ammonium sulphate - $(NH_4)_2SO_4$

Hazards:

May be harmful if swallowed

May cause irritation if it comes into contact with the skin, eyes and respiratory tract

Personal Protective Equipment:

Safety gloves

Barium chloride - $BaCl_2.2H_2O$

Hazards:

Poison, may be fatal if swallowed, damages to central nervous system

Harmful if inhaled

May cause irritation if it comes into contact with the skin, eyes and respiratory tract

Personal Protective Equipment:

Safety gloves

Ferrous sulphate - $FeSO_4.7H_2O$

Hazards:

Poison, harmful if swallowed, damages liver

May cause irritation if it comes into contact with the skin, eyes and respiratory tract

Personal Protective Equipment:

Safety gloves

Potassium sulphate - K_2SO_4

Hazards:

May be harmful if swallowed

May cause irritation if it comes into contact with the skin, eyes and respiratory tract

Personal Protective Equipment:

Safety gloves

Phenanthroline monohydrate - $C_{12}H_8N_2.H_2O$

Hazards:

Harmful if inhaled, swallowed or absorbed through skin

Eye, skin and respiratory tract irritant

Personal Protective Equipment:

Safety glasses, adequate ventilation

Sodium hydroxide – *NaOH*

Hazards:

Poison, may be fatal if swallowed

Extremely corrosive, liquid and mist cause severe burns to all body parts

Water reactive

Personal Protective equipment

Safety gloves, mask if potential of producing fumes

Sulphuric acid conc. - H_2SO_4 (98%)

Hazards:

Poison, may be fatal if swallowed

Extremely corrosive, liquid and mist cause severe burns to all body parts

Water reactive

Can cause cancer

Personal Protective equipment

Safety gloves, mask if potential of producing fumes

Tris-hydroxymethylanimomethane – *H'NC(CH'OH)"*

Hazards:

May be harmful if swallowed

Eye, skin and respiratory tract irritant

Personal Protective equipment

Safety gloves